LERC-3695-1

LABORATORY EVALUATION OF SELECTED SHALE OIL ASPHALTS IN PAVING MIXTURES

Report RF 3403-1

By
Joe W. Button
Jon A. Epps
Bob M. Gallaway

January 1978

Work Performed Under Contract No. EY-76-C-04-3695

Texas Transportation Institute
Texas A&M University
College Station, Texas

TECHNICAL INFORMATION CENTER
UNITED STATES DEPARTMENT OF ENERGY

This report has been reproduced directly from the best available copy.

Available from the National Technical Information Service, U. S. Department of Commerce, Springfield, Virginia 22161.

Price: Paper Copy $7.25
Microfiche $3.00

Printed in the United States of America
USDOE Technical Information Center, Oak Ridge, Tennessee

LERC-3695-1
Distribution Category UC-92b

Laboratory Evaluation

of

Selected Shale Oil Asphalts in Paving Mixtures

by

Joe W. Button
Assistant Research Engineer

Jon A. Epps
Research Engineer

and

Bob M. Gallaway
Research Engineer

Report RF 3403-1

Work Performed Under Contract No. E(29-2)-3695

Prepared for

Department of Energy
Laramie Energy Research Center
Laramie, Wyoming 82071

by

Texas Transportation Institute
Texas A&M University
College Station, Texas 77843

January 1978

TABLE OF CONTENTS

LIST OF TABLES

LIST OF FIGURES

DISCLAIMER

The contents of this report reflect the veiws of the authors who are responsible for the facts and accuracy of the data presented herein. The contents do not necessarily reflect the official views or policies of the Department of Energy. This report does not constitute a standard, specification, or regulation.

ABSTRACT

Shale oil asphalt cements originating from the Green River formation in Colorado were characterized by laboratory tests commonly used in specifying paving asphalts. The asphalt cements were mixed with two common aggregates to fabricate laboratory specimens which were tested to identify paving mixture characteristics such as compactibility, stability, stiffness, tensile strength, and water susceptiblity. Test results were compared to similar characteristics of a petroleum asphalt cement and petroleum asphalt-aggregate mixtures. Laboratory test results indicate no fundamental differences between shale oil asphalt and petroleum asphalt and furthermore properties of the mixtures are shown to be satisfactory when compared to standard specifications.

INTRODUCTION

Since the 1850's, interest in shale oil as a fuel source has been fluctuating. Each time the interest in shale oil went up the price of conventional crude went down. Following this established pattern, commercial interest in shale oil was again pushed aside until recently. But now, due to dwindling domestic oil supplies and increased prices on foreign oil, oil shale, as a major fossil fuel resource, again appears promising.

Although interest in shale oil has seriously lagged during the last three decades, one group, the Laramie Energy Research Center (LERC) in Laramie, Wyoming has continued to conduct research on oil shale since 1944. Due primarily to their efforts, the development of new ideas, processes, and equipment may allow competitive production of oil from shale in the near future. LERC research includes in-situ processing, which eliminates the problem of disposing of spent shale; recovery of other marketable minerals from shale, which helps offset the cost of producing shale oil; and hydrogenation of raw shale oil to reduce nitrogen and sulfur content, thus yielding a product acceptable to conventional refineries.

It was this group with their interest in the properties of asphalt from shale oil which initiated the research described herein. Since 75 percent of the asphalt produced is used in the paving industry it behooves one to determine whether or not asphalt from shale oil is suitable for paving applications.

The objective of this research study is to determine the suitability of shale oil asphalts for paving purposes. Selected shale oil asphalt cements were characterized by tests commonly utilized to specify paving asphalt together with certain special tests. Asphalt-aggregate mixtures were made utilizing these asphalts and they too were subjected to tests used in specifying paving mixtures. The test results were compared to similar characteristics of petroleum asphalt cements and petroleum asphalt-aggregate mixtures. Based on the laboratory test results, there appears to be no basic differences in shale oil asphalt and petroleum asphalts and further, the performance in paving mixtures should be quite satisfactory.

ASPHALT CEMENT PROPERTIES

General

Crude shale oil was produced from oil shale from the Green River formation in Colorado by the gas combustion process. A sample of the resulting shale oil residue (LERC # SOA-71-98) was used to produce three grades of asphalt cement. A soft asphalt cement was produced by vacuum distillation and labeled SO AC-5 and a dewaxed asphalt cement produced by Kerr-McGee Company using the ROSE high-pressure process with pentane solvent was labeled SO AC-10. The first attempts by the refiner at distillation of the residue to produce an AC-20 resulted in a material that was much too hard. There was only enough original residuum for one trial. Since the distillate from the residuum had been retained, a predetermined portion was re-blended with the hard asphalt to produce a material with the appropriate viscosity at 140°F (60°C) and it was labeled SO AC-20. The material selected as the control asphalt (1) was a viscosity graded AC-10 petroleum asphalt cement produced by vacuum reduction by the American Petrofina Company at their Mt. Pleasant, Texas refinery.

Laboratory Tests and Results

Standard laboratory tests (2, 3, 4) were performed on each asphalt to determine the basic physical and chemical characteristics, including consistency, durability, purity and safety.

Two non-standard tests were also conducted. They are entitled Thermal Neutron Activation Analysis used to determine the vanadium content of the asphalt and Actinic Light Hardening Test, used to determine the asphalt hardening effects of chemically active (ultraviolet) light (5). Hardening Index was computed by dividing viscosity at 77°F (25°C) of the asphalt after exposure to actinic light by its initial viscosity.

The types of tests performed and the results are presented in Table 1. The Bitumen Test Data Chart was developed by Heukelom (6) to provide a means of describing both penetration and viscosity as functions of temperature with the aid of the reference temperature (ring and ball softening point, theoretically the temperature at 800 penetration) and the temperature susceptibility of a given bitumen. For convenience, the appropriate properties of each asphalt are displayed on Bitumen Test Data Charts (Figures 1 through 4). The arrows indicate specification limits (2, 3) for the nomial viscosity graded asphalts. The asphalt viscosities are presented collectively on an ASTM standard viscosity chart in Figure 5. Asphalt penetrations are graphically depicted in Figure 6 to facilitate comparison.

TABLE 1. Original Asphalt Cement Properties

Characteristic Measured	Lab Std. AC-10	SO AC-5	SO AC-10	SO AC-20
Viscosity, 77°F (25°C) poise (4)	5.8×10^5	4.8×10^5	2.6×10^6	2.5×10^6
Viscosity, 140°F (60°C) poise	1580	490	1300	1990
Viscosity, 275°F (135°C) poise	3.8	1.3	2.3	2.2
Penetration, 77°F (25°C), dmm	118	123	43	70
Penetration, 39°F (4°C), dmm	26	32	8	31
Softening Point, (R & B) °F (°C)	107(42)	115(46)	119(48)	121(49)
Penetration Index	-1.4	+0.25	-1.9	-0.5
Specific Gravity, 77°F (25°C)	1.02	1.01	1.03	1.03
Ductility, 77°F (25°C), cm	150+	127	150+	93
Solubility (CH Cl:CCl_2), %	99.99	100	99.97	100
Flash Point, °F (°C)	615(324)	582(306)	561(294)	519(271)
Fire Point, °F (°C)	697(370)	670(355)	633(334)	586(308)
Spot Test	Neg.	Neg.	Neg.	Neg.
Thin Film Oven Test				
Penetration of Residue, 77°F	68	48	24	22
Ductility of Residue, 77°F	150+	148	150+	9
Viscosity of Residue, 140°F	3050	2070	3650	Too high
Loss on Heating	Neg.	Neg.	Neg.	2%
Hardening Index (due to Actinic light)	1.9	2.5	2.2	1.7
Vanadium Content, ppm	3.4	2.6	---	3.2

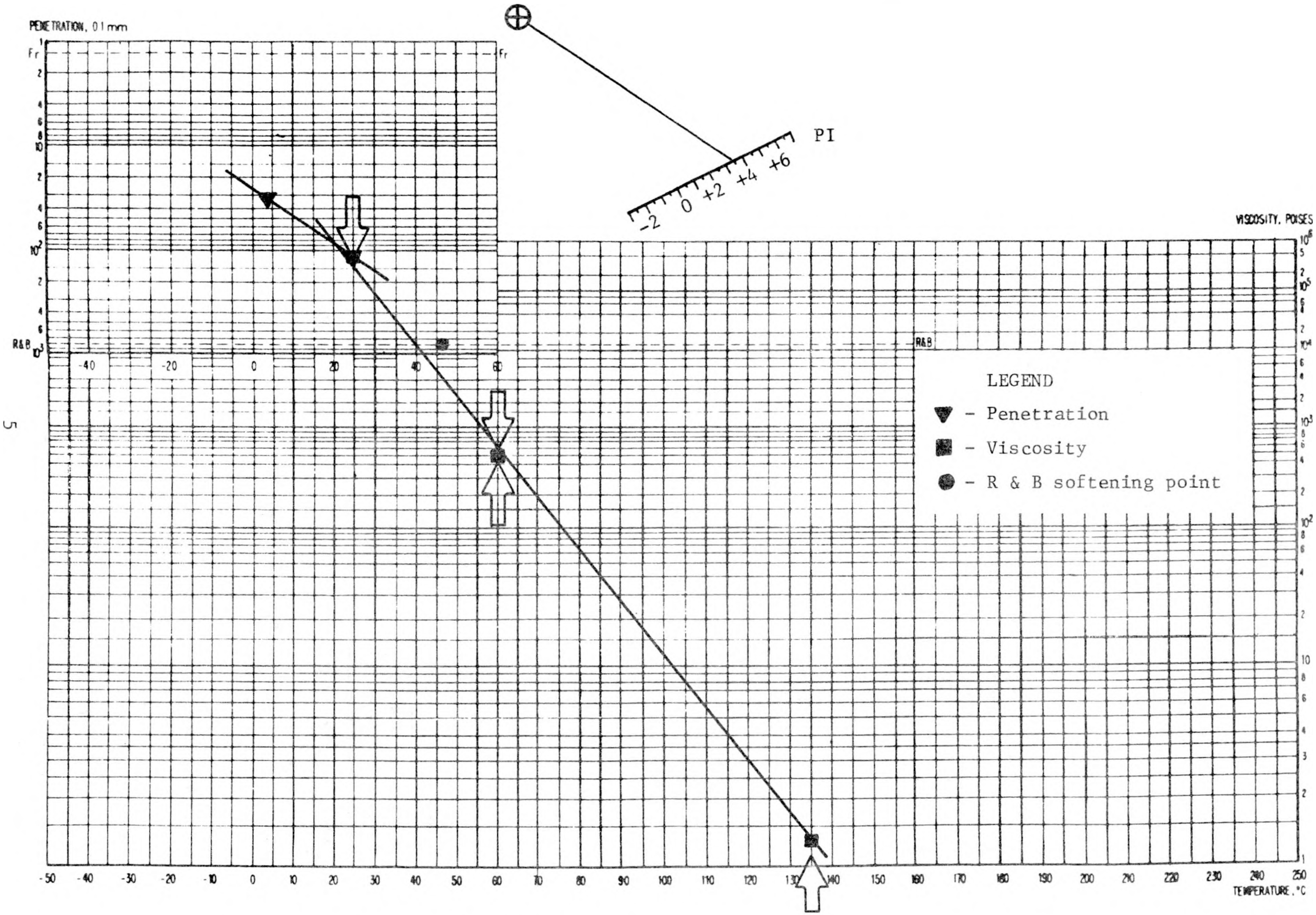

Figure 1. Bitumen Test Data Chart Showing Properties of SO AC-5

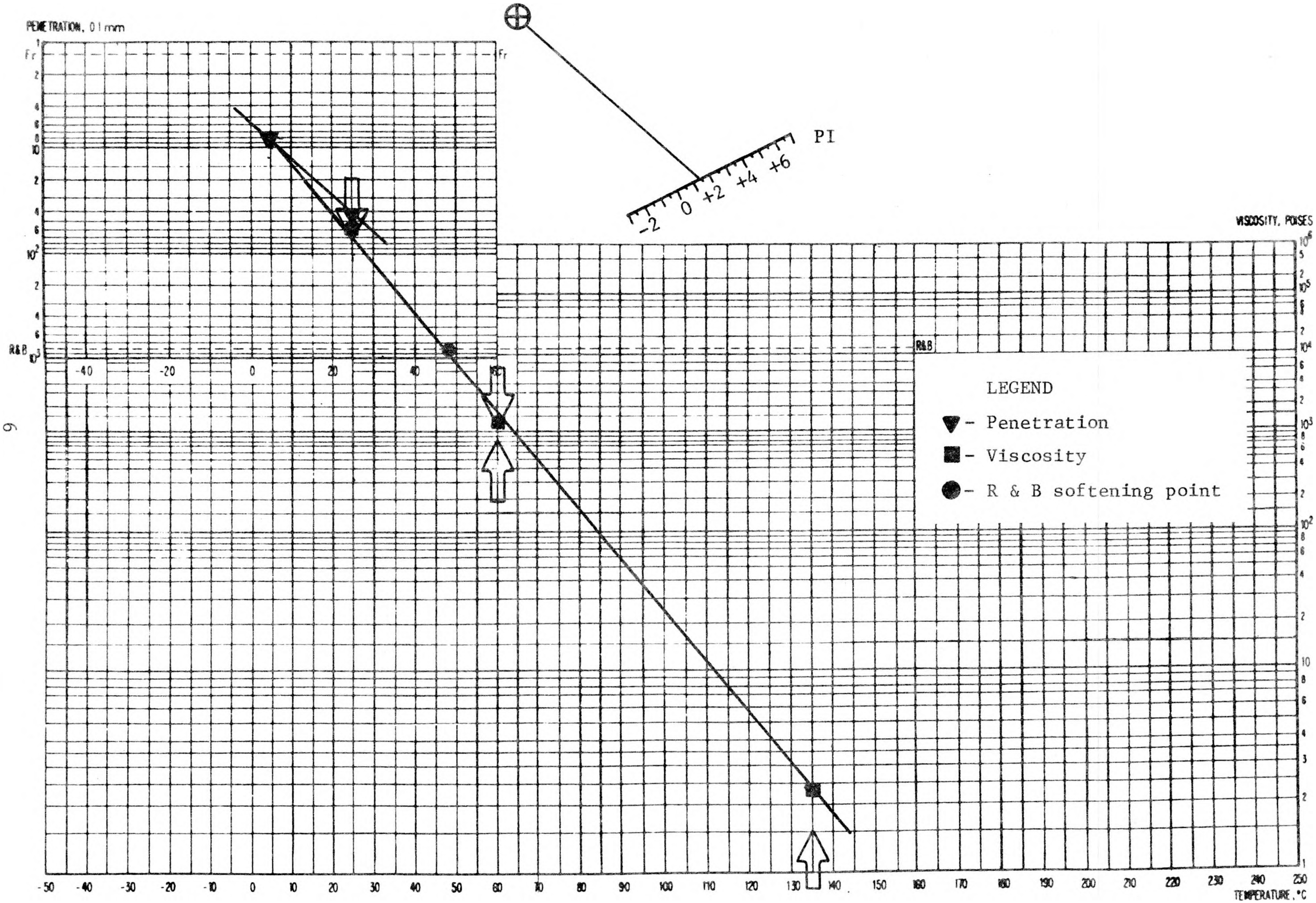

Figure 2. Bitumen Test Data Chart Showing Properties of SO AC-10.

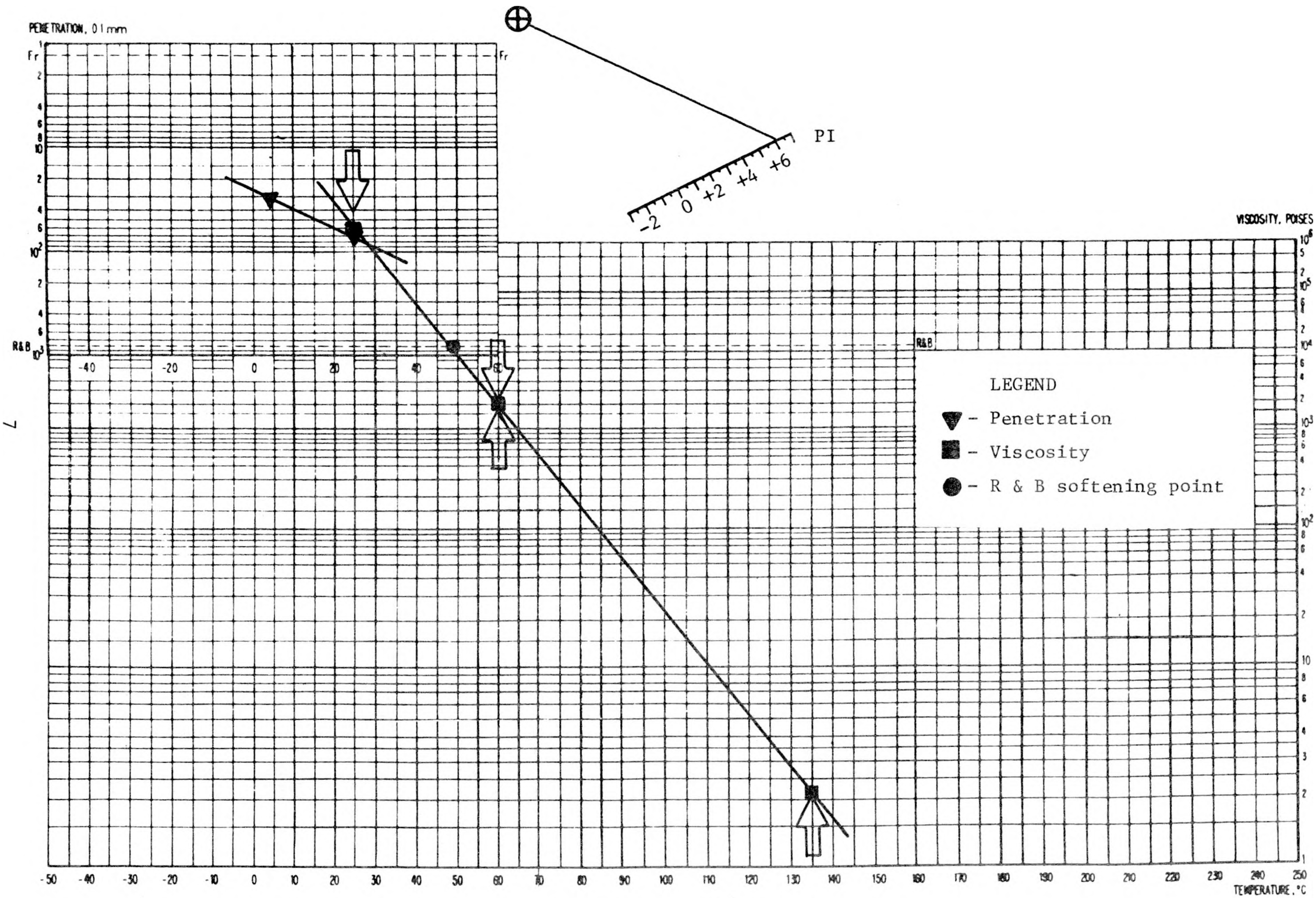

Figure 3. Bitumen Test Data Chart Showing Properties of SO AC-20

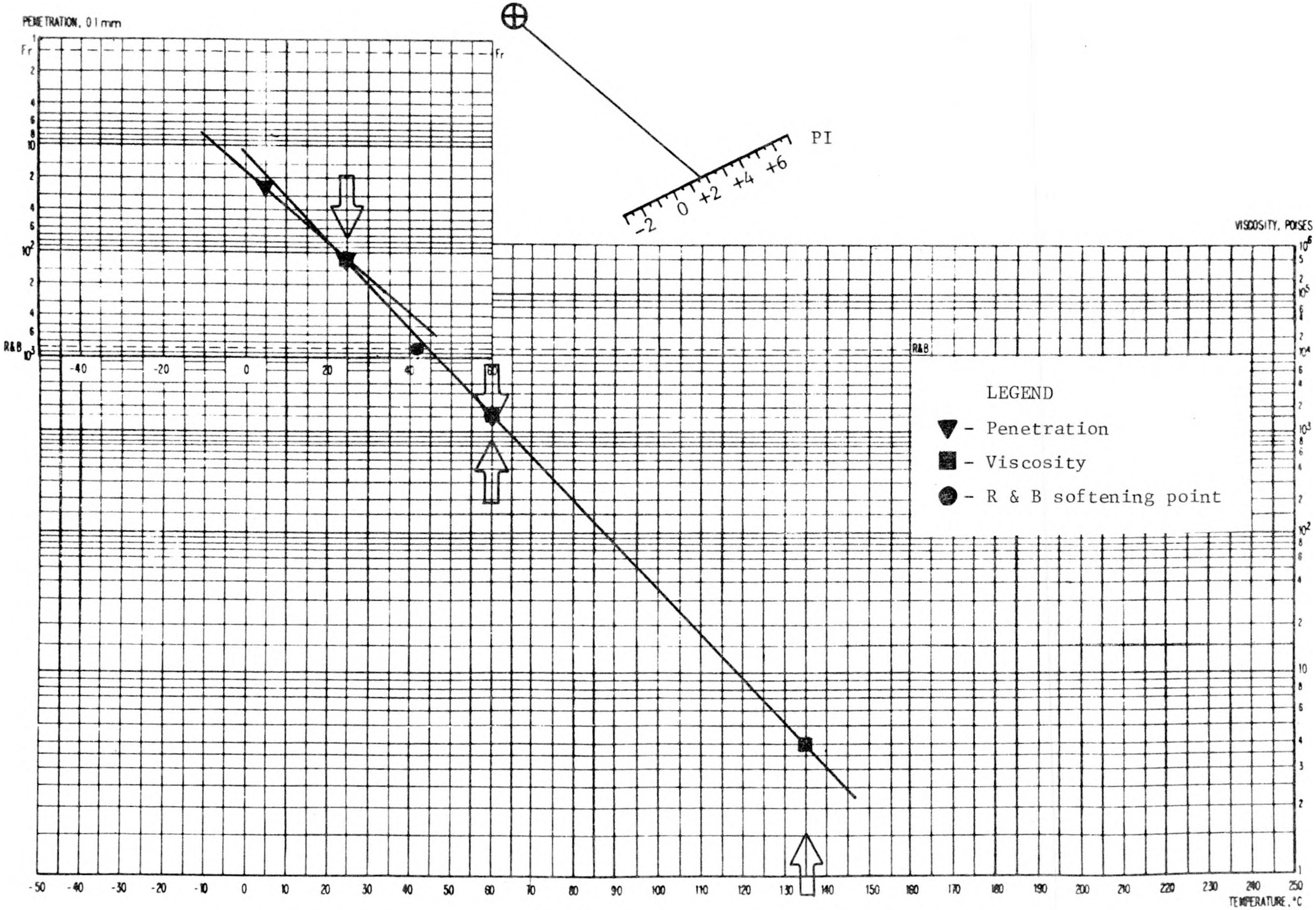

Figure 4. Bitumen Test Data Chart Showing Properties of Laboratory Standard Asphalt

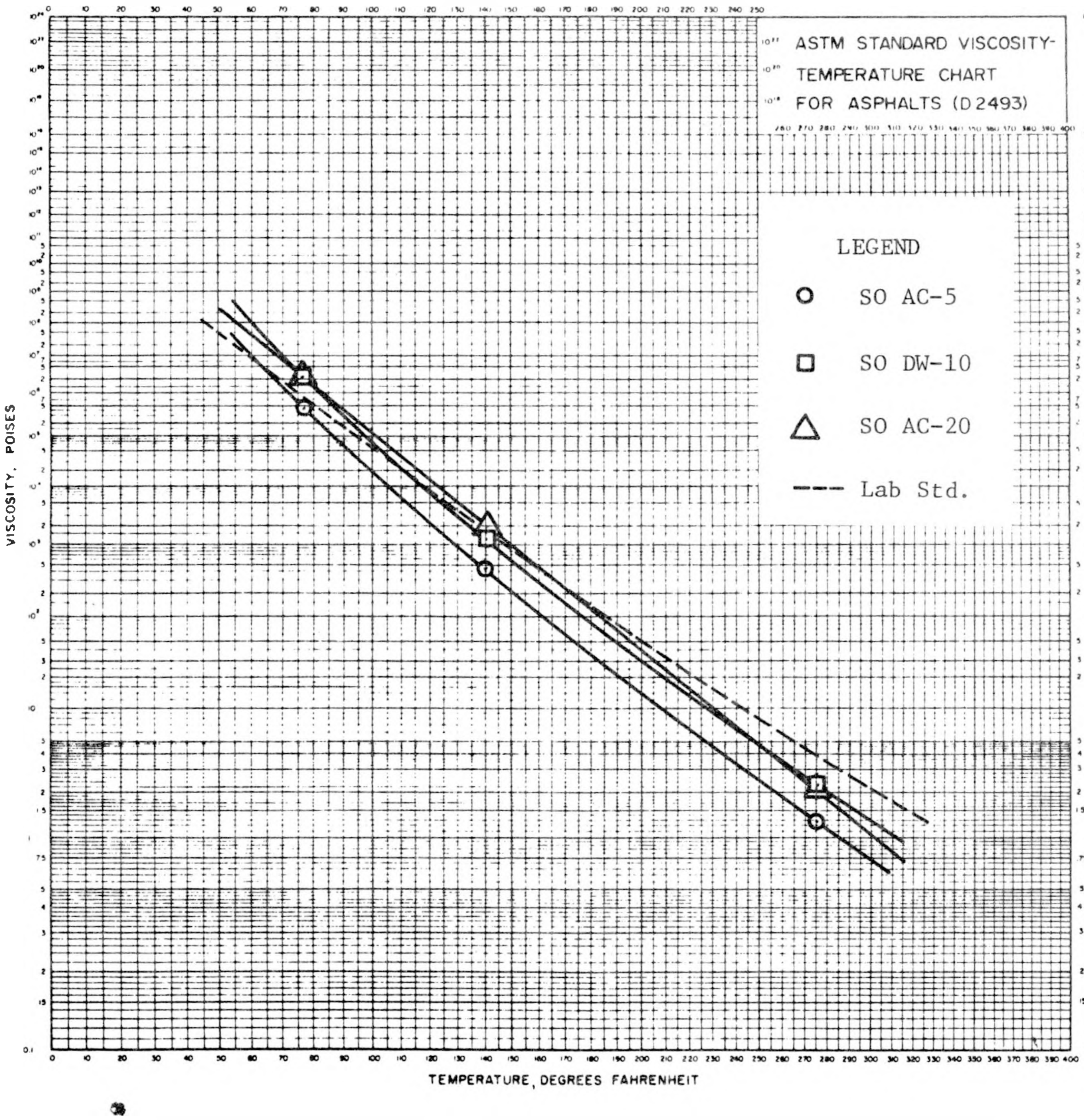

Figure 5. Viscosity of Shale Oil Asphalts as a Function of Temperature

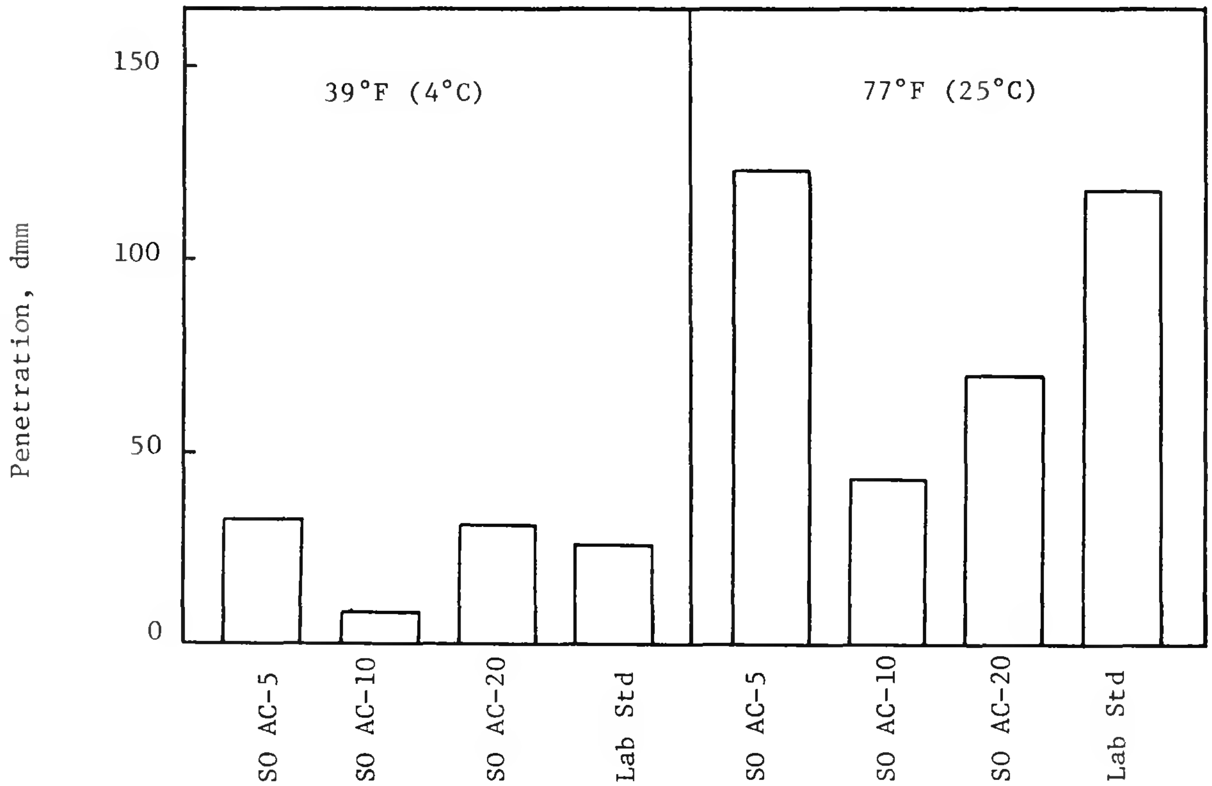

Figure 6. Penetration of Asphalt Cements at Two Temperatures

Discussion of Test Results

In review, it should be pointed out that the SO AC-20 should not be considered a "normal" asphalt primarily because of the aforementioned method of production. The addition of the distillate to the hard asphalt would introduce light hydrocarbons that would not otherwise be present in the final product. The calculated penetration index (-0.5) and penetration ratio (44%) indicate the material is a normal asphalt with a relatively low temperature susceptibility. The asphalt is, however, quite susceptible to heat damage as evidenced by its properties after the thin film oven test (Table 1). A 2% loss on heating indicates the presence of volatile materials and when they were evaporated the viscosity at 140°F (60°C) became too high to be measured with conventional test equipment while the penetration and ductility fell below specified limits for an AC-20. Also the flash point and fire point were even lower than those of SO AC-5. Further evidence of abnormality is the difference in slope of the penetration and viscosity vs. temperature plots (Figure 3) which Heukelom (6) claims to indicate an air blown (oxidized) asphalt (probably a result of "overcooking" the base asphalt during distillation). Figure 3 also indicates an abnormally high penetration index. In view of the previous discussion, it is not recommended that the results from tests on SO AC-20 be generally applied to evaluate the performance of hard shale oil asphalts.

Another relatively hard shale oil asphalt (SO AC-10), prepared using conventional techniques, was resistant to heat damage as evidenced by the properties after the thin film oven test (Table 1). The loss on heating was negligible and the ductility remained greater than 150 cm. The changes in viscosity and penetration are such as to be expected and are of the order of the corresponding changes in the laboratory standard asphalt. Overall, the properties of the SO AC-10 actually fell nearer to AC-20 specifications (2, 3), however, it was termed SO AC-10 primarily because of the viscosity at 140°F (60°C). With a penetration index of -1.9 and a penetration ratio of 19%, SO AC-10 may be described as a normal asphalt with a slightly high temperature susceptibility.

The soft shale oil asphalt (SO AC-5) possessed a temperature susceptibility in the higher temperature range almost identical to that of the SO AC-10 and SO AC-20 (Figures 1, 2 and 3) which is to be expected since they are of a common origin. The penetration index (+0.25) and the penetration ratio (26%) indicate a normal asphalt. Results from the thin film oven test indicate a durable asphalt that will resist excessive hardening during mixing and compaction.

In comparison to tests conducted by Traxler (5), the shale oil asphalts as well as the laboratory standard asphalt have very low vanadium contents. Since damage by ultraviolet light in the sun's rays apparently increases with vanadium content, these asphalts may be expected to resist surface hardening due to sunlight. This deduction is manifested by the very low hardening indices that were determined from the actinic light hardening tests.

AGGREGATE PROPERTIES

Prior to discussing the mixture properties contributed by asphalt cements the basic characteristics of the aggregates should be presented. The two types of aggregates selected for use in this research study are laboratory standard aggregates at the Texas A&M University materials laboratory (1).

The rounded, siliceous gravel was obtained from a Gifford-Hill plant near the Brazos River at College Station, Texas. A very hard crushed limestone was obtained from White's Mines at a quarry near Brownwood, Texas. Standard sieves (ASTM E-11) were used to separate the aggregates into fractions sized from 3/4 inch to minus No. 200 mesh. A photograph of the sized aggregates is shown in Figures 7 and 8. Prior to mixing with asphalt, the various aggregate sizes were recombined according to the ASTM D 3515-77 5A grading specification. The project gradation design as well as the upper and lower limits of the specifications are shown in Figure 9. Standard tests were conducted to determine various physical properties of these aggregates such as specific gravity, absorption capacity, abrasion resistance, and unit weight. One additional test (7) was conducted to estimate the optimum asphalt content.

The types of tests and results are presented in Table 2 for the rounded gravel and in Table 3 for the crushed limestone.

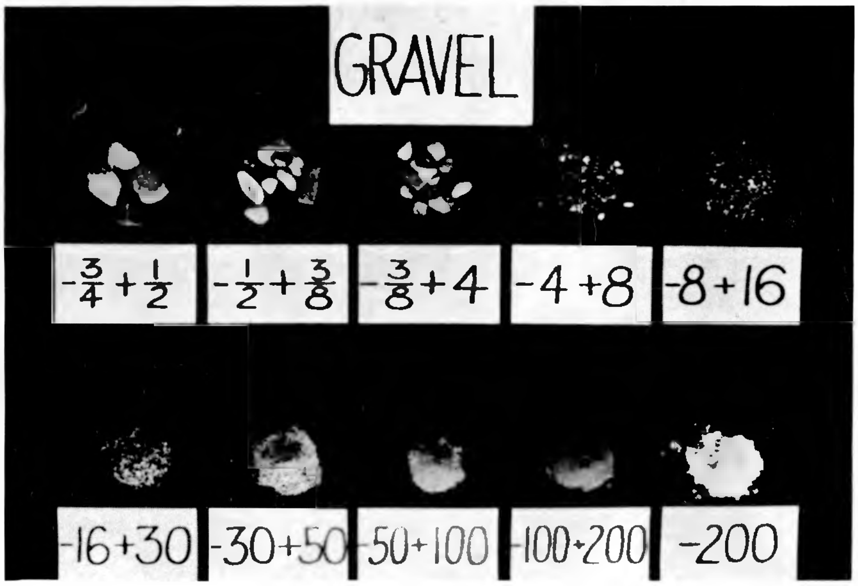

Figure 7. Rounded Gravel Aggregate Showing Size and Shape of Particles.

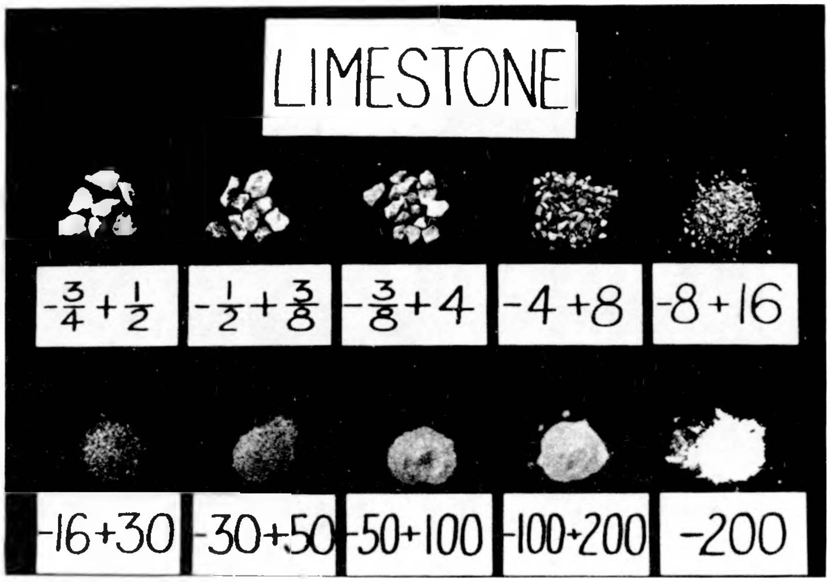

Figure 8. Crushed Limestone Aggregate Showing Size and Shape of Particles.

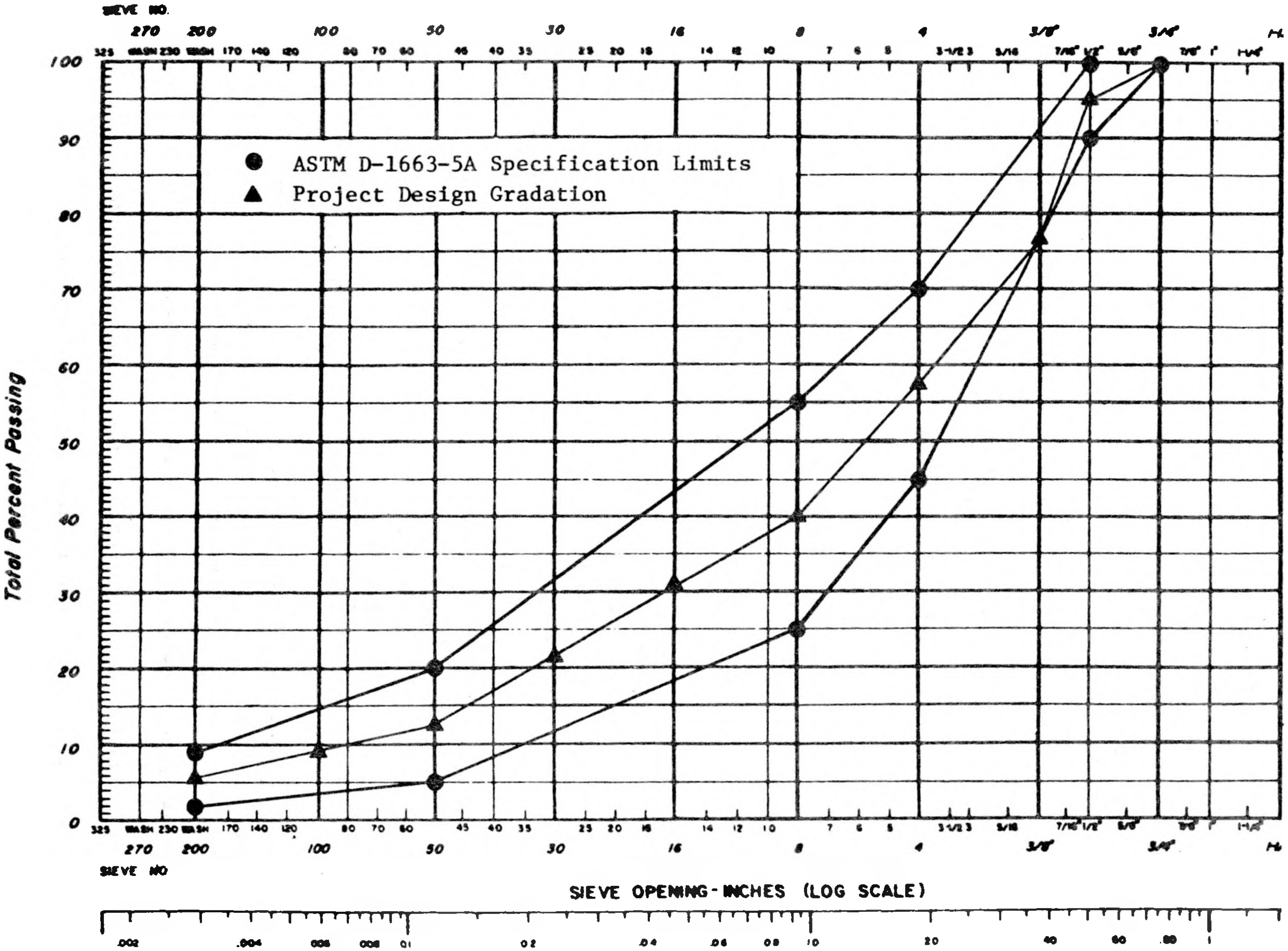

Figure 9. ASTM D-1663 - Aggregate Gradation 5A Specification and Project Gradation Design.

TABLE 2. Physical Properties of Rounded Gravel

Physical Property	Test Designation	Aggregate Grading	Test Results
Bulk Specific Gravity	ASTM C 127 AASHTO T 85	Coarse Material*	2.621
Bulk Specific Gravity (SSD)			2.640
Apparent Specific Gravity			2.672
Absorption, percent			0.72
Bulk Specific Gravity	ASTM C 218 AASHTO T 84	Fine Material**	2.551
Bulk Specific Gravity (SSD)			2.597
Apparent Specific Gravity			2.675
Absorption, percent			1.8
Bulk Specific Gravity	ASTM C 127 & C 128 AASHTO T 84 & T 85	Project Design Gradation	2.580
Apparent Specific Gravity			2.671
Absorption, percent			1.3
Abrasion Resistance, percent loss	ASTM C 131 AASHTO T 96	Grading C	19
Compacted Unit Weight, pcf	ASTM C 29 AASHTO T 19	Project Design Gradation	129
Surface Capacity, percent by wt. dry aggregate	Centifuge Kerosene Equivalent	Fine Material**	3.0
Surface Capacity, percent oil retained by wt. agg.	Oil Equivalent	-3/8 inch to + No. 4	1.8
Estimated Optimum Asphalt Content, percent by wt. dry aggregate	C.K.E. and Oil Equivalent	Project Design Gradation	4.7

* Material retained on No. 4 sieve from Project Design Gradation

**Material passing No. 4 sieve from Project Design Gradation

TABLE 3. Physical Properties of Crushed Limestone

Physical Property	Test Designation	Aggregate Grading	Test Results
Bulk Specific Gravity Bulk Specific Gravity (SSD) Apparent Specific Gravity Absorption, percent	ASTM C 127 AASHTO T 85	Coarse Material*	2.663 2.678 2.700 0.7
Bulk Specific Gravity Bulk Specific Gravity (SSD) Apparent Specific Gravity Absorption, percent	ASTM C 128 AASHTO T 84	Fine Material**	2.537 2.597 2.702 2.2
Bulk Specific Gravity Apparent Specific Gravity Absorption, percent	ASTM C 127 & C 128 AASHTO T 84 & T 85	Project Design Gradation	2.589 2.701 1.56
Abrasion Resistance, percent loss	ASTM C 131 AASHTO T 96	Grading C	23
Compacted Unit Weight, pcf	ASTM C 29 AASHTO T 19	Project Design Gradation	122
Surface Capacity, percent by wt. dry aggregate	Centrifuge Kerosene Equivalent	Fine Material**	4.1
Surface Capacity, percent by wt. dry aggregate	Oil Equivalent	-3/8 inch to + No. 4	2.3
Estimated Optimum Asphalt Content, percent by wt. dry aggregate	C.K.E. and Oil Equivalent	Project Design Gradation	5.5

*Material retained on No. 4 sieve from Project Design Gradation

**Material passing No. 4 sieve from Project Design Gradation

DETERMINATION OF OPTIMUM ASPHALT CONTENT

General

One of the first steps in producing asphalt-aggregate mixtures for paving purposes is to determine the optimum asphalt content. The optimum asphalt content for each of the two laboratory standard aggregates was determined using the laboratory standard asphalt. Then the identical asphalt content was used when mixing each of the shale oil asphalts with these aggregates, although some design procedures would indicate somewhat different optimums for different viscosities of binder. Determination of optimum asphalt content was accomplished in accordance with the test program shown by the flow chart in Figure 10.

Mixing of Laboratory Standard Asphalt with Aggregate

As mentioned earlier, the various aggregate fractions were recombined to meet specifications. The mixing and compacting temperatures for the asphalt-aggregate mixtures were determined to be 305 ± 5°F (152°C) and 283 ± 5°F (140°C), respectively, by using the test procedure described in ASTM D 1559. (The procedure requires mixing at the temperature that produces an asphalt viscosity of 170 ± 20 centistokes and compacting at the temperature then produces an asphalt viscosity of 280 ± 30 centistokes kinematic). Prior to mixing with asphalt cement, the aggregates were heated a minimum of four hours at 305 ± 5°F. The asphalt cement was heated in the same oven a minimum of 3/4 hour and a maximum of 2 hours. The appropriate quantity of asphalt cement was added to the heated aggregate then the mixture was blended in a mechanical mixer while heat was applied using a Bunsen burner. When blending was completed (all aggregate particles coated with asphalt cement), the mixture was carefully divided into three aliquots of predetermined weight and placed in an oven of appropriate compaction temperature. The mixing and batching operation was completed in approximately four minutes. A data summary of the asphalt-aggregate mixtures is presented in Table 4.

Marshall Compaction and Testing

Compaction and testing were conducted in accordance with ASTM D 1559, "Resistance to Plastic Flow of Bituminous Mixtures Using Marshall Apparatus". As soon as the temperature of each batch reached 283 ± 5°F (140°C), each was compacted by applying 50 blows to each face of the specimen. When the specimens were sufficiently cool (less than 140°F) they were extruded from the molds. The weight and height of each specimen was accurately measured. The 4-inch (10.2 cm) diamter specimens are approximatley 1200 grams in

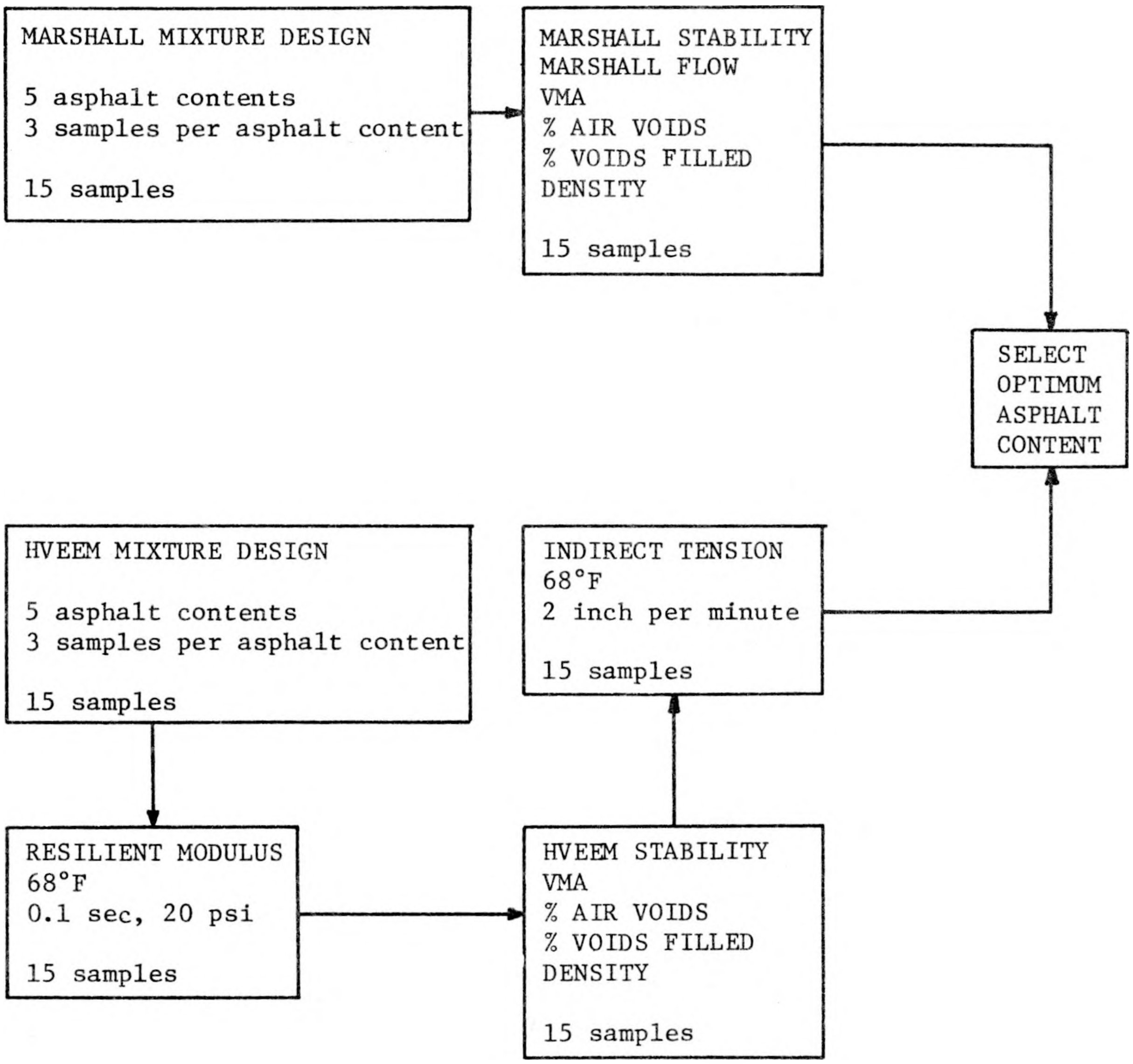

Figure 10. Test Program for Determination of Optimum Asphalt Content

TABLE 4. Data Summary of Asphalt-Aggregate Mixtures

Asphalt Content, percent by wt. aggregate	2.5	3.0	3.5	4.0	4.5	5.0	5.5	6.0
Asphalt Content, percent by wt. total mix	2.4	2.9	3.4	3.9	4.3	4.8	5.2	5.7
Coarse Aggregate, percent by wt. total mix	41.5	41.3	41.1	40.9	40.7	40.5	40.3	40.1
Fine Aggregate, percent by wt. total mix	50.7	50.5	50.2	50.0	49.8	49.5	49.3	49.1
Mineral Filler, percent by wt. total mix	5.4	5.3	5.3	5.3	5.3	5.2	5.2	5.2
Total Aggregate, percent by wt. total mix	97.6	97.1	96.6	96.2	95.7	95.2	94.8	94.3

in weight and 2.5-inches (6.4 cm) in height. The bulk specific gravity of each specimen was determined in accordance with ASTM D 2726 "Bulk Specific Gravity of Compacted Bituminous Mixtures Using Saturated Surface-Dry Specimens". Marshall stability tests were conducted on the day following compaction of the test specimens. Some of the previously failed specimens were reheated and finely divided in order to determine the maximum specific gravity of the mixture in accordance with ASTM D 2041 "Maximum Specific Gravity of Bituminous Paving Mixtures".

The Marshall compaction tests were accomplished as an aid to the determination of the optimum asphalt cement content for the given aggregate gradation. A summary of the test results for the Marshall Specimens is presented in Appendix A. Each value in the figures and tables represents an average for three tests unless otherwise indicated.

Gyratory Compaction and Testing

The aggregate gradation, asphalt, and mixing procedure used in making the gyratory compacted specimens were identical to those used in making the Marshall specimens. However, compaction (Figure 11) was conducted in accordance with Texas State Department of Highways and Public Transportation test method TEX-206-F, Part II, "Motorized Gyratory-Shear Molding Press Operating Procedure" (4).

Upon completion of mixing, each batch was placed in an oven and as soon as the required temperature was attained the mixtures were compacted. This test method required a compaction temperature of 250 ± 5°F (121°C) for all asphalt-aggregate mixtures. When the specimens were sufficiently cool, the weight and height of each was accurately determined. These 4-inch (10.2 cm) diameter specimens were approximately 1000 grams in weight and 2-inches (5.1 cm) in height. The bulk specific gravity of each specimen was determined in accordance with ASTM D 2726.

On the day following compaction the resilient modulus, M_R (a measure of stiffness), was determined for each specimen at 68°F (20°C) using the Mark III Resilient Modulus Device (Figures 12 and 13) developed by Schmidt (8). A diametral load of approximately 72 lbs (33 kg) was applied for a duration of 0.1 seconds while monitoring the lateral deformation in accordance with Schmidt (9).

The Hveem stability of the specimens was determined in accordance with the Texas State Department of Highways and Public Transportation test method TEX-208-F "Test for Stabilometer Value of Bituminous Mixtures", which is a modification of ASTM D 1560.

The final test performed on these specimens was the splitting tensile test (indirect tension), which is described in detail by Hadley, Hudson,

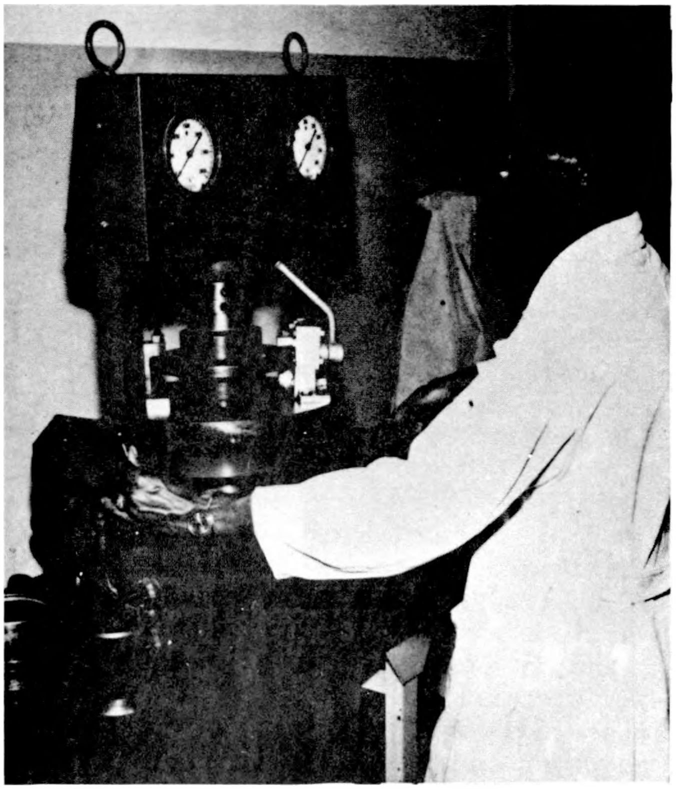

Figure 11. Gyratory Molding Press Used to Compact 2-inch Test Specimens

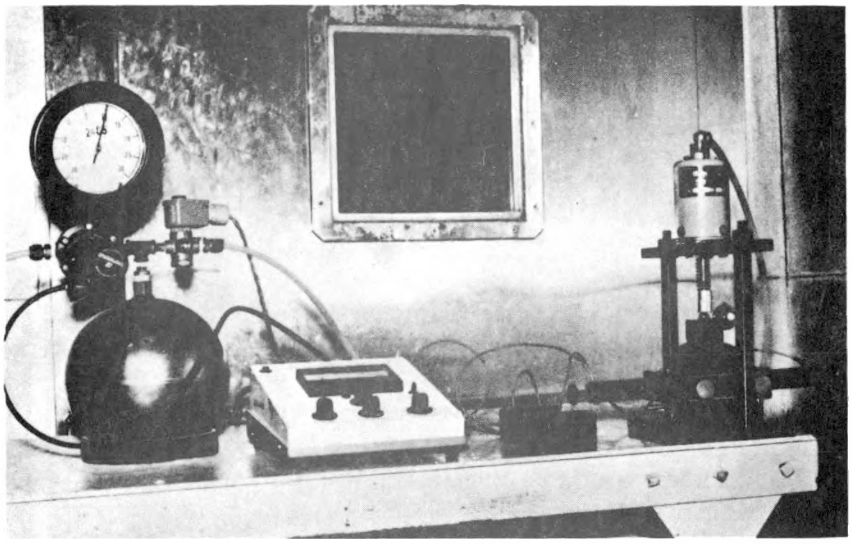

Figure 12. Overall View of Mark III Resilient Device

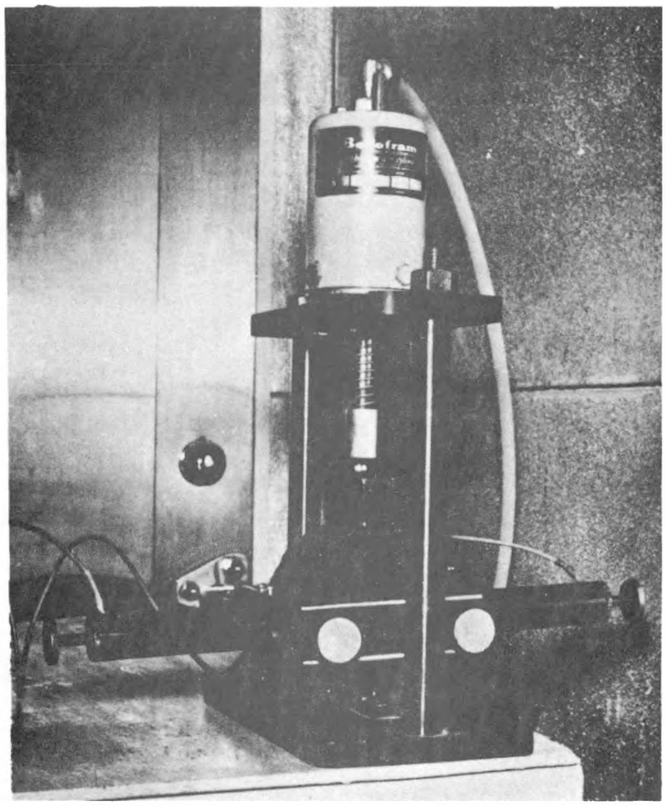

Figure 13. Close-up View of Loading Frame and Transducers

and Kennedy (10). The splitting tensile test (Figure 14 and 15) was conducted at 68°F (20°C) with a loading rate of 2-inches per minute. Stress, strain and modulus of elasticity were computed for each specimen at the point of failure using a value of 0.35 for Poisson's ratio. A summary of the test results for the Hveem specimens is given in Appendix B, where each value in the figures and tables represents an average of three tests.

Optimum Asphalt Content

The optimum asphalt cement content was selected for both types of aggregate to be used in all mixtures for further testing and evaluation of shale oil asphalts. The selection was based primarily on the results of the test series conducted on the Marshall specimens using the mixture design selection procedures described by the Asphalt Institute (11). However, the results of the test series conducted on the Hveem specimens and engineering judgement also entered into the final selection. The properties of the mixtures using rounded gravel and crushed limestone at optimum asphalt content are given in Table 5.

It should be noted that some of the properties of the compacted mixtures at optimum asphalt content did not meet the criteria established by the Asphalt Institute (11). For example, considering the rounded gravel mixtures, the average values for Marshall flow, air void content, VMA and Hveem stability were less than those specified. Considering the crushed limestone mixtures, the average values for air void content and VMA were also less than specified. The action of traffic on an asphalt concrete pavement with qualities such as those mentioned above is likely to display plastic instability or, possibly flushing after a period of time. Undoubtedly, the quality of these mixtures could have been improved by adjusting the aggregate gradation and/or the asphalt content. However, since these mixtures were to be used as laboratory standards for test comparisons and not highway paving, no attempt was made to further adjust the mixture design.

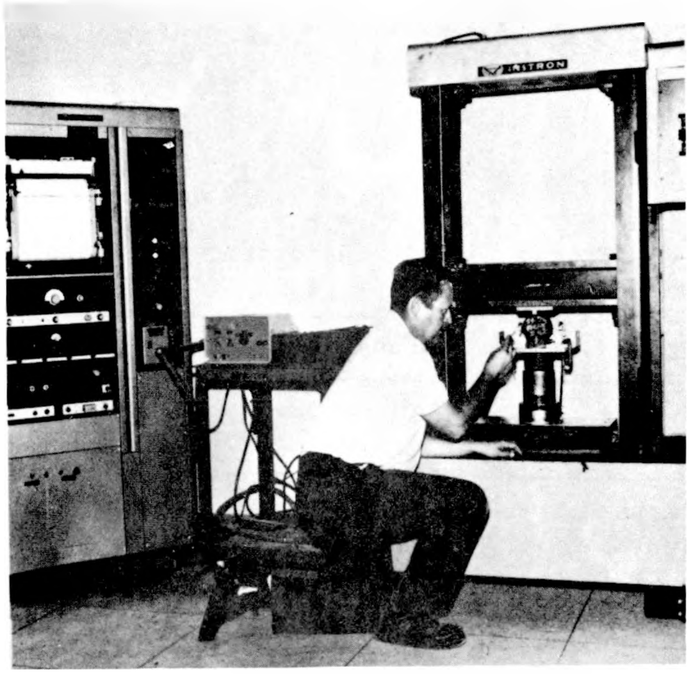

Figure 14. Splitting Tensile Tester

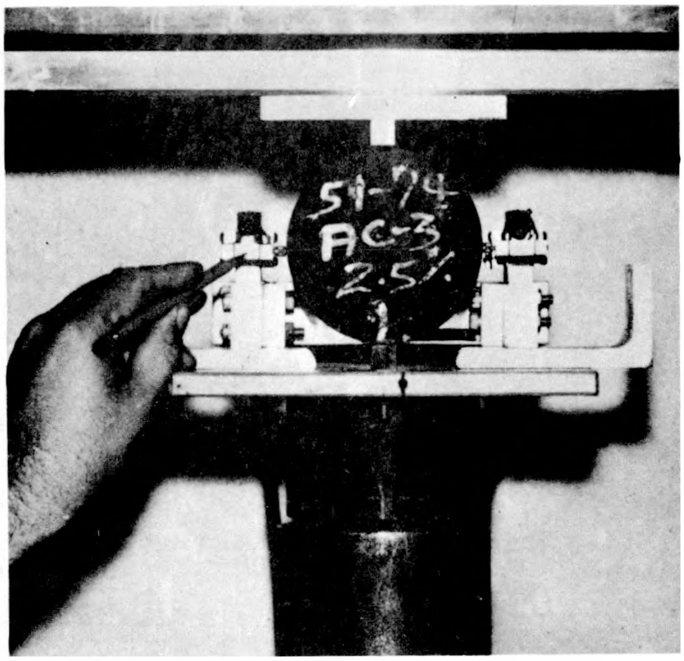

Figure 15. Specimen in Test Frame of Splitting Tensile Tester

TABLE 5. Mixture Properties with Laboratory Standard Asphalt at Optimum Asphalt Content

Property	Rounded Gravel	Crushed Limestone
Design Asphalt Content, percent by wt. aggregate	3.8	4.5
Marshall Specimens		
Unit Weight, pcf	152	153
Air Void Content, percent	2.1	3.0
VMA, percent	9.1	10.5
VMA Filled w/Asphalt, percent	80	78
Marshall Stability, lbs	1270	2740
Marshall Flow, .01 inch	7	11
Hveem Specimens		
Unit Weight, pcf	151	154
Air Void Content, percent	2.9	2.5
VMA, percent	9.7	9.1
VMA Filled w/Asphalt, percent	76	81
Hveem Stability, percent	25	54
Resilient Modulus, psi	570,000	590,000
Elastic Modulus, @ Failure *	39,000	26,000

* From Splitting Tensile Test

Test Results on Gyratory Compacted Specimens

Table 6 presents the basic physical properties of the gyratory compacted specimens. The test sequence performed on the gyratory compacted specimens is presented in the flow chart in Figure 16 and is discussed in the following four paragraphs.

Resilient Modulus. Using the optimum asphalt contents previously determined for each of the aggregates, thirty specimens of each of the eight asphalt-aggregate mixtures (4 asphalts with 2 aggregates) were compacted in accordance with test method TEX-206-F. The resilient modulus of each of these specimens was measured at 68°F (20°C) using the Schmidt device as described before and the results for the individual specimens are tabulated in Appendix C. To provide a comparison, resilient moduli at 73°F (23°C) for various types of asphalt-aggregate mixtures are indcluded in Appendix C. Summarized statistical information on these data are given in Table 7 and the mean resilient moduli of the different mixtures are presented in the bar graph of Figure 17.

Tensile Strength. Twenty-seven of the thirty specimens were selected and divided into three groups of nine each and conditioned at temperatures of -13, 33, 68°F (-25, 1, 20°C respectively). Then they were subdivided into groups of three each and the splitting tensile test was conducted at loading head displacement rates of 2, 0.2, 0.02 inches per minute (5.1, 0.51, 0.051 cm/min). A computer program with a plotting subroutine was used to reduce the data. Typical stripcharts showing raw data, sketches of plots, test results for each specimen and plots of the summarized data are presented in Appendix D. A summary of the test results is presented in Table 8 where each value represents an average of three values, unless otherwise indicated by the number in parentheses.

Recovered Asphalt Properties. Following the splitting tensile test, certain specimens were selected for extraction and recovery of each of the asphalt cements. Extraction was conducted in accordance with ASTM D 2172-75 (Method B). Recovery was conducted using a special method as described in Appendix E. Penetration at 77°F (25°C), viscosity at 77°F (25°C) and 140°F (60°C) and ring and ball softening point were measured to quantify any asphalt hardening that may have taken place during the mixing and compacting procedures. The properties of the asphalts recovered from gravel and limestone are given in Table 9.

Resilient Modulus and Water Susceptibility. The remaining three specimens of the original thirty were tested to determine whether or not the asphalts were susceptible to damage by water. The resilient modulus of the specimens was measured at -13, 33, 68, 77 and 104°F (-25, 1, 20, 25

TABLE 6. Basic Physical Properties of Gyratory Compacted Specimens*

Type of Aggregate	Rounded Gravel				Crushed Limestone			
Type of Asphalt Cement	Lab. Std.	SO AC-5	SO AC-10	SO AC-20	Lab. Std.	SO AC-5	SO AC-10	SO AC-20
Bulk Specific Gravity of Compacted Mix	2.43	2.40	2.42	2.42	2.42	2.45	2.45	2.46
Maximum Specific Gravity of Mixture	2.50	2.51	2.50	2.50	2.51	2.50	2.52	2.51
Asphalt Absorption, percent by wt. agg.	1.0	1.2	0.91	0.91	1.6	1.3	1.6	1.3
Effective Asphalt Content, percent total mix	2.7	2.5	2.8	2.8	2.8	3.1	2.8	3.0
Voids in Mineral Aggregate, percent bulk volume	9.3	10.4	9.6	9.6	10.6	9.5	9.5	9.1
Air Void Content, percent total volume	2.8	4.4	3.2	3.2	3.6	2.0	2.8	2.0
VMA Filled with Asphalt, percent VMA	76	67	73	73	74	84	79	84

*Each value represents an average of thirty specimens.

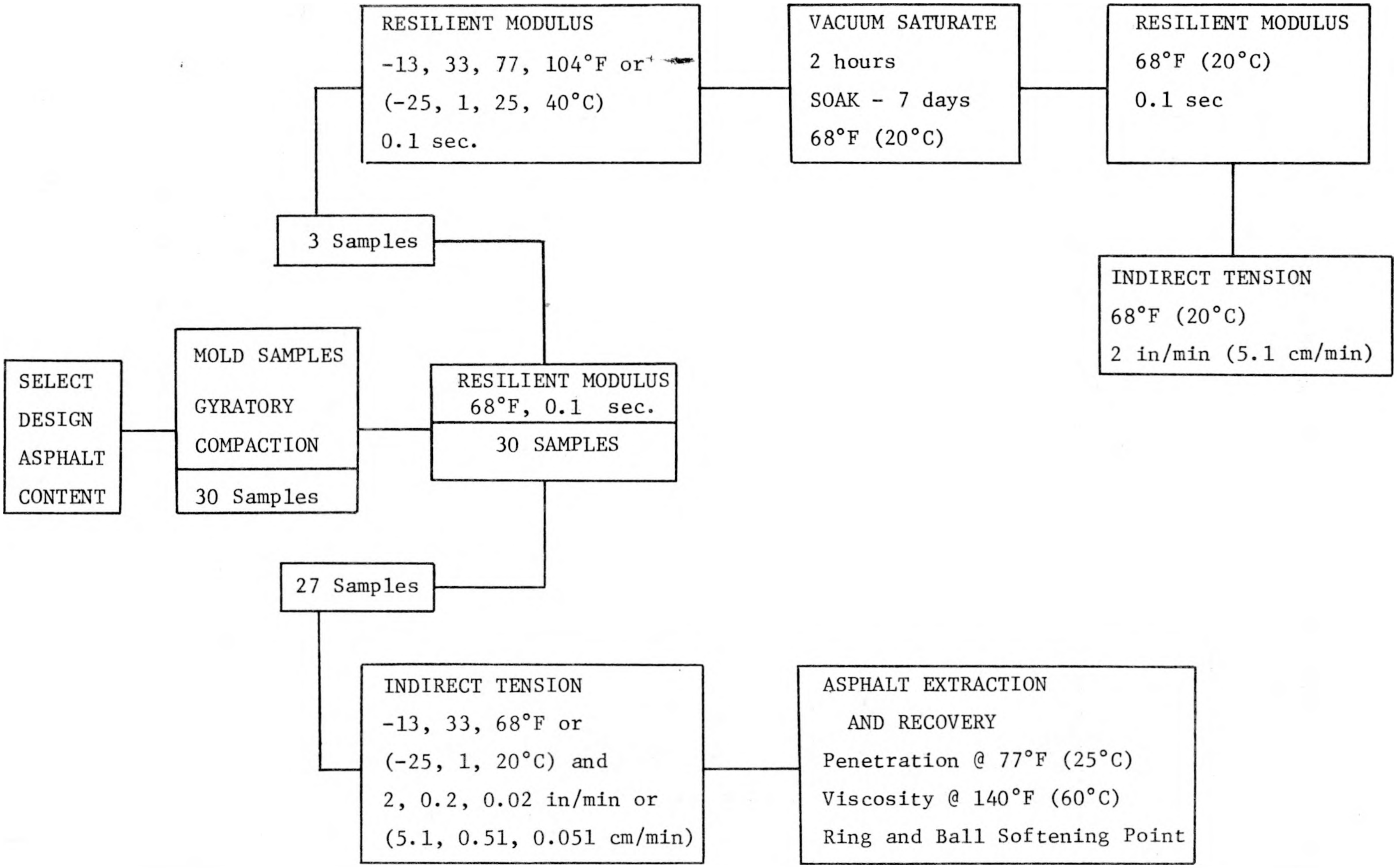

Figure 16. Test Program to Determine Strength and Water Susceptibility of Mixes

TABLE 7. Simple Statistics of Resilient Modulus or Gyratory Compacted Specimens at 68°F (20°C)

Aggregate	Asphalt	Mean psi x 10^{-6} (KPa x 10^{-6})	Standard Deviation, psi x 10^{-6} (KPa x 10^{-6})	Coefficient of Variation, percent
Gravel	Lab Std	0.52 (3.55)	0.06 (.414)	12
	SO AC-5	0.95 (6.55)	0.16 (1.13)	17
	SO AC-10	1.88 (13.0)	0.16 (1.07)	8
	SO AC-20	1.23 (8.47)	0.19 (1.31)	16
Limestone	Lab Std	0.72 (4.98)	0.10 (0.69)	14
	SO AC-5	1.06 (7.35)	0.11 (0.73)	10
	SO AC-10	1.95 (13.4)	0.21 (1.47)	11
	SO AC-20	1.42 (9.79)	0.15 (1.04)	11

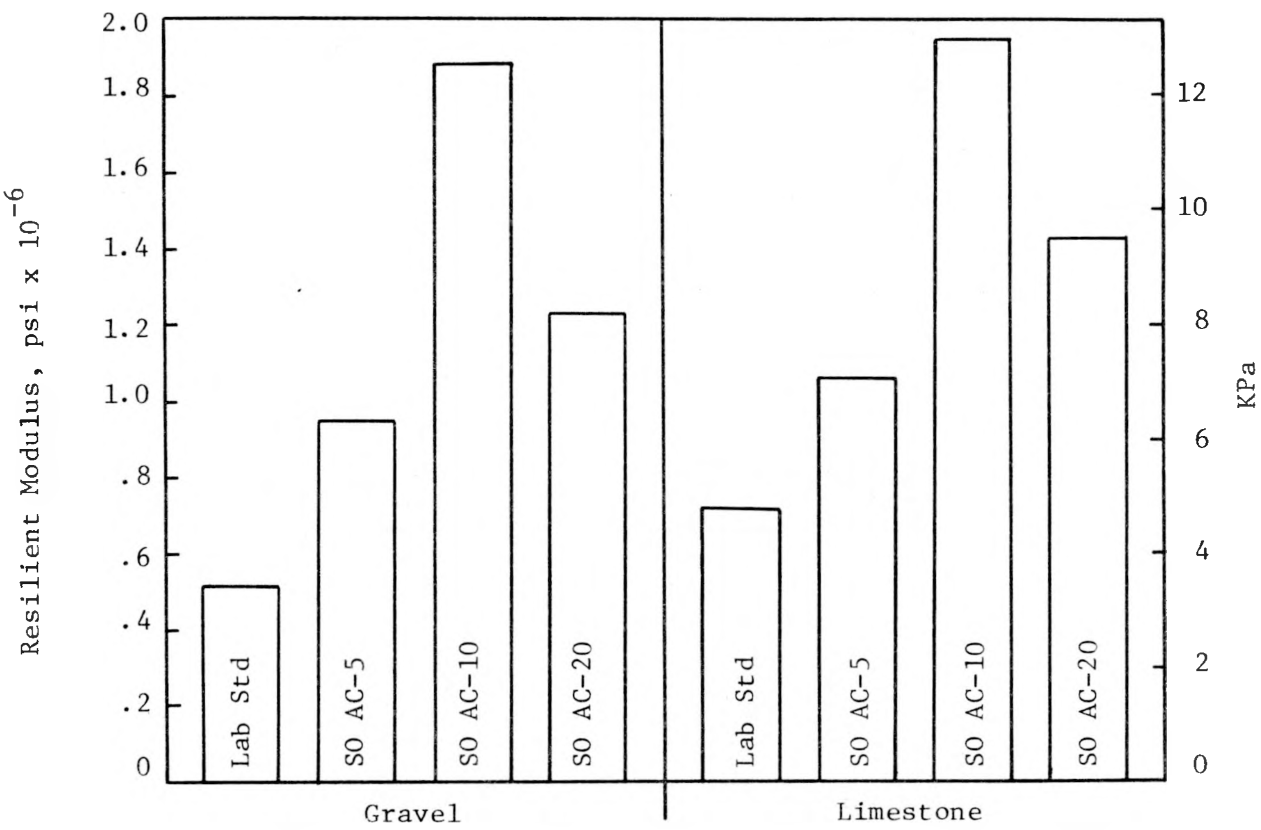

Figure 17. Mean Resilient Modulus of All Test Specimens

TABLE 8. Summary of Splitting Tensile Test Data.

Aggregate	Displacement Rate in/min (cm/min)	Temperature °F (°C)	Lab Standard			SO AC-5			SO AC-10			SO AC-20		
			Stress, psi	Strain, in/in	Modulus, psi	Stress, psi	Strain, in/in	Modulus, psi	Stress, psi	Strain, in/in	Modulus, psi	Stress, psi	Strain, in/in	Modulus, psi
Gravel	2.0 (5.1)	68 (20)	110	0.0029	38,000	140	0.0026	58,000	310	0.0038	82,000	160	0.0025	75,000
		33 (1)	390	0.0027	170,000	410	0.0013	354,000	450	0.0007	984,000	400	0.0009	470,000
		-13 (-25)	490	0.0012	418,000	360	0.0006	625,000	340	0.0004	1,042,000	370	0.0006	668,000
	Soak	68 (20)	100	0.0050	21,000	200	0.0026	76,000	200	0.0038	55,000	230	0.0020	114,000
	0.2 (0.51)	68 (20)	50	0.0043	12,000	80	0.0032	25,000	230	0.0032	87,000	100	0.0023	46,000
		33 (1)	250	0.0020	130,000	380	0.0018	212,000	400	0.0016	257,000	300	0.0014	232,000
		-13 (-25)	380	0.0009	498,000	460	0.0008	578,000	370	0.0009	457,000	430	0.0009	519,000
	0.02 (0.051)	68 (20)	20	0.0041	5,000	30	0.0037	9,000	80	0.0048	18,000	60	0.0022	30,000
		33 (1)	110	0.0018	59,000	110	0.0021	61,000	250(2)	0.0024(2)	102,000(2)	340	0.0011	348,000
		-13 (-25)	340	0.0012(2)	331,000(2)	270	0.0011	246,000	390(1)	0.0014(1)	271,000(1)	410	0.0011	385,000
Limestone	2.0 (5.1)	68 (20)	150	0.0025	60,000	130	0.0023	69,000	250	0.0029	89,000	150	0.0017	94,000
		33 (1)	520	0.0018	290,000	480(2)	0.0011(2)	462,000(2)	590	0.0006	1,089,000	500	0.0011	479,000
		-13 (-25)	630(2)	0.0012(2)	553,000(2)	500	0.0011	553,000	470	0.0005	955,000	590	0.0010	598,000
	Soak	68 (20)	90	0.0059	16,000	120	0.0038	32,000	190	0.0031	63,000	240	0.0022	109,000
	0.2 (0.51)	68 (20)	90	0.0041	23,000	70	0.0034	19,000	270	0.0030	97,000	120	0.0017(2)	70,000(2)
		33 (1)	310	0.0022	150,000	420	0.0013	337,000	490	0.0014	361,000	400	0.0014	280,000
		-13 (-25)	630	0.0030(2)	226,000(2)	540	0.0012	479,000	470	0.0011	456,000	600	0.0012	500,000
	0.02 (0.051)	68 (20)	40	0.0040	11,000	40	0.0028	12,000	90	0.0042	21,000	70	0.0023	32,000
		33 (1)	140	0.0021	70,000	470	0.0014	340,000	380(2)	0.0020(2)	200,000(2)	200	0.0017	120,000
		-13 (-25)	410	0.0030	156,000	500	0.0011	481,000	480(2)	0.0024(2)	205,000(2)	570	0.0013	462,000

*All values measured at the point of failure
English to Metric Conversion: 1 psi = 6.895 x 10^3 pascals

TABLE 9. Recovered Asphalt Properties

Aggregate	Test	Lab. Std.	SO AC-5	SO AC-10	SO AC-20
Extracted from Gravel	Penetration @ 77°F, dmm	55	46	19	30
	Viscosity @ 77°F, poise	3.9×10^6	2.8×10^6	2.3×10^7	2.0×10^7
	Viscosity @ 140°F, poise	4630	1430	8810	33,000
	R&B Softening Point, °F (°C)	129 (54)	122 (57)	134 (57)	152 (67)
Extracted from Limestone	Penetration @ 77°F, dmm	53	50	17	35
	Viscosity @ 77°F, poise	3.8×10^6	3.2×10^6	2.4×10^7	1.5×10^7
	Viscosity @ 140°F, poise	4320	1520	8010	13,100
	R&B Softening Point, °F (°C)	128 (54)	120 (49)	136 (58)	141 (61)

and 40°C) using a load of approximately 72 pounds (33 kg) for a duration of 0.1 seconds (Figures 18 and 19). Then the specimens were submerged in water and vacuum saturated (Figure 20) at approximately one inch (25 mm) of mercury (absolute pressure) for two hours and allowed to soak at atmospheric pressure for seven days. After soaking, while still in the saturated condition, the resilient modulus of each specimen was again measured at 68°F then the splitting tensile test was conducted at 68°F and two inches per minute (5.08 cm/min). Resilient moduli from these tests are tabulated in Appendix F. (Due to an error in testing sequence the resilient modulus of the original specimens containing SO AC-5 and SO AC-20 was not measured at -13, 33, 77 and 104°F (-25, 1, 25 and 40°C) however, similar specimens were fabricated and tested to fill in this gap in the data. These specimens are recognizable in Tables F1 and F2 by observing the sample numbers. The splitting tensile test data are included in Appendix D (Table D9). A summary of these data is given in Tables 10 and 11 where each value represents an average of three values. Figures 21 through 26 are bar graphs showing comparisons of mixture characteristics before and after soaking in water.

Test Results on Marshall Compacted Specimens

This test sequence (Figure 27) was performed primarily to determine the compactibility and stability of mixtures containing shale oil asphalt and to afford a direct comparison of Marshall specimens containing shale oil asphalt cement with Marshall specimens containing the laboratory standard asphalt cement as discussed in the section entitled Optimum Asphalt Content.

Mixing at the optimum asphalt contents, each of the three shale oil asphalts were combined with the two laboratory standard aggregates to prepare Marshall specimens by applying fifty blows to each face of the specimens. After determining the dimensions and density of each specimen, the resilient modulus was determined at 68°F (20°C) using a load of approximately 72 lbs (33 kg) for a duration of 0.1 sec.

The Marshall stability test was then conducted in accordance with ASTM D 1559. The test results for the Marshall compacted specimens is presented in Table 12.

Discussion of Laboratory Test Results

Gyratory Compacted Specimens. The resilient modulus (Table 7), which is a measure of stiffness, indicates the order of stiffness of the asphalt mixtures is the same for mixtures containing gravel and limestone. The order from low to high follows: laboratory standard, SO AC-5, SO AC-20 and SO AC-10. From the original asphalt properties, SO AC-10 and SO AC-20

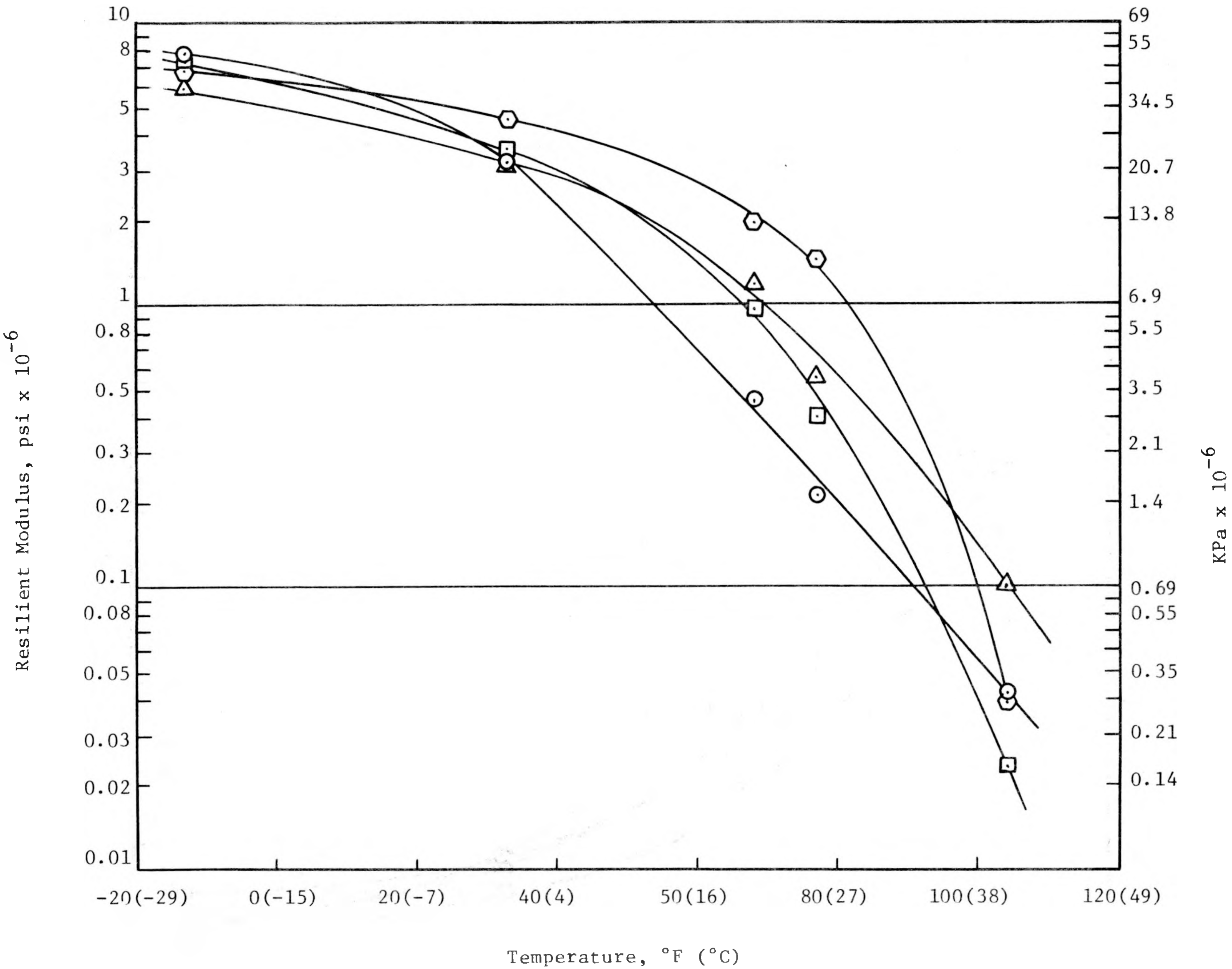

Figure 18. Resilient Modulus of Water Susceptibility Specimens of Gravel as a Function of Temperature

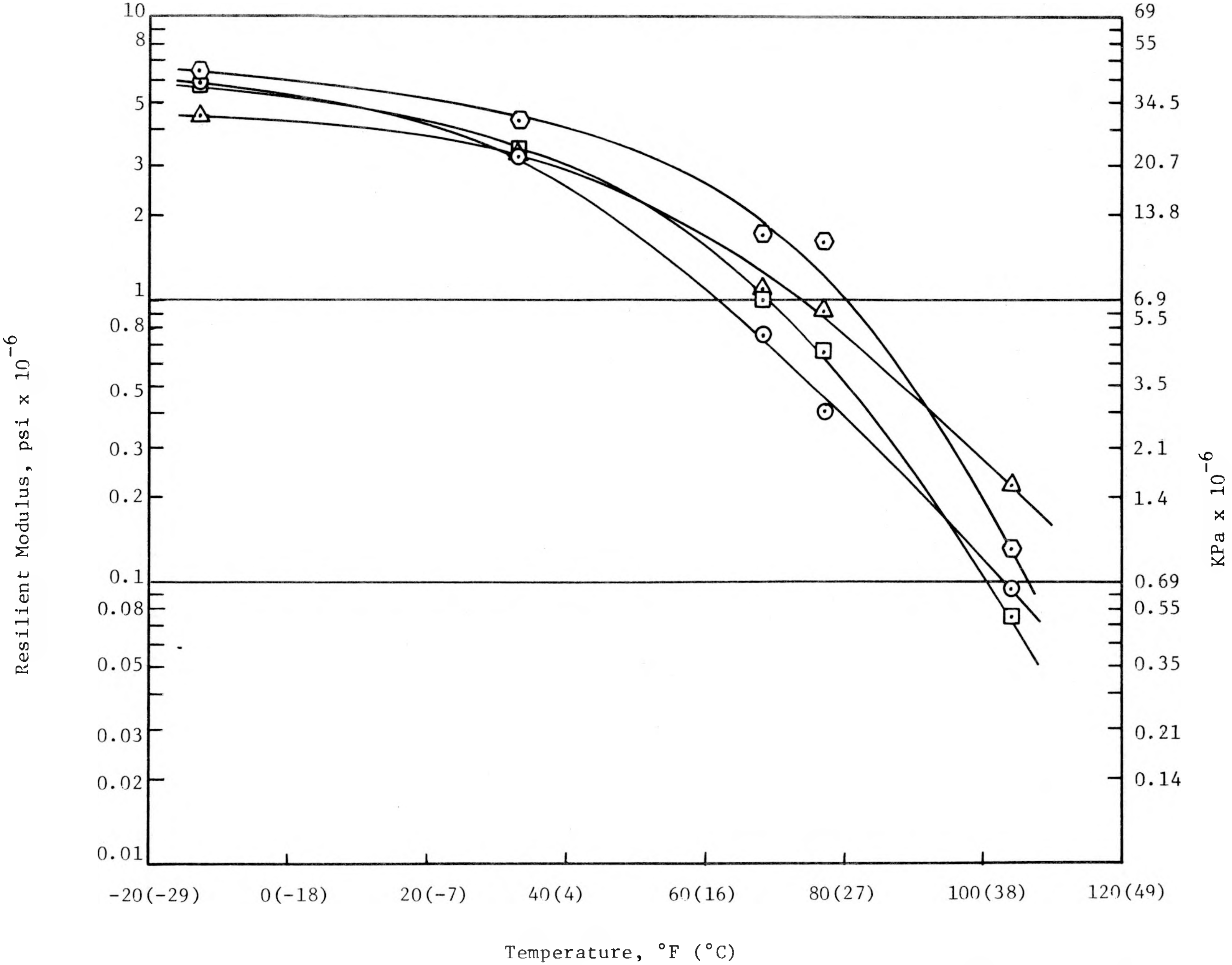

Figure 19. Resilient Modulus of Water Susceptibility Specimens of Limestone as a Function of Temperature

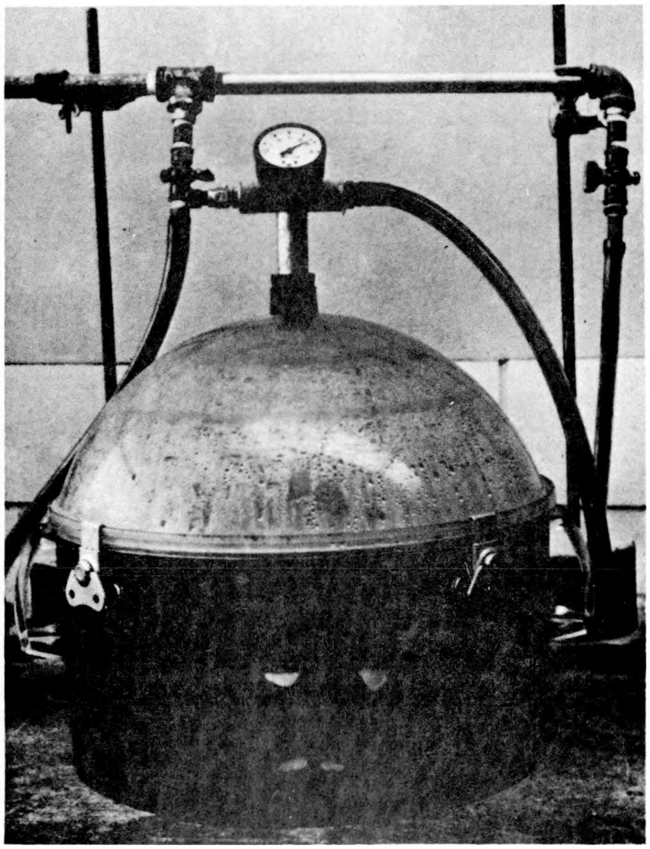

Figure 20. Apparatus Used for Vacuum Saturation and Soaking of Asphalt Concrete Specimens

Table 10. Average Resilient Moduli of Water Susceptibility Specimens Prior to Soaking*

Aggregate	Asphalt	Resilient Modulus, psi x 10^{-6} (KPa x 10^{-6})				
		-13°F (-25°C)	33°F (1°C)	68°F (20°C)	77°F (25°C)	104°F (40°C)
Gravel	Lab Std	7.83 (53.9)	3.19 (21.9)	0.45 (3.1)	0.21 (1.4)	0.042 (.29)
	SO AC-5	7.47 (51.5)	3.47 (23.9)	0.96 (6.60)	0.40 (2.8)	0.023 (0.16)
	SO AC-10	6.80 (46.8)	4.50 (31.6)	1.92 (13.2)	1.41 (9.7)	0.039 (0.27)
	SO AC-20	5.83 (40.2)	3.19 (21.9)	1.19 (8.18)	0.55 (3.8)	0.10 (0.69)
Limestone	Lab Std	5.79 (39.9)	3.17 (21.9)	0.75 (5.2)	0.40 (2.8)	0.093 (0.64)
	SO AC-5	5.77 (39.8)	3.39 (23.4)	1.00 (6.9)	0.66 (2.8)	0.074 (.51)
	SO AC-10	6.28 (43.3)	4.29 (29.6)	1.67 (11.5)	1.61 (11.1)	0.13 (.89)
	SO AC-20	4.44 (30.6)	3.31 (22.3)	1.13 (9.1)	0.92 (6.3)	0.22 (1.5)

*Each value is an average of three values.

TABLE 11. Summary of Data From Water Susceptibility Study*

Agg.	Asphalt	Res. Mod. Before Soaking psi x 10^6 (KPa x 10^6)	Res. Mod. After Soaking psi x 10^6 (KPa x 10^6)	Tensile Stress @ Failure** psi (KPa)	Tensile Strain @ Failure** in/in or cm/cm	Elastic Modulus @ Failure** psi (KPa)
Gravel	Lab Std	0.46 (3.17)	0.30 (2.07)	100 (660)	0.0054	19,000 (1.27×10^5)
	SO AC-5	1.07 (7.38)	1.10 (7.58)	200 (1360)	0.0026	76,000 (5.22×10^5)
	SO AC-10	1.93 (13.3)	1.17 (8.06)	200 (1360)	0.0038	55,000 (3.79×10^5)
	SO AC-20	1.50 (10.3)	1.64 (11.3)	230 (1570)	0.0020	114,000 (7.83×10^5)
Limestone	Lab Std	0.75 (5.17)	0.45 (3.10)	90 (610)	0.0059	16,000 (1.11×10^5)
	SO AC-5	0.94 (6.48)	1.02 (7.03)	120 (840)	0.0038	32,000 (2.23×10^5)
	SO AC-10	1.67 (1.15)	1.22 (8.41)	190 (1290)	0.0031	63,000 (4.34×10^5)
	SO AC-20	1.51 (10.4)	1.42 (9.79)	240 (1660)	0.0022	109,000 (7.53×10^5)

*Each value is an average of three values at 68°F (20°C).

**From splitting tensile tests at 68°F (20°C) and 2 in/min (5.1 cm/min) after 7 day soak.

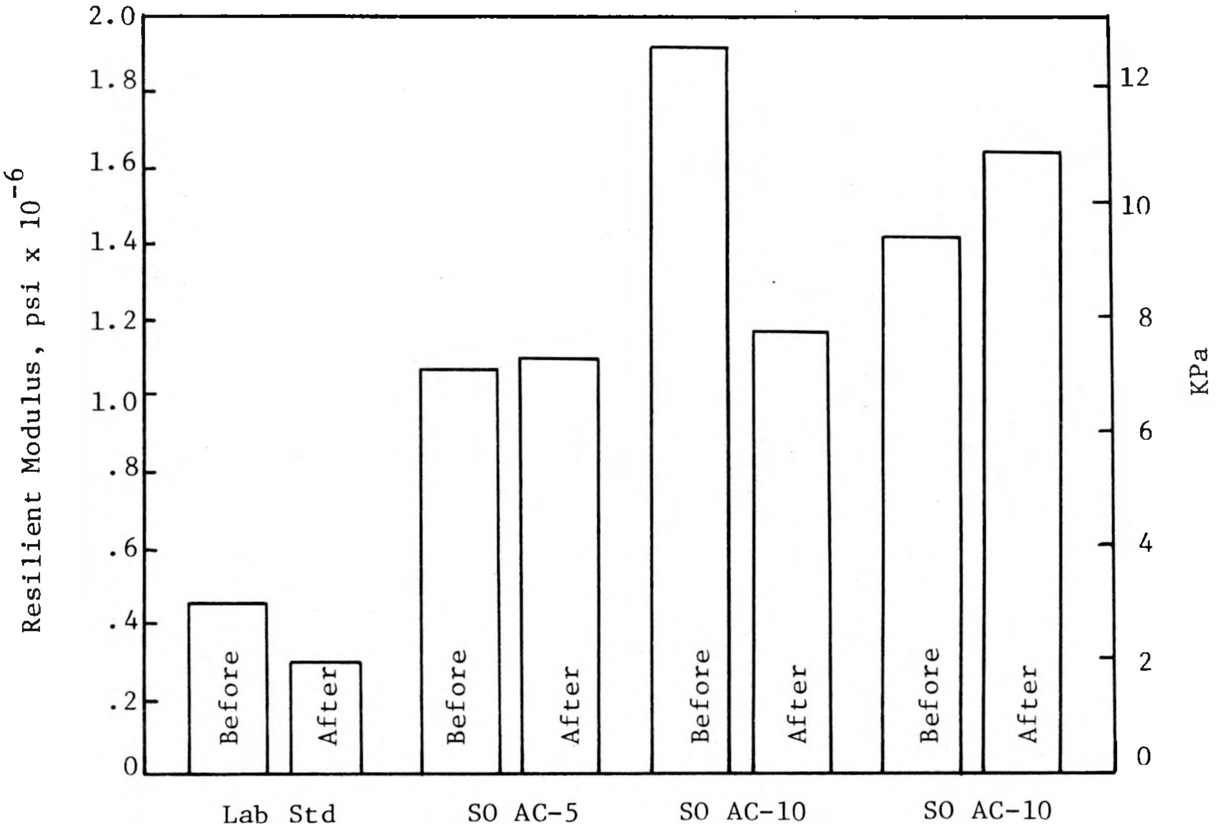

Figure 21. Resilient Modulus at 68°F (20°C) of Gravel Specimens Before and After Soaking

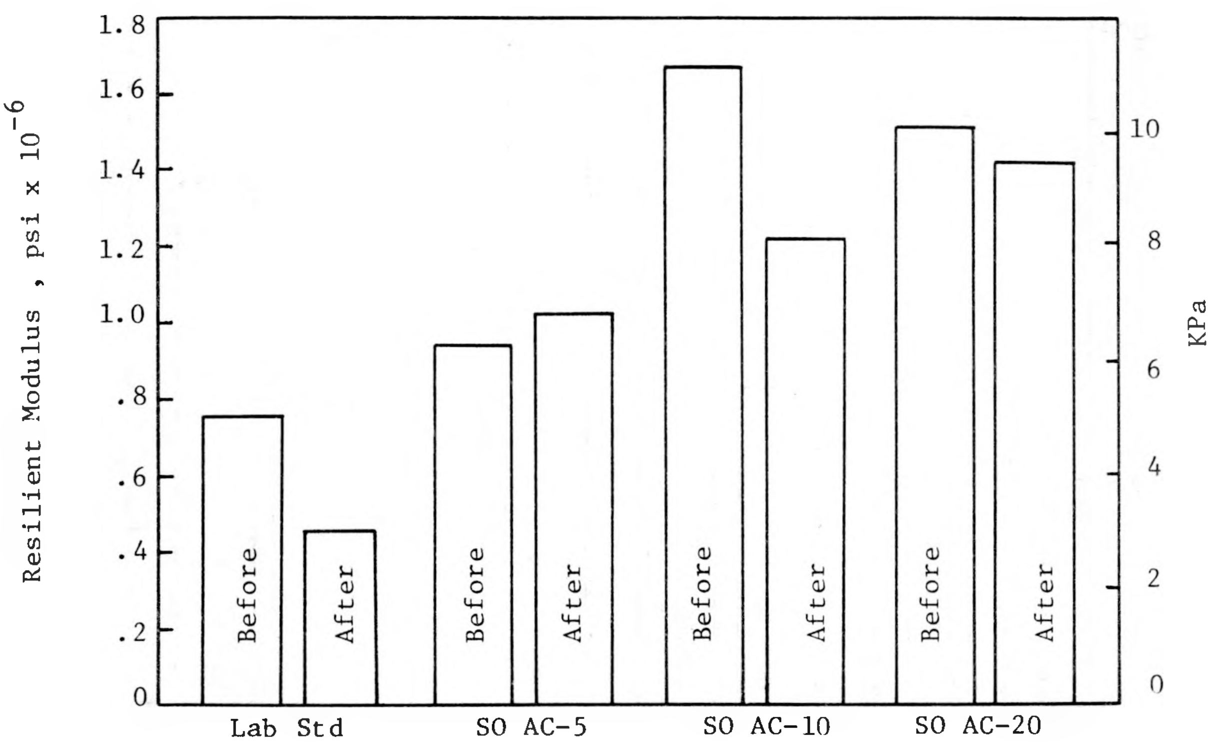

Figure 22. Resilient Modulus at 68°F (20°C) of Limestone Specimens Before and After Soaking

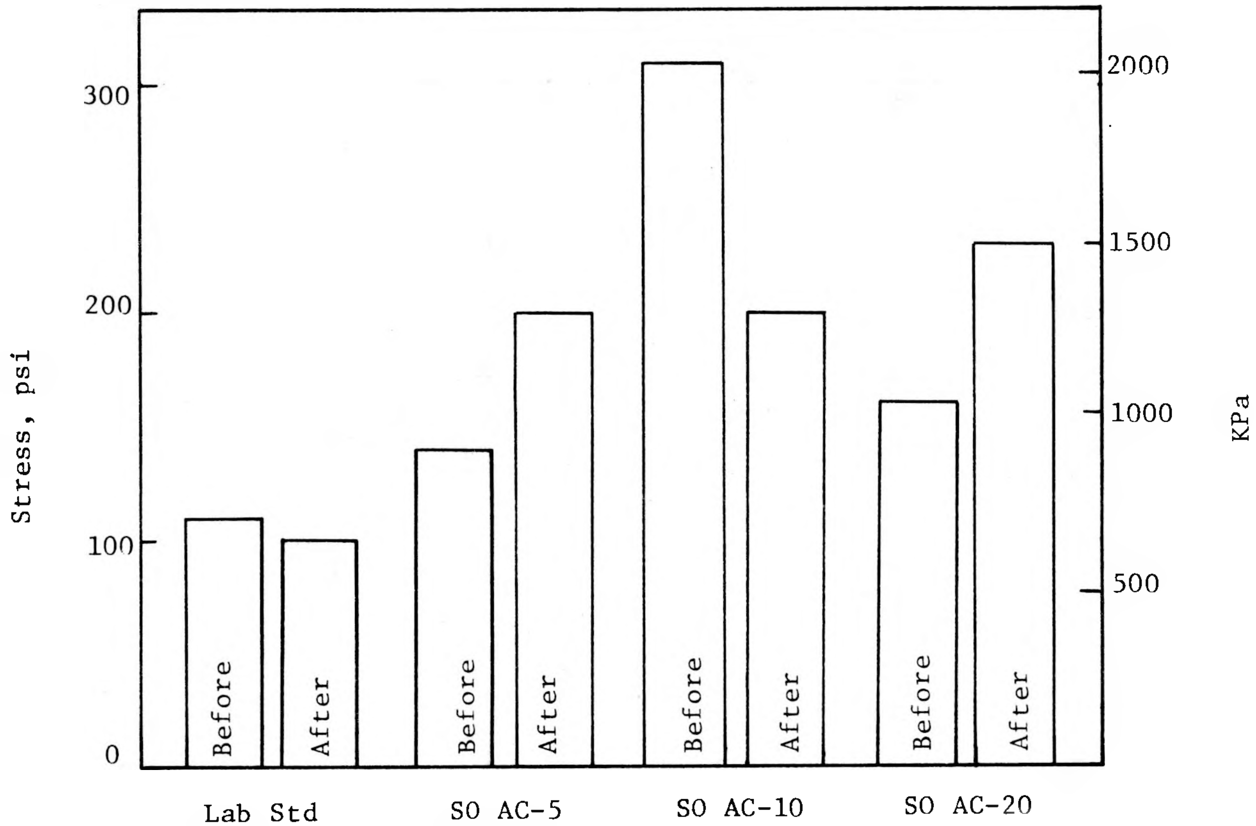

Figure 23. Splitting Tensile Strength of Gravel Specimens at 68°F (20°C) Before and After Soaking

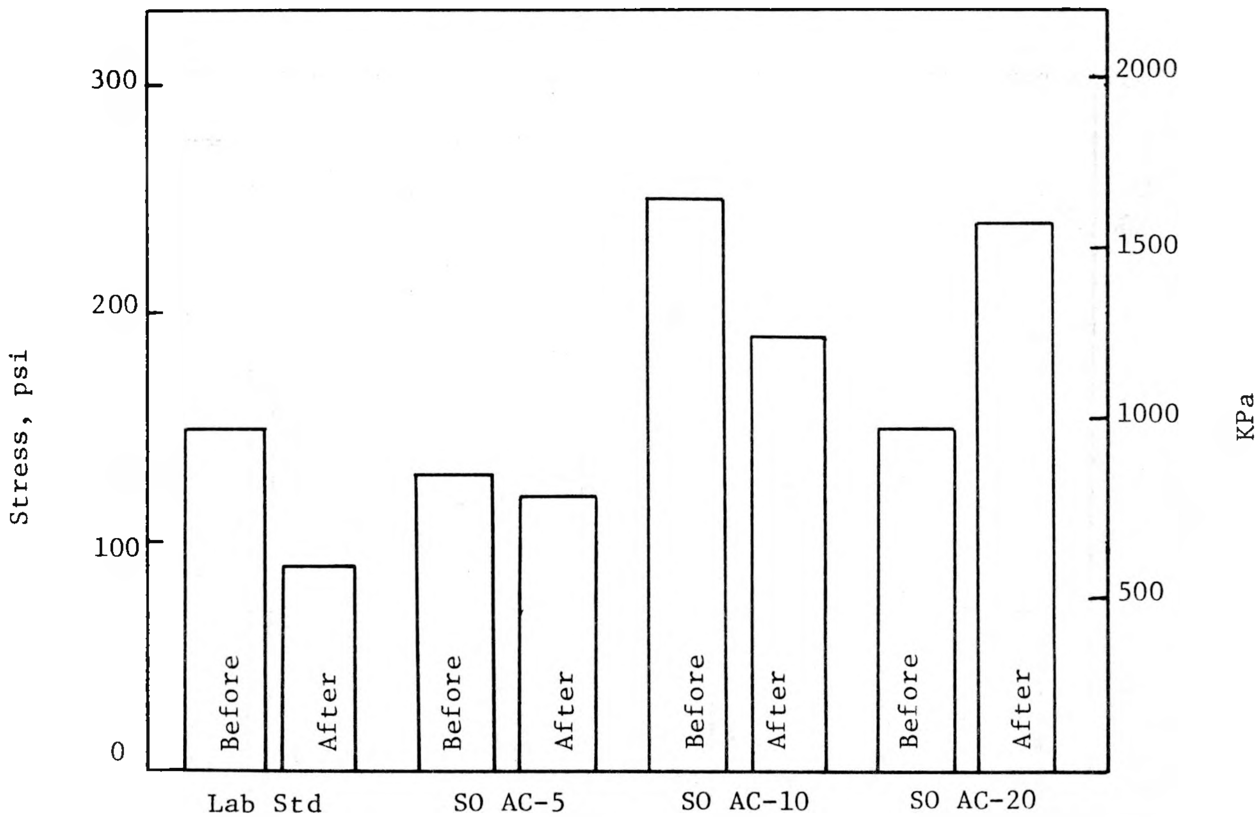

Figure 24. Splitting Tensile Strength of Limestone Specimens at 68°F (20°C) Before and After Soaking

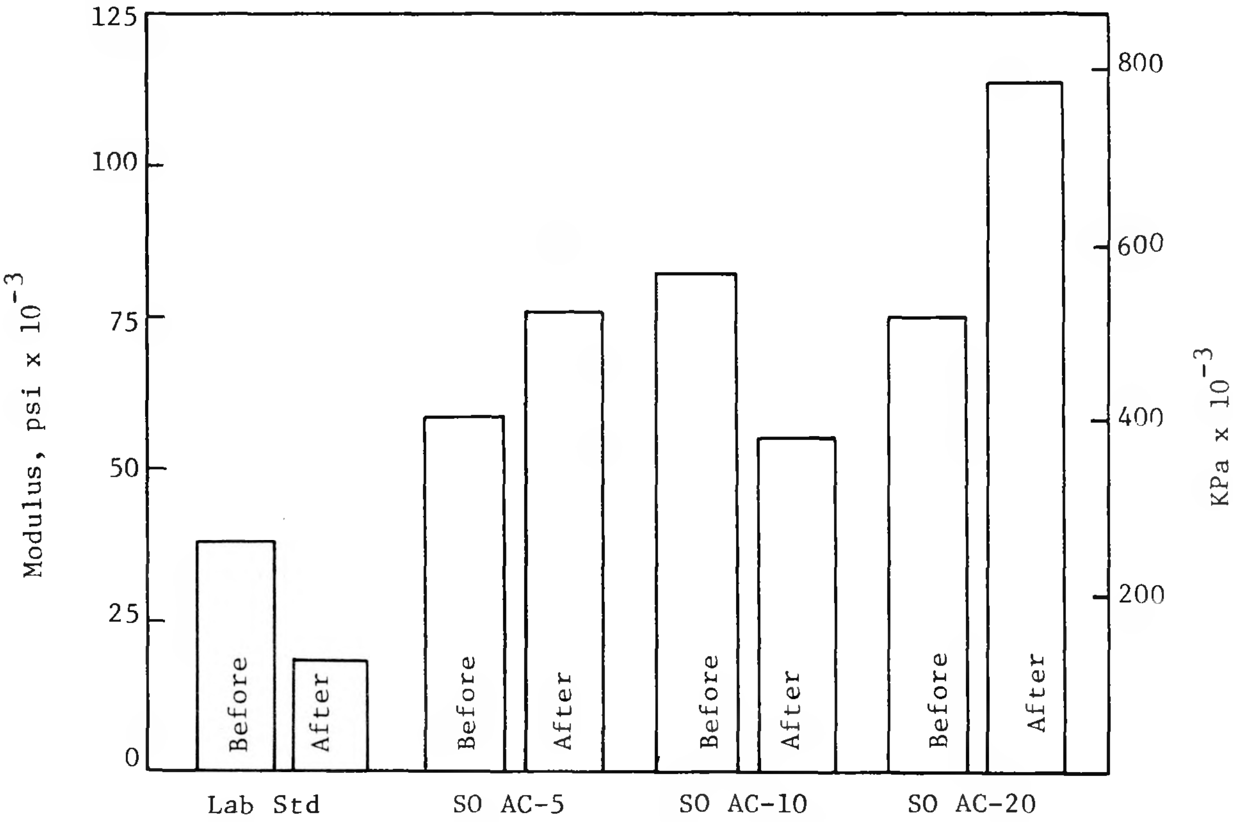

Figure 25. Splitting Tensile Modulus of Gravel Specimens at 68°F (20°C) Before and After Soaking

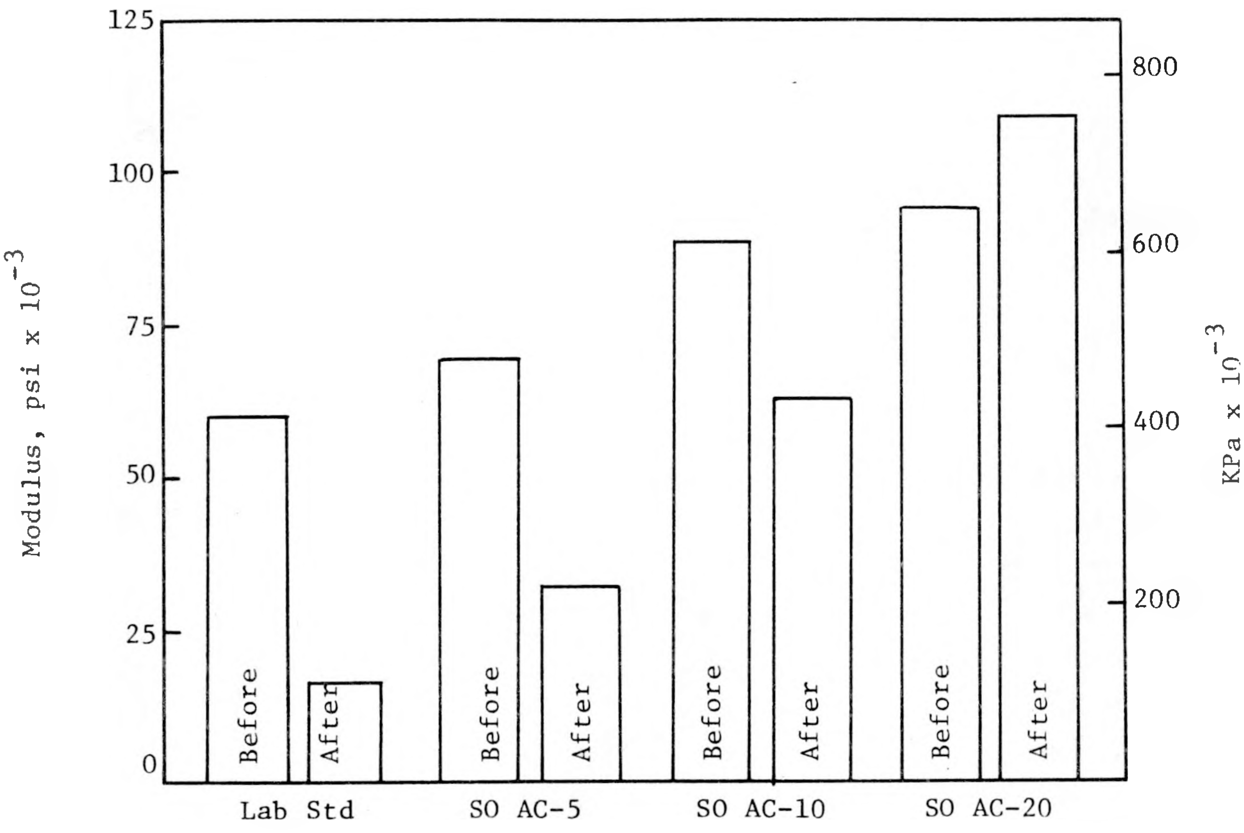

Figure 26. Splitting Tensile Modulus of Limestone Specimens at 68°F (20°C) Before and After Soaking

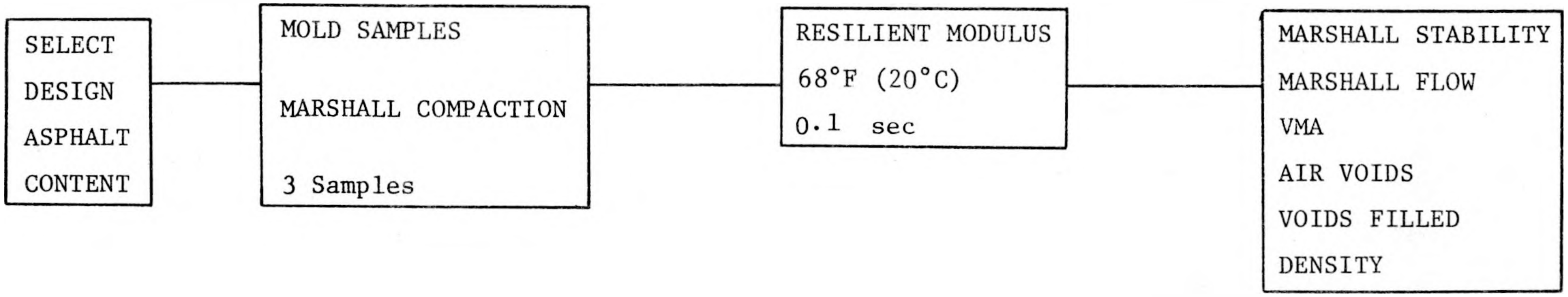

Figure 27. Test Program to Determine Stability and Compactabiliy of Mixes

TABLE 12. Test Results for Marshall Specimens

Type of Aggregate	Rounded Gravel				Crushed Limestone			
Type of Asphalt Cement	Lab. Std.	SO AC-5	SO AC-10	SO AC-20	Lab. Std.	SO AC-5	SO AC-10	SO AC-20
Bulk Specific Gravity of compacted mix	2.44	2.42	2.43	2.39	2.45	2.42	2.46	2.42
Maximum Specific Gravity of compacted mix	2.49	2.51	2.50	2.50	2.53	2.50	2.52	2.51
Asphalt Absorption, % by wt. agg.	0.75	1.2	0.91	0.91	1.7	1.3	1.6	1.3
Effective Asphalt Content, % of total mix	2.9	2.5	2.8	2.8	2.6	3.1	2.7	3.0
Voids in Mineral Aggregate, % bulk volume	9.1	9.8	9.3	10.8	10.5	10.7	9.1	10.6
Air Void Content, % total volume	2.1	3.7	2.8	4.2	3.0	3.5	2.3	3.6
VMA Filled with Asphalt, % VMA	80	70	76	67	78	75	81	74
Marshall Stability, lbs	1270	1380	1540	2470	2740	2310	2560	3430
Marshall Flow, 0.01 in	7	6	6	7	11	8	12	10
Resilient Modulus @ 68°F (20°C), psi x 10^6	0.57	1.14	——	1.62	0.59	1.16	——	1.68

were expected to produce mixtures with higher stiffness values than the laboratory standard asphalt. However, this would not be expected of the SO AC-5 unless the material was a better adhesive or more hardening occurred during mixing and compacting. By observing the results from the recovered asphalt properties (Table 9), it is obvious that although hardening occurred in every case it was not excessive in any case.

The simple statistics for the resilient modulus tests are given in Table 7. For a laboratory test such as this, coefficients of variation of 10 percent or less are considered excellent, therefore, coefficients of variation in the 15 to 20 percent range should be considered reasonable.

Splitting tensile test results would normally be expected to yield the highest tensile strength and highest elastic moduli at the highest loading rate and the lowest temperature and the converse should be true regarding tensile strain. Generally, this trend is fairly consistent with the data presented herein (Table 8), however, there are specific instances where this is not true. Due to the lack of precision inherent to data of this type, the heterogeneity of individual asphalt specimens, and the fact that only three specimens were tested at each condition it is reasonable to expect some inconsistencies.

If the overall averages of stress and modulus at failure are observed, the results indicate an order of tensile strength and stiffness of the asphalt mixtures identical to that shown before in the discussion of resilient modulus. Inspection of the graphs in Appendix D (stress and modulus as a function of loading head displacement rate) reveal curves with significant slopes at 68 and 33°F (20 and 1°C) and almost flat curves at -13°F (-25°C). At -13°F (-25°C) the tensile strengths and elastic moduli of the mixtures appeared to depend very little on displacement rate, therfore the materials behaved almost elastically. At 33 and 68°F (1 and 20°C) the mixtures behaved more viscoelastically, in that the moduli were more dependent on displacement rate. There was no noticeable difference in the behavior of the shale oil asphalts with respect to the petroleum asphalt. However as expected, the specimens containing limestone usually exhibited higher tensile strengths and elastic moduli than those containing gravel.

The mode of failure of the splitting tensile test specimens ranged from physically unnoticeable at 68°F (20°C) and 0.02 in/min (0.051 cm/min) to catastrophic at -13°F (-25°C) and 2 in/min (5.1 cm/min). Evidence of this is shown by comparing Figures D2 and D4 in Appendix D. At -13°F (-25°C) the failure plane was well defined such that the larger aggregates within the failure plane were severed, indicating the tensile strength of the matrix equaled or exceeded that of the aggregates.

By comparing the recovered asphalt properties (Table 8) with the original asphalt properties (Table 1), it is seen that as a result of heating during mixing and compacting, the penetration at 77°F (25°C) of each asphalt cement decreased slightly more than 50% and the viscosity at

77°F increased by slightly less than one order of magnitude. The viscosity at 140°F (60°C) of the "soft" asphalts (laboratory standard and SO AC-5) increased by a factor of three, whereas, that of the "hard" asphalts (SO AC-10 and SO AC-20) increased by approximately one order of magnitude. The ring and ball softening point of the SO AC-5 increased only 6°F (3°C) while the others showed an increase of near 20°F (11°C). Hardening of all the shale oil asphalts was quite comparable to that of the petroleum asphalt. Interestingly, the penetration of the recovered asphalt indicates the same order of stiffness of the asphalt cements as mentioned before in discussion of resilient modulus.

The most apparent result of the water susceptibility study was that the resilient moduli of the mixtures using laboratory standard asphalt and SO AC-10 (dewaxed) with both aggregates were adversely affected by soaking in water while the mixtures using SO AC-5 and SO AC-20 were not appreciably affected (Figures 21 and 22). This same trend was generally prevalent in the post-soaking results of the splitting tensile test at 68°F (20°C) and 2 in/min (5.1 cm/min). With one inexplicable exception, that of SO AC-5 plus limestone, those mixtures containing SO AC-5 and SO AC-20 actually displayed an increase in tensile strength after water soaking. Consider a theory to explain this phenomenon: Highly aromatic constituents or high amounts of basic nitrogen in the shale oil asphalts act as anti-stripping agents (13). Shale oil contains large amounts of basic nitrogen when compared with petroleum asphalts and shale oil asphalts with a source common to these discussed herein have been found to contain aromatic compounds (14) and would therefore display low water susceptibility unless the aromatic compounds were removed by some procedure such as the pentane deasphalting process. Petroleum (and naturally the derivatives thereof) from the American midcontinent do not contain substantial quantities of aromatic compounds (15). Hence, the laboratory standard and the dewaxed SO AC-10 asphalts should be more water susceptible than the SO AC-5 and SO AC-20. Further, assuming the water had no effect on the mixtures containing SO AC-5 and SO AC-20, the increase in strength and stiffness may have been due to thixotrophy since the specimens had aged at least one week more and the "before soaking" tests were normally conducted on the day following specimen fabrication.

Resilient modulus (stiffness) as a function of temperature of the mixtures made with shale oil asphalt was not strikingly different from those made with petroleum asphalt (Figures 18 and 19). However, it is interesting to note that both of these figures showed a "crossover" of the resilient modulus of the mixtures containing laboratory standard asphalt. That is, at moderate temperatures (68 and 77°F) those mixtures containing laboratory standard asphalt are measurably less stiff than those containing shale oil asphalt. Then, particularly at -13°F (-25°C) and even at 33 and 104°F (1 and 40°C), the stiffness of these mixtures becomes as high or higher than those containing the shale oil asphalts. Using the Shell nomograph for determining the stiffness modulus of asphalts (16) in conjunction with a chart giving the ratio of the stiffness of the mix to the stiffness of the asphalt (17), it was possible to predict the stiffness of some of these mixtures at moderate temperatures. The predicted stiffness was approximately one order of magnitude greater than the measured stiffness for the shale oil asphalts as well as the petroleum asphalt.

Marshall Compacted Specimens. According to the Asphalt Institute (11) the medium traffic category requires fifty blows per face of each specimen and should result in a Marshall stability exceeding 500 lbs (2224 N). The stability of all the mixtures exceeded this value (Table 12). Based on the stiffness of the SO AC-10 relative to the other asphalts tested, the Marshall stability of mixtures containing this material was surprisingly low. However, the comparatively low stability of the rounded gravel specimens was not surprising since round, smooth aggregates usually produce mixtures with low stabilities. The bulk specific gravity of the compacted mixtures with similar aggregates indicated all the mixtures were about equal in compactibility. Since all the mixtures of a given aggregate contained identical quantities of asphalt cement, received equal compactive effort, and were in the same viscosity range during compaction, it can be stated that the air void contents indicated SO AC-20 was least compactible while SO AC-10 was the most compactible.

CONCLUSIONS

Based on the previous discussions of shale oil asphalts from the Green River formation, the following conclusions appear warranted:

1. Shale oil asphalt can be produced by conventional methods in acceptable grades for highway paving mixtures.

2. Difficulties encountered in producing a given grade of asphalt from shale oil for this research were due to the refiner's inexperience in the distillation of small batches and had nothing to do with the fact that the residuum came from shale oil.

3. The vanadium content of shale oil asphalt is low compared to about 65 petroleum asphalts tested by Traxler (5).

4. Adhesive properties of shale oil asphalt are sufficient to produce adequate paving mixtures and compare favorably with those of petroleum asphalts.

5. Paving mixtures containing shale oil asphalts appear to be quite resistant to damage by water, however, dewaxing of shale oil asphalts apparently causes some water susceptibility as well as loss of Marshall stability in mixtures utilizing the dewaxed binder.

6. Hardening of the shale oil asphalts due to heating during mixing and compacting was about the same as that of the petroleum asphalt.

7. The stiffness of mixtures made with shale oil asphalt was not strikingly different from the stiffness of those made with petroleum asphalt.

8. The Marshall stability of mixtures made with shale oil asphalt was more than adequte and compared well with the Marshall stability of those made with petroleum asphalt.

REFERENCES

1. Button, J. W., Epps, J. A., Gallaway, B. M., "Test Results of Laboratory Standard Asphalts, Aggregates, and Mixtures", Materials Laboratory Note No. 1, Texas Transportation Institute, Texas A&M University, 1977.

2. Annual Book of Standards, Part 15, Road and Paving Materials; Bituminous Materials for Highway Construction, Waterproofing, and Roofing and Pipe; Skid Resistance, American Society for Testing and Materials, 1977.

3. Standards Specifications for Transportation Materials and Methods of Sampling and Testing, Part II, American Association of State Highway and Transportation Officials, 1974.

4. Manual of Testing Procedures, Vol. 1, Texas State Department of Highways and Public Transportation, 1970.

5. Traxler, R. N., Scrivner, F. H., Kuykendall, W. E., Jr., "Loss of Durability in Bituminous Pavement Surfaces - Importance of Chemically Active Solar Radiation", Research Report 127-3, Texas Transportation Institute, Texas A&M University.

6. Heukelom, W., "An Improved Method of Characterizing Asphaltic Bitumens With the Aid of Their Mechanical Properties", Aspahlt Paving Technology, Vol. 42, Association of Asphalt Paving Technologist, 1973.

7. Hveem, F. N., "Establishing the Oil Content for Dense-Graded Bituminous Mixtures", California Highways and Public Works, July - August 1942.

8. Schmidt, R. J., "A Practical Method for Measuring the Resilient Modulus of Asphalt - Treated Mixes", Highway Research Record No. 404, Highway Research Board, 1972, pp. 22-32.

9. Schmidt, R. J., "Operating Instructions for the Mark III Resilient Modulus Device", An operations manual.

10. Hadley, W. O., Hudson, W. R., Kennedy, T. W., "Evaluation and Prediction of the Tensile Properties of Asphalt - Treated Materials", Research Report No. 98-9, Center for Highway Research, University of Texas at Austin, May 1971, pp. 63-76.

11. "Mix Design Methods for Asphalt Concrete", The Asphalt Institute, Manual Series No. 2 (MS-2), Fourth Edition, March 1974, Section 3.13.

12. Traxler, R. N., "Hardening of Asphalt Cements During Service in Pavements, 1963 - 66 Program", Texas Transportation Institute, Research Report 59-11, Texas A&M University, College Station, Texas, 1966.

13. Verbal Communication with J. Claine Petersen, U. S. Department of Energy, Laramie, Research Center, Laramie, Wyoming.

14. Kommes, W. C., and Stanfield, K. E., "Properties of Shale - Oil Asphalts form Colorado Oil Shale", Intra - Bureau Report OSRD-45, Petroleum and Oil - Shale Experiment Station, Laramie, Wyoming, 1951.

15. Linstromberg, W. W., Organic Chemistry, D. C. Heath and Company, Boston, Massachusetts, p. 101, 1966.

16. C. Vander Poel, Journal of Applied Chemistry, Vol. 4, Part 5 (May 1954), p. 221, Shell Bitumen Reprint No. 9.

17. W. Heukelom and A. J. G. Klomp, "Road Design and Dynamic Loading", Proceedings of the Associatoin of Asphalt Paving Technologists, Vol. 33 (1964), pp. 111.

APPENDIX A

Test Results for Marshall Specimens Using Laboratory Standard Asphalt

TABLE A1. Summary of Test Results for Marshall Specimens Using Rounded Gravel

Asphalt Cement Content, percent by wt. aggregate	2.5	3.0	3.5	4.0	4.5
Bulk Specific Gravity of compacted mix	2.37	2.39	2.42	2.44	2.45
Maximum Specific Gravity of mixture	2.53	2.52	2.50	2.48	2.46
Effective Specific Gravity of aggregate	2.63	2.64	2.63	2.63	2.63
Asphalt Absorption, percent by wt. aggregate	0.72	0.83	0.81	0.76	0.71
Effective Asphalt Content, percent by total mix	1.7	2.1	2.6	3.1	3.6
Voids in Mineral Aggregate, percent bulk volume	10.5	10.0	9.4	9.0	9.3
VMA Filled w/Asphalt, percent VMA	47	57	71	85	95
Air Void Content, percent total volume	6.4	5.1	3.2	1.6	0.6
Marshall Stability, lbs	1190	1150	1220	1290	1160
Marshall Flow, 0.01 in	7	7	7	7	8

TABLE A2. Summary of Test Results for Marshall Specimens Using Crushed Limestone

Asphalt Cement Content, percent by wt. aggregate	3.5	4.0	4.5	5.0	5.5
Bulk Specific Gravity of compacted mix	2.40	2.41	2.45	2.48	2.48
Maximum Specific Gravity of mixture	2.55	2.55	2.53	2.50	2.49
Effective Specific Gravity of aggregate	2.70	2.69	2.71	2.69	2.70
Asphalt Absorption, percent by wt. aggregate	1.6	1.5	1.8	1.5	1.6
Effective Asphalt Content, percent by wt. total mix	1.8	2.4	2.6	3.4	3.7
Voids in Mineral Aggregate, percent bulk volume	10.5	10.5	9.4	8.8	9.2
VMA Filled with Asphalt, percent VMA	57	65	78	94	97
Air Void Content, percent total volume	5.9	4.8	3.0	0.8	0.4
Marshall Stability, lbs	2410	2610	2740	2430	2230
Marshall Flow, 0.01 in	9	9	11	15	14

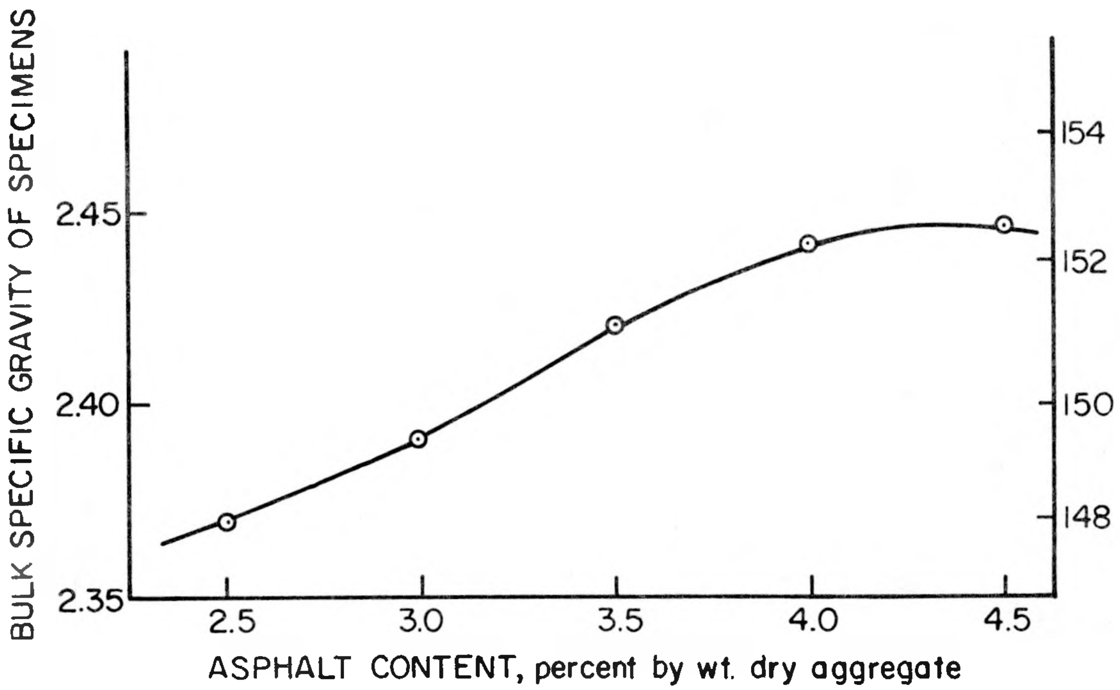

Figure A1. Bulk specific gravity of Marshall specimens using rounded gravel.

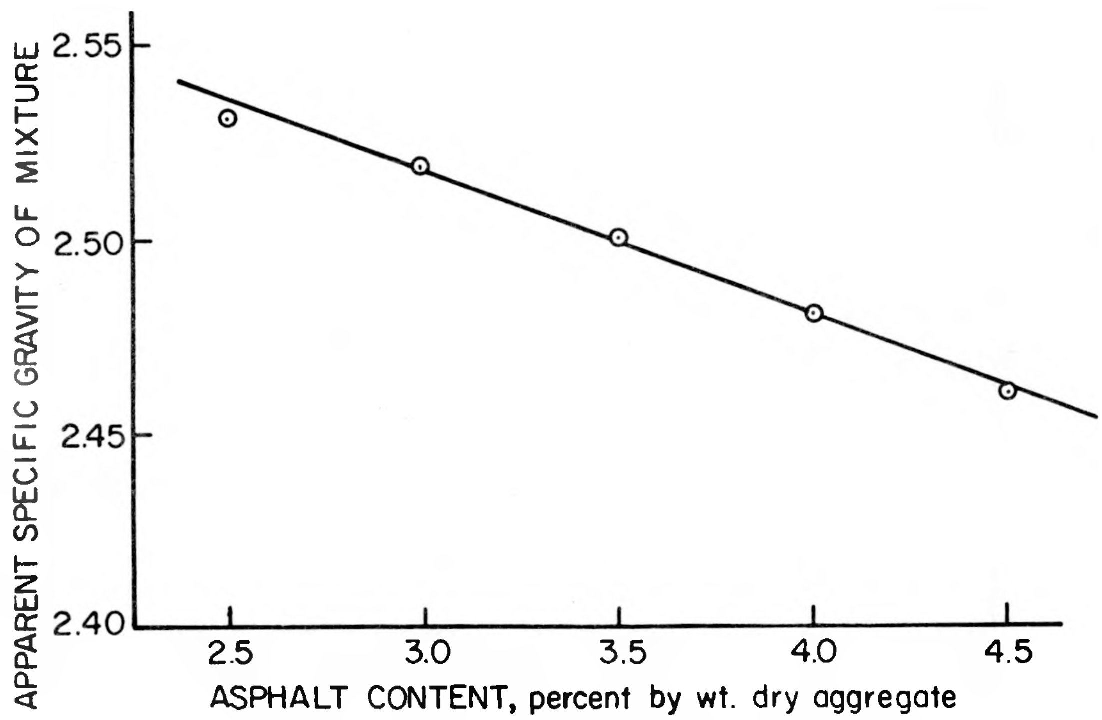

Figure A2. Apparent specific gravity of mixtures using rounded gravel.

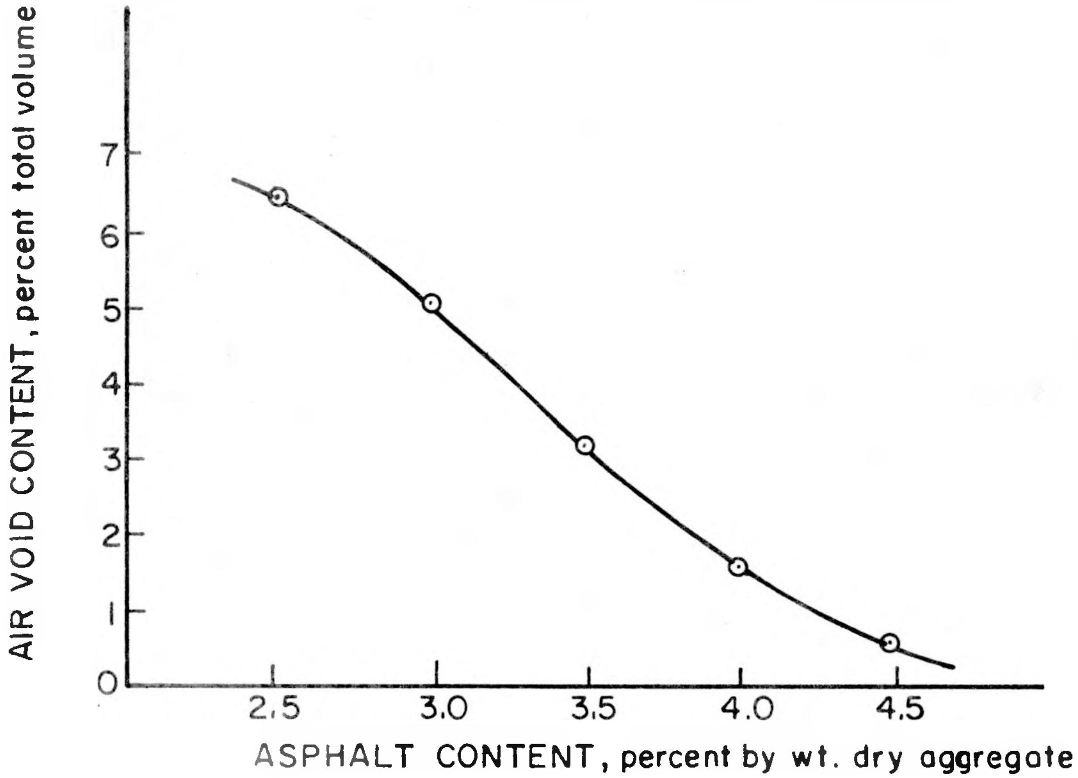

Figure A3. Air voids in Marshall specimens using rounded gravel.

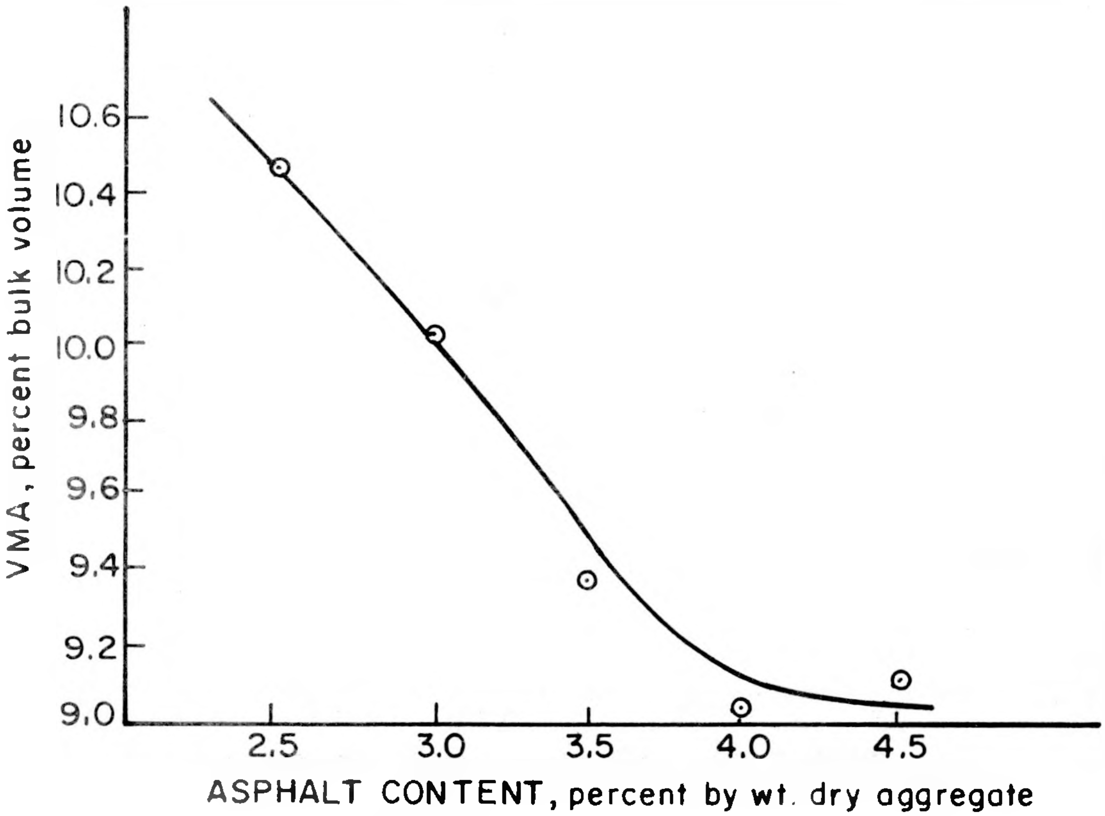

Figure A4. Voids in mineral aggregate for Marshall specimens using rounded gravel.

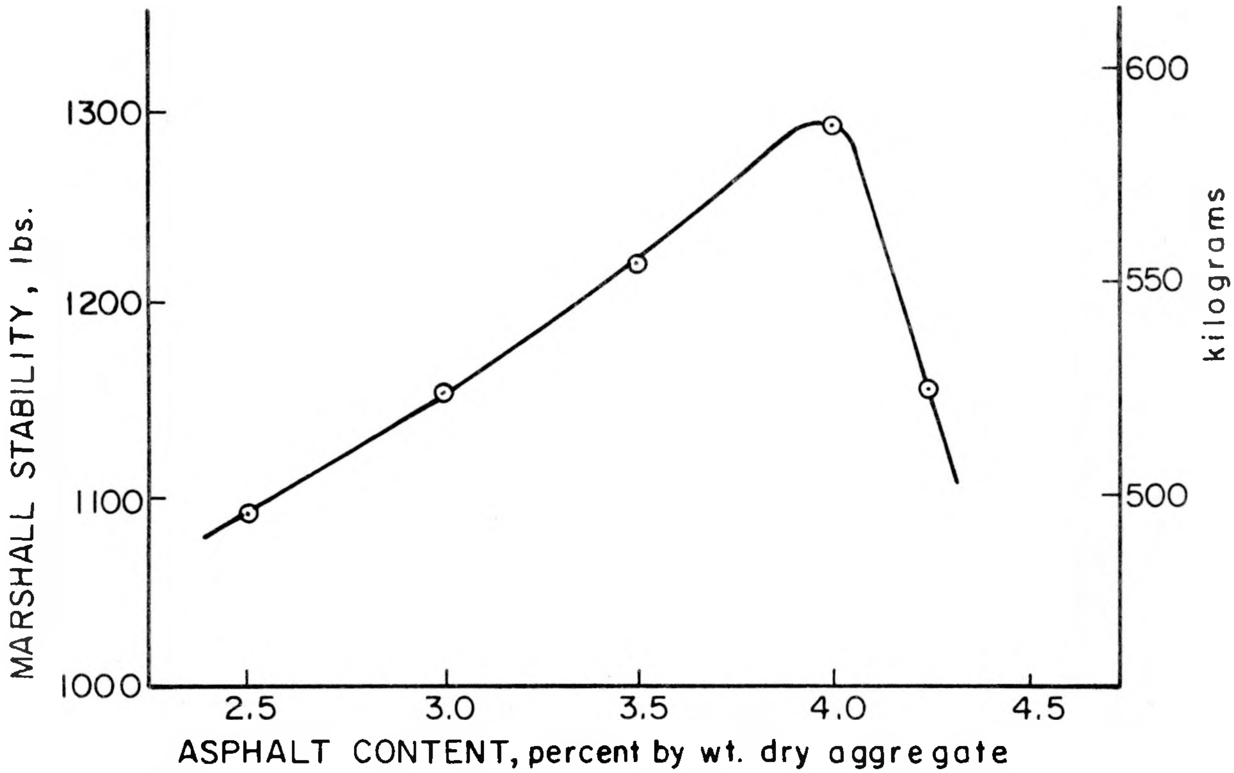

Figure A5. Marshall stability of specimens using rounded gravel.

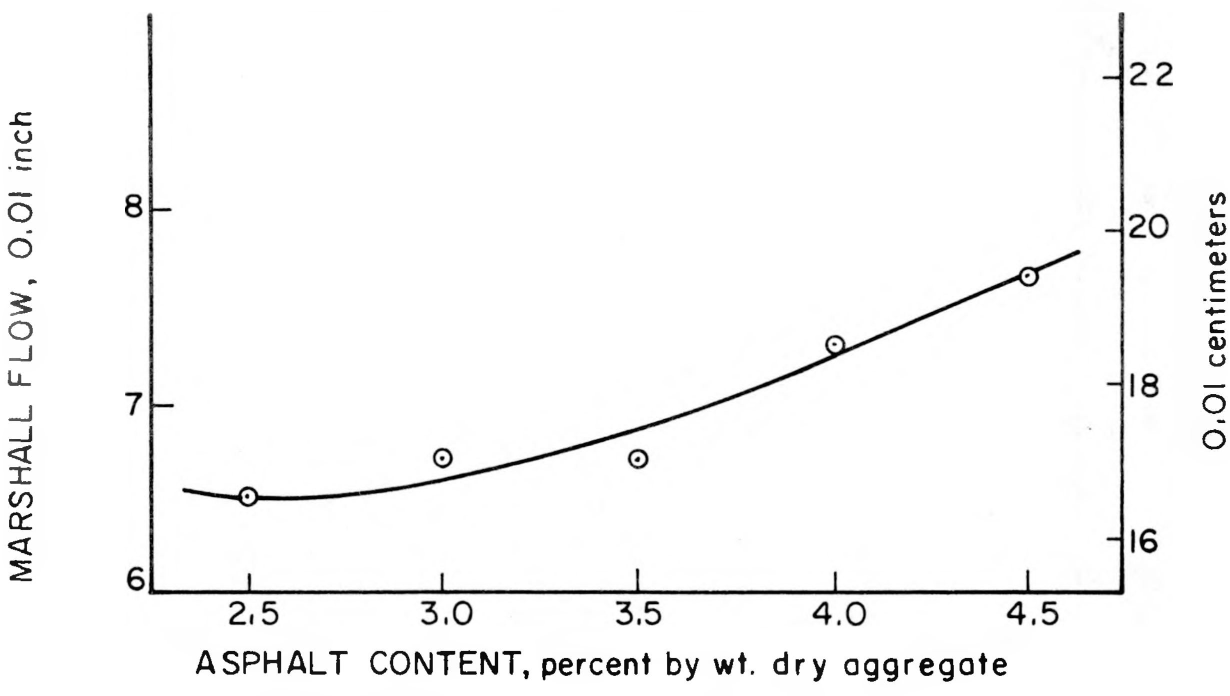

Figure A6. Marshall flow of specimens using rounded gravel.

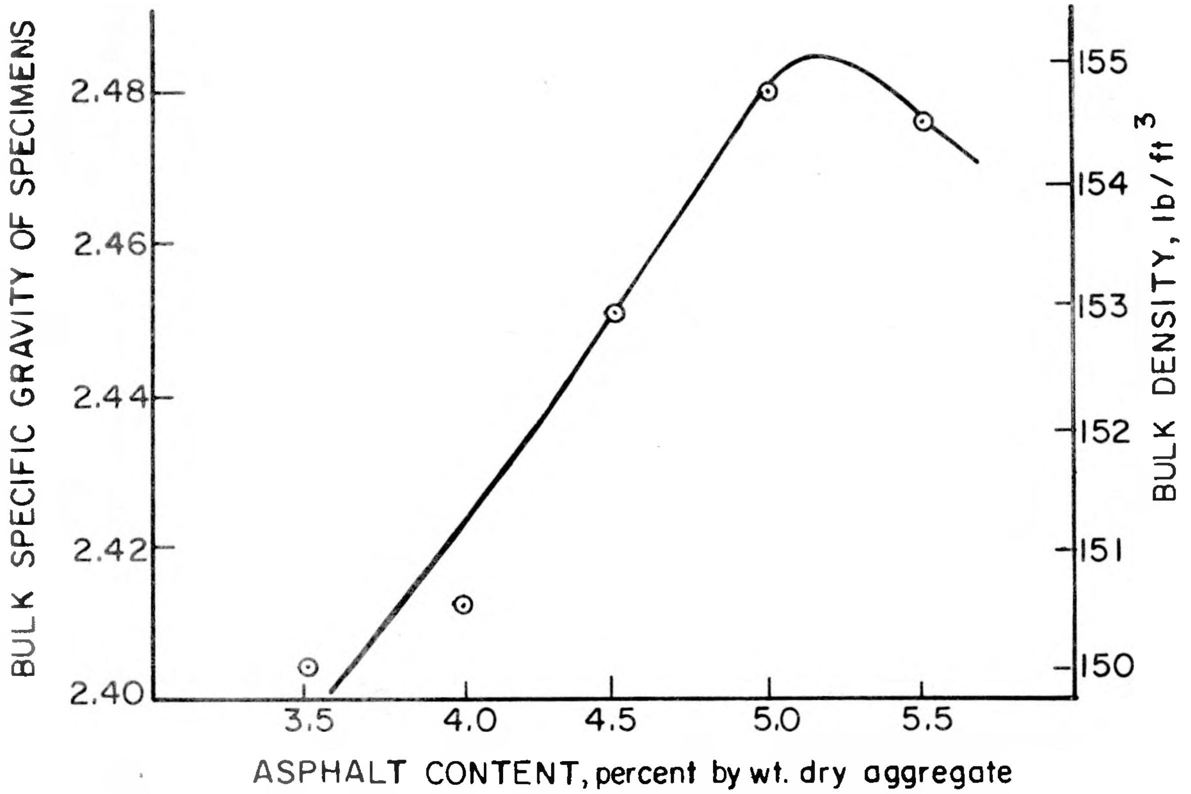

Figure A7. Bulk specific gravity of Marshall specimens using crushed limestone.

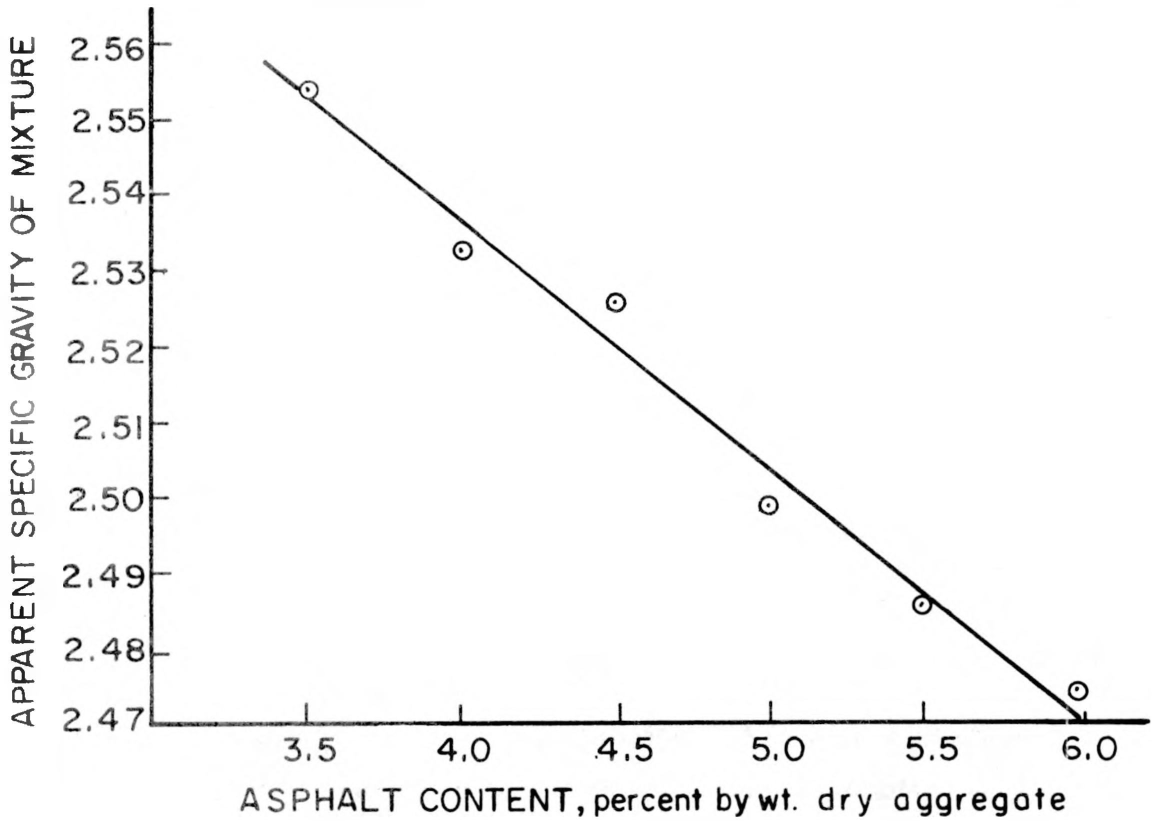

Figure A8. Apparent specific gravity of mixtures using crushed limestone.

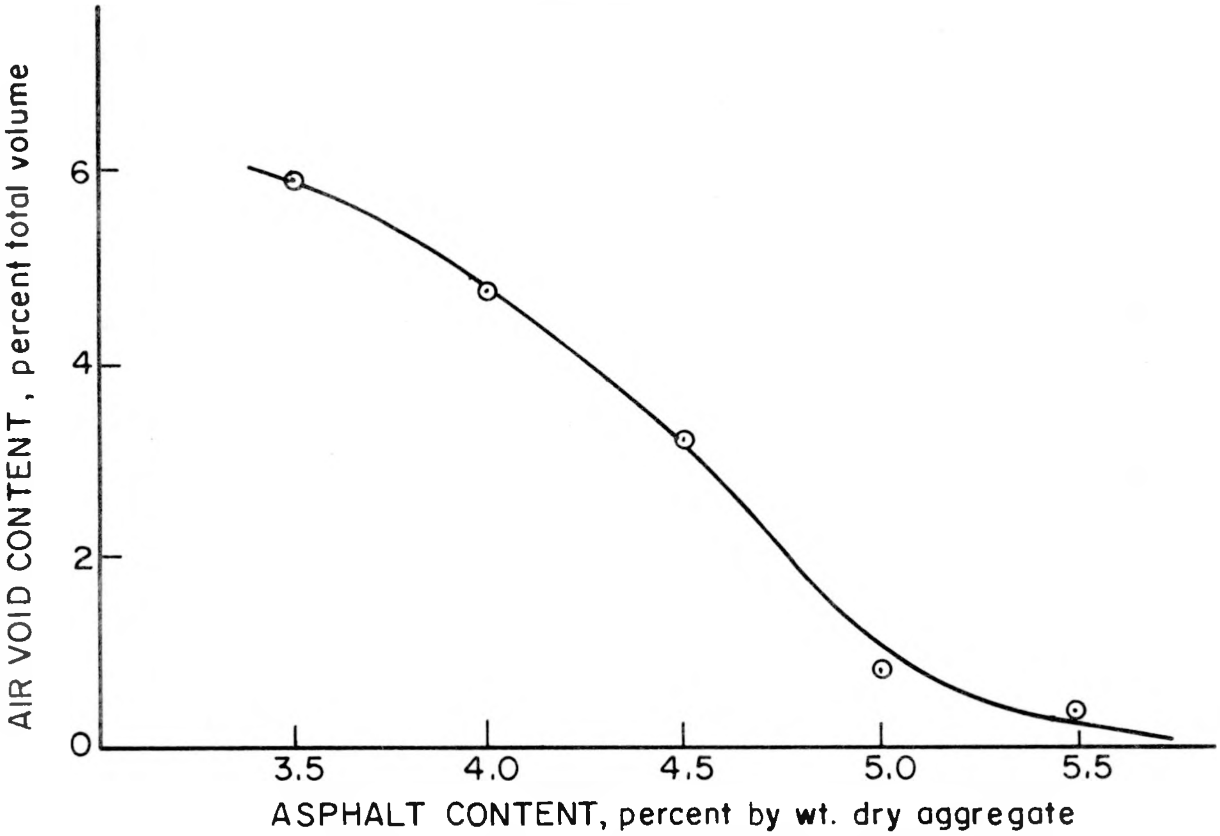

Figure A9. **Air voids in Marshall specimens using crushed limestone.**

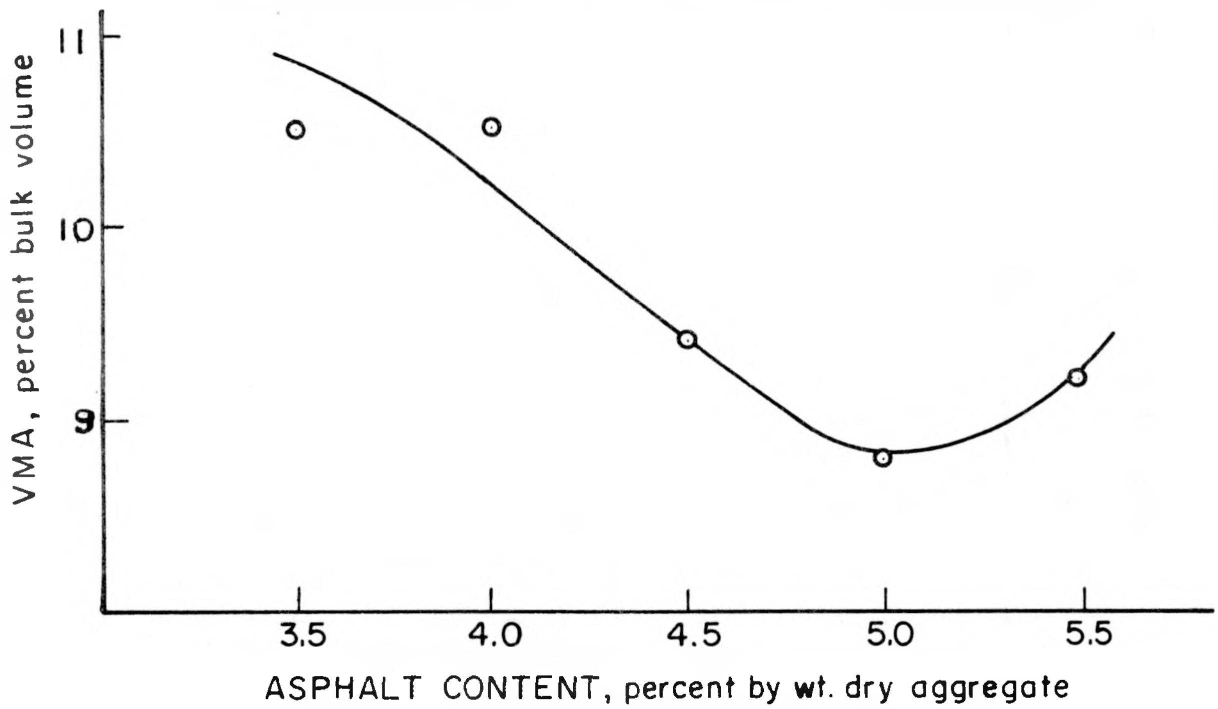

Figure A10. **Voids in mineral aggregate for Marshall specimens using crushed limestone.**

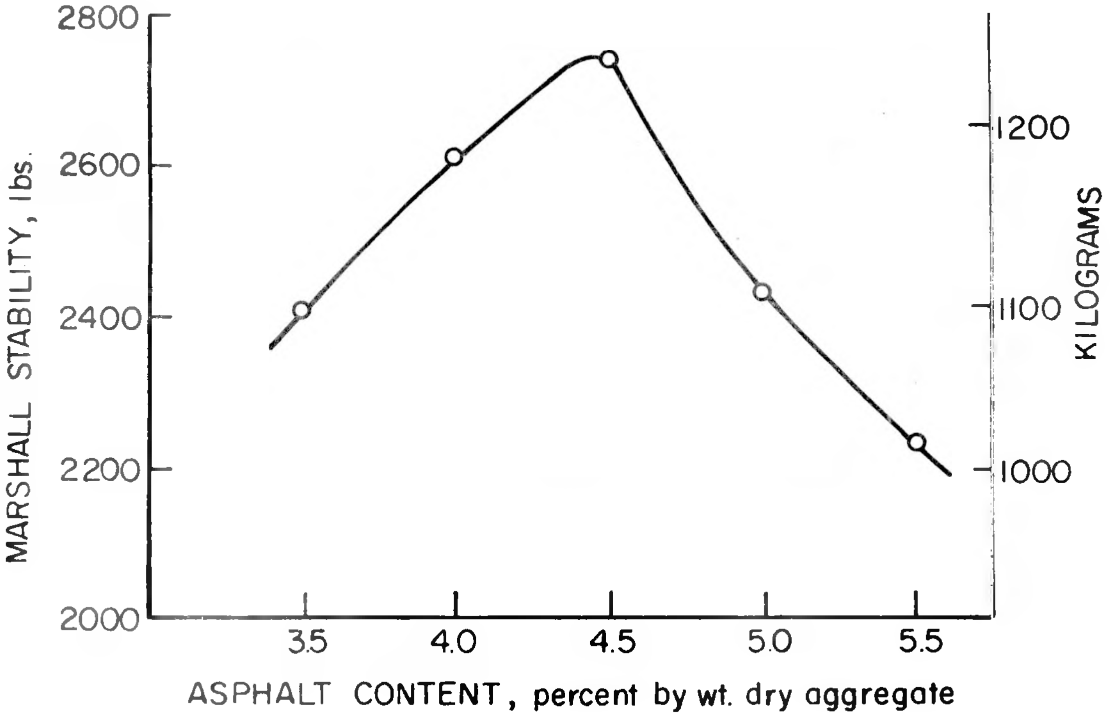

Figure A11. Marshall stability of specimens using crushed limestone

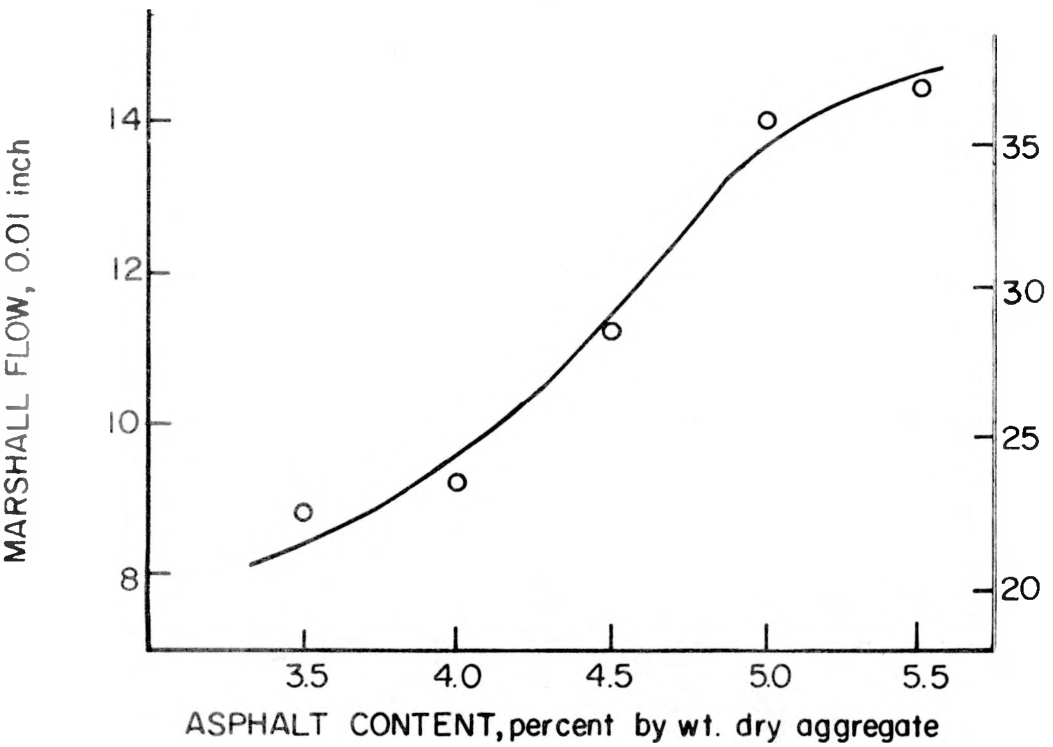

Figure A12. Marshall flow of specimens using crushed limestone

APPENDIX B

Test Results for Gyratory Compacted Specimens

Using Laboratory Standard Asphalt

TABLE B1. Data Summary of Hveem Specimens Using Rounded Gravel

Asphalt Content, percent by wt. dry aggregate	2.5	3.0	3.5	4.0	4.5
Bulk Specific Gravity of compacted mix	2.34	2.39	2.40	2.43	2.45
Maximum Specific Gravity of mixture	2.53	2.52	2.50	2.48	2.46
Effective Specific Gravity of aggregate	2.63	2.64	2.63	2.63	2.63
Asphalt Absorption, percent by wt. aggregate	0.72	0.83	0.81	0.77	0.71
Effective Asphalt Content, percent by wt. total mix	1.7	2.1	2.6	3.1	3.6
Voids in Mineral Aggregate, percent bulk volume	11.7	10.0	10.0	9.6	9.3
VMA Filled with Asphalt, percent VMA	42	58	68	81	95
Air Void Content, percent total volume	7.7	5.0	3.8	2.2	0.6
Resilient Modulus (M_R), 68°F(20°C), psi	407,000	515,000	513,000	562,000	477,000
Hveem Stability, percent	33	30	27	22	21
Splitting Tensile Stress @ Failure, 68°F(20°C), psi	92	103	121	114	119
Splitting Tensile Strain @ Failure 68°F(20°C), in/in	0.0025	0.0027	0.0027	0.0032	0.0037
Splitting Tensile Modulus (E) @ Failure, 68°F(20°C), psi	36,500	38,400	44,100	36,100	33,100

TABLE B2. Data Summary of Hveem Specimens Using Crushed Limestone

Asphalt Content, percent by wt. aggregate	3.5	4.0	4.5	5.0	5.5	6.0
Bulk Specific Gravity of compacted mix	2.44	2.45	2.46	2.44	2.47	2.47
Maximum Specific Gravity of mixture	2.55	2.53	2.53	2.50	2.49	2.48
Effective Specific Gravity of aggregate	2.70	2.69	2.71	2.69	2.70	2.71
Asphalt Absorption, percent by wt. aggregate	1.6	1.5	1.8	1.5	1.6	1.8
Effective Asphalt Content, percent by wt. total mix	1.8	2.4	2.6	3.4	3.7	4.0
Voids in Mineral Aggregate, percent bulk volume	9.0	9.0	9.1	10.3	9.6	10.0
VMA Filled with Asphalt, percent VMA	64	74	81	84	94	97
Air Void Content, percent total volume	4.5	3.2	2.5	2.2	0.8	0.4
Resilient Modulus (M_R), psi	618,000	620,000	590,000	499,000	571,000	249,000
Hveem Stability, percent	57	54	54	50	46	24
Splitting Tensile Stress @ Failure 68°F(20°C), psi	119	112	112	106	105	82
Splitting Tensile Strain @ Failure 68°F(20°C), in/in	.0032	.0032	.0044	.0041	.0035	.0069
Splitting Tensile Modulus (E) @ Failure, 68°F(20°C), psi	37,200	34,800	26,000	27,400	30,000	12,000

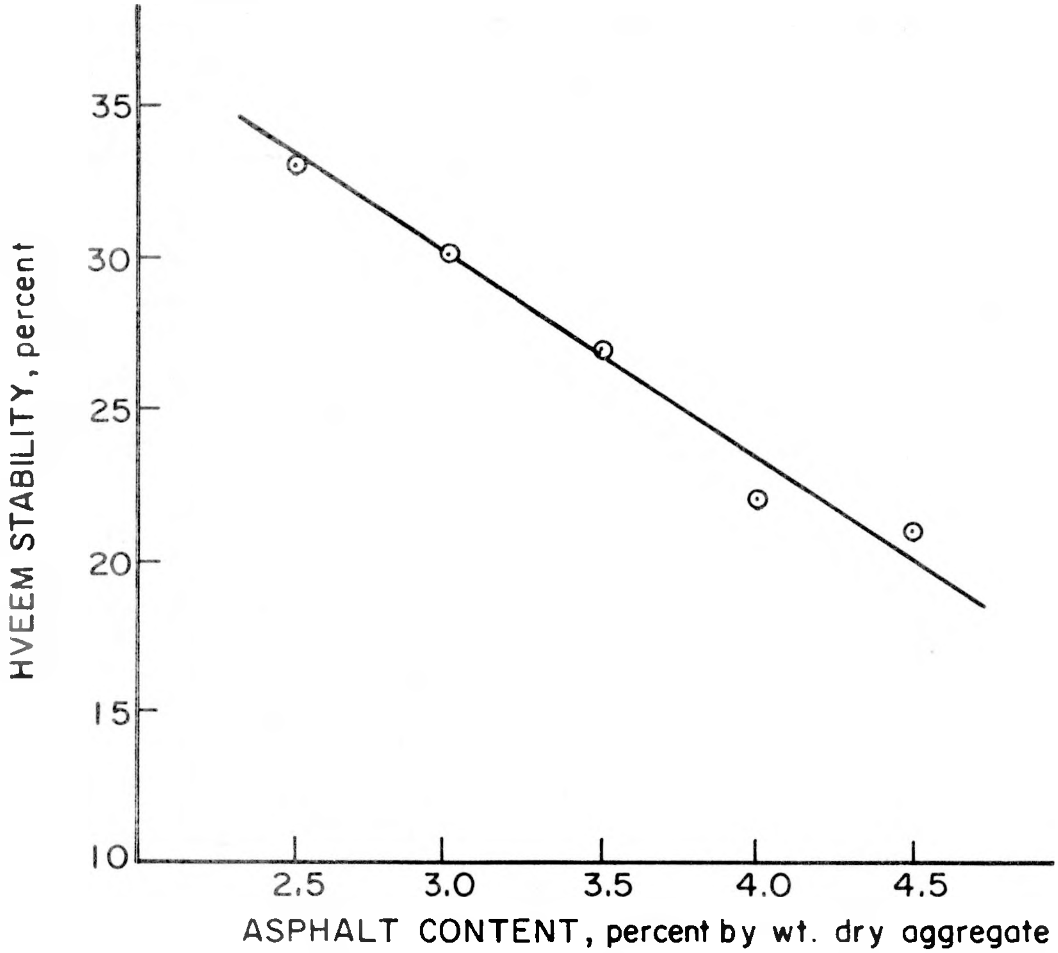

Figure B1. Hveem stability of specimens using rounded gravel.

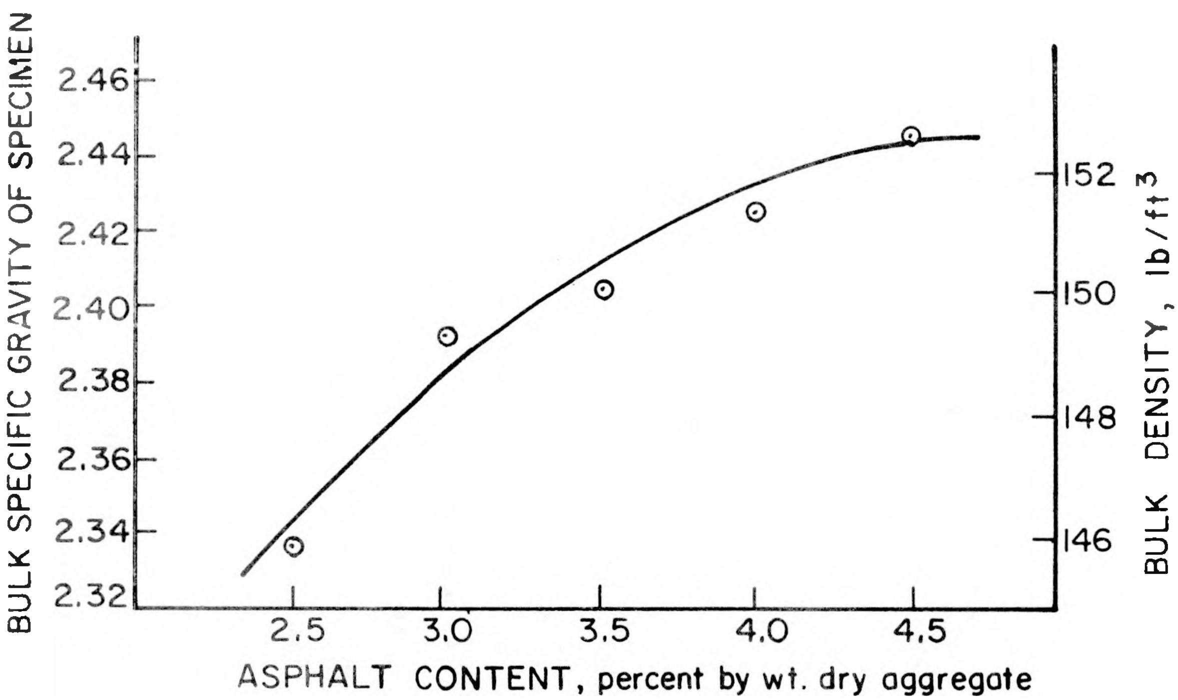

Figure B2. Bulk specific gravity of Hveem specimens using rounded gravel.

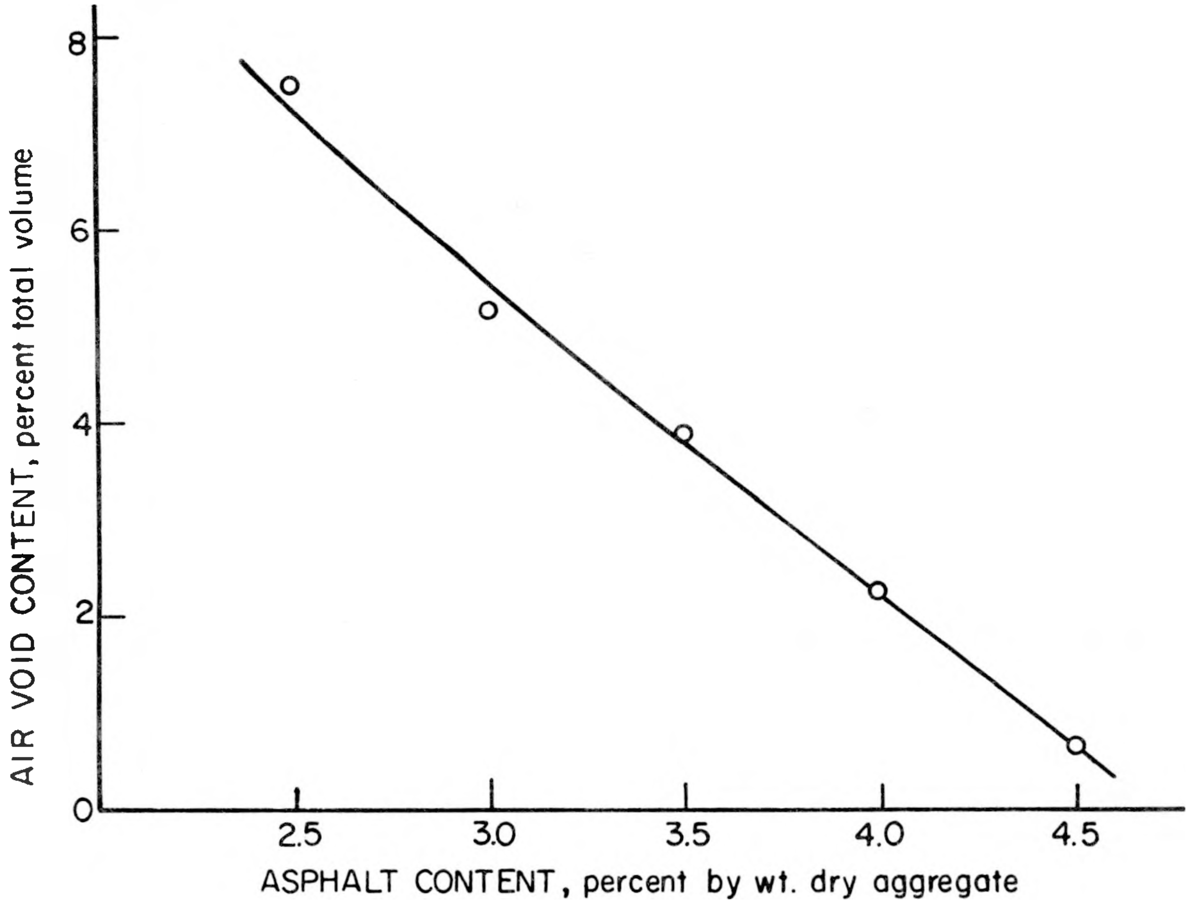

Figure B3. Air void content of Hveem Specimens using rounded gravel.

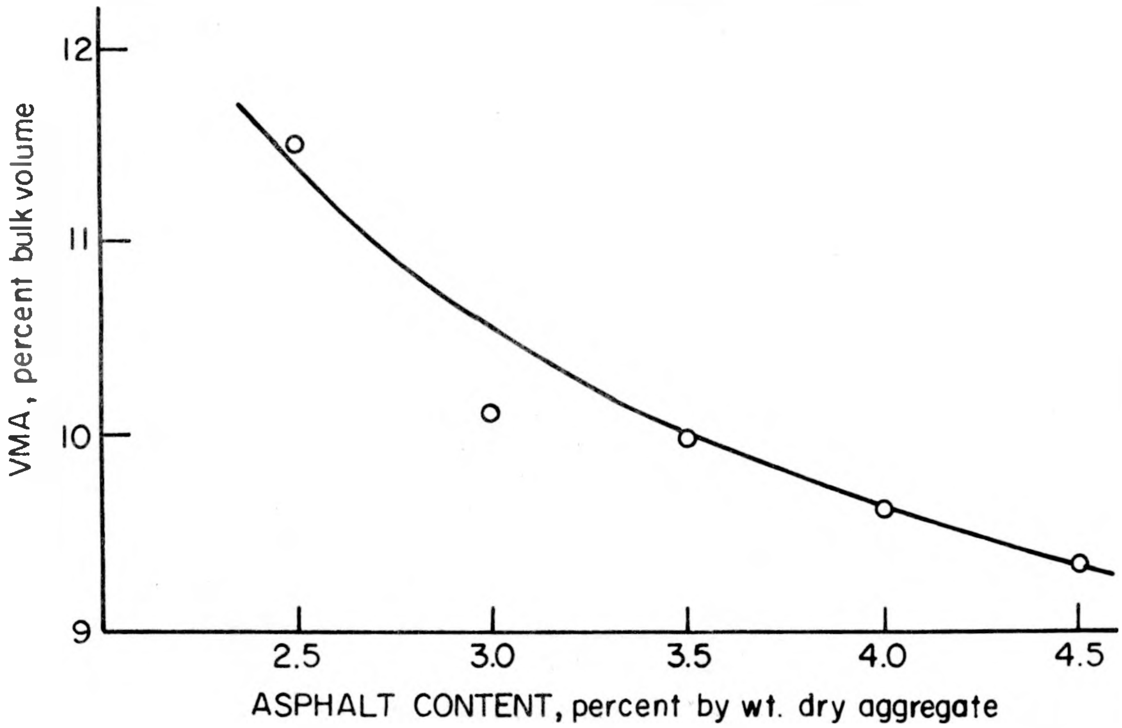

Figure B4. Voids in mineral aggregate for Hveem specimens using rounded gravel.

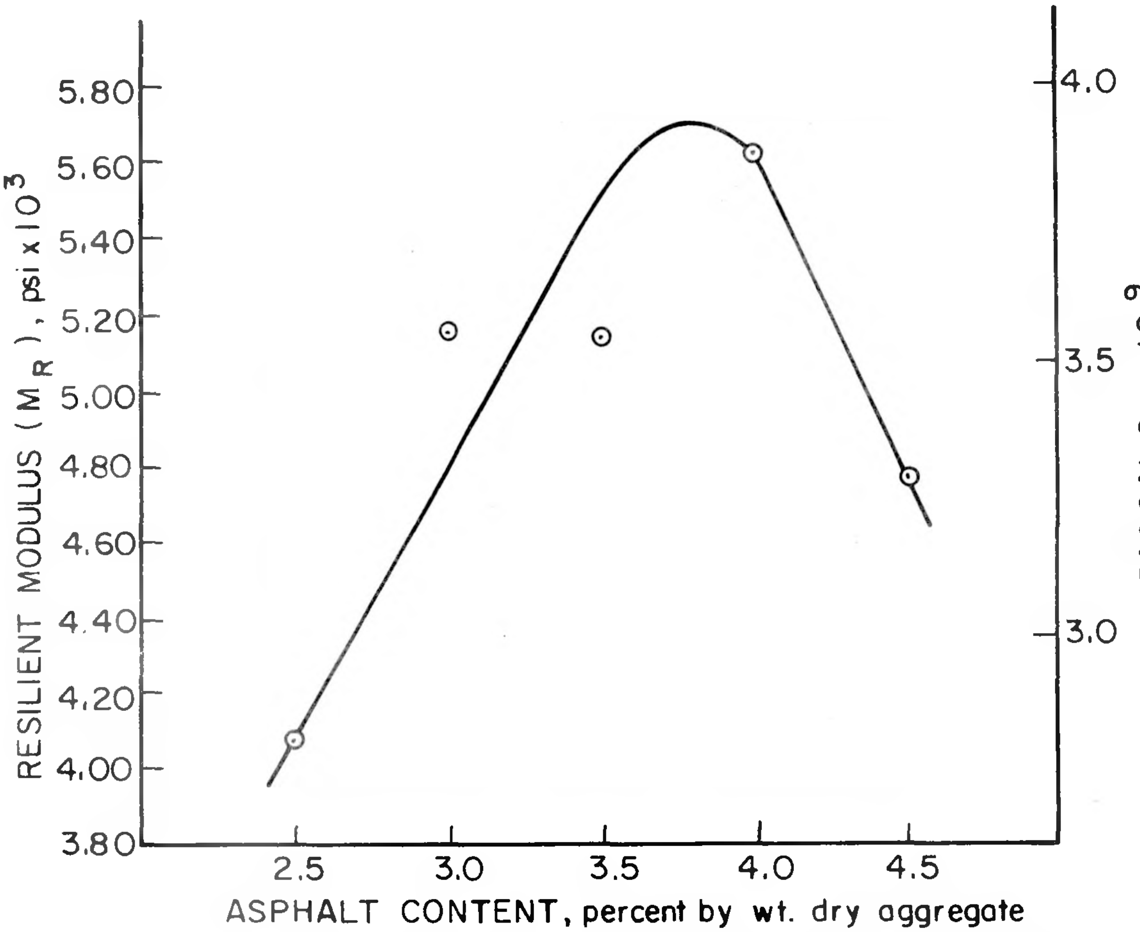

Figure B5. Resilient modulus of Hveem specimens at 68°F using rounded gravel.

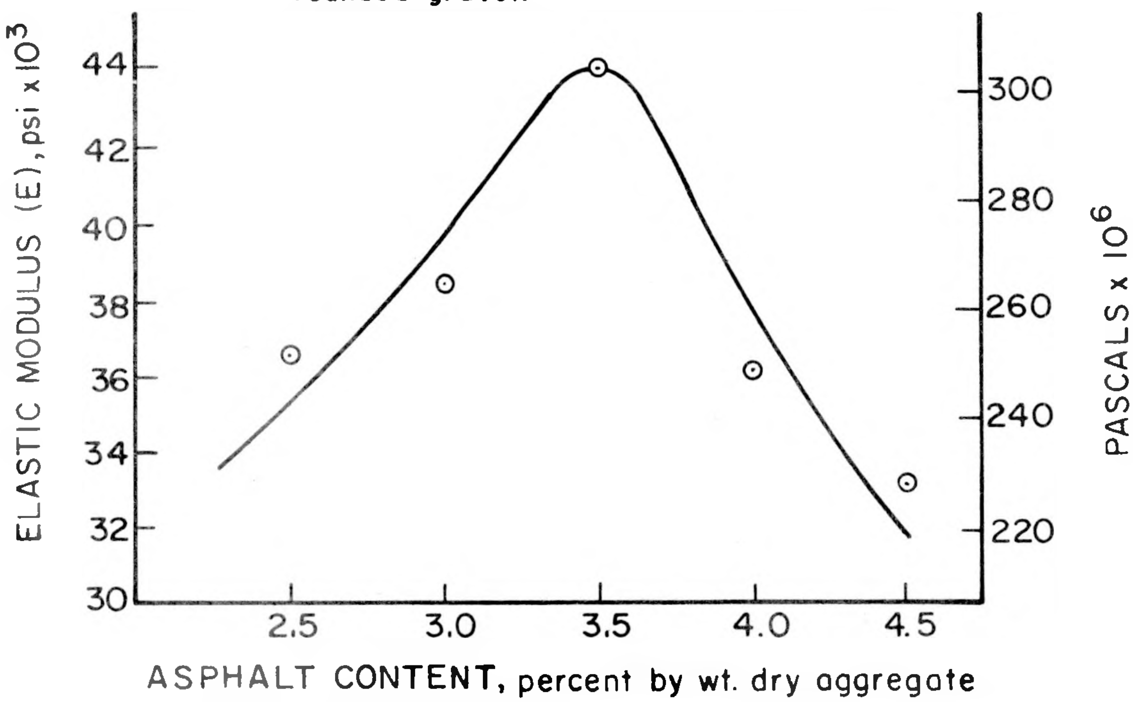

Figure B6. Splitting tensile modulus at failure for Hveem specimens at 68°F using rounded gravel.

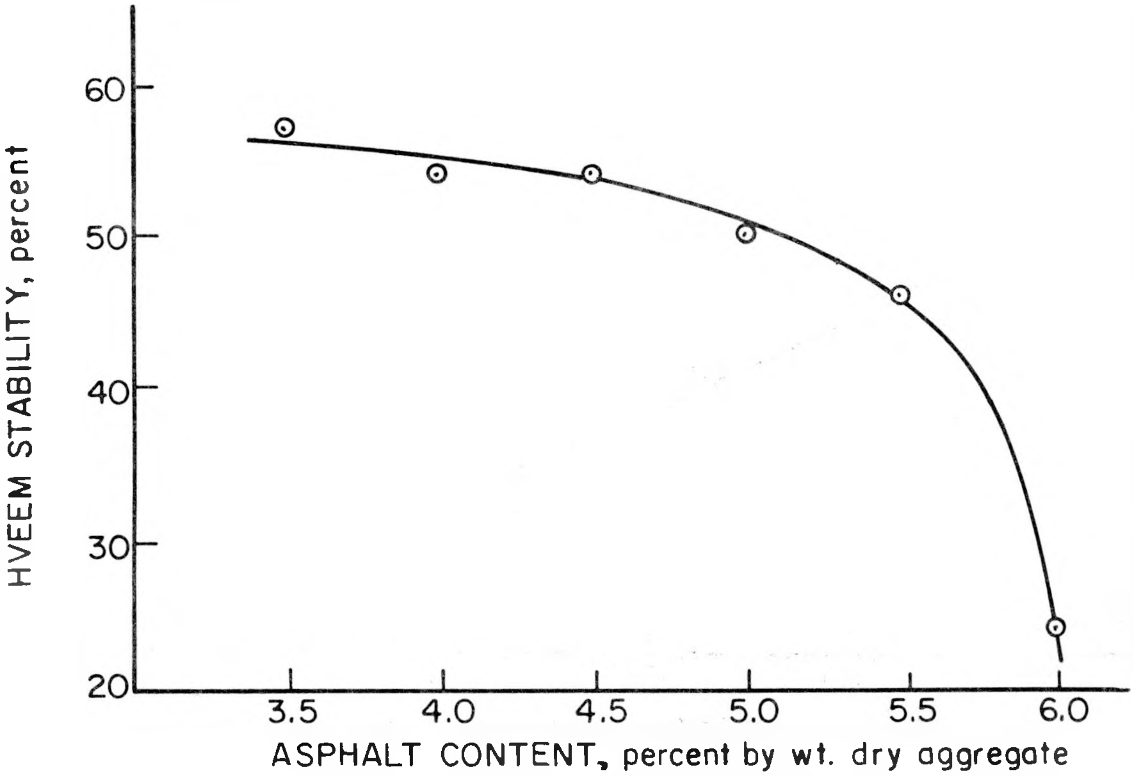

Figure B7. Hveem stability of specimens using crushed limestone.

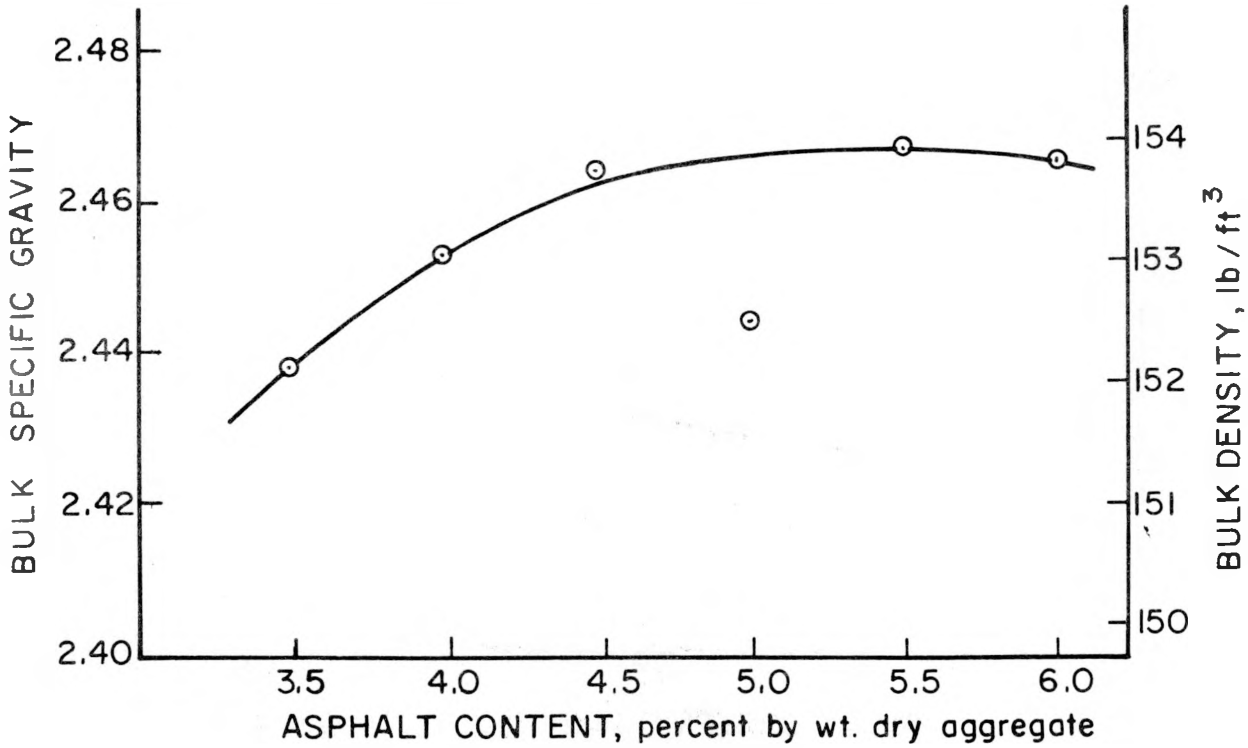

Figure B8. Bulk specific gravity of Hveem specimens using crushed limestone.

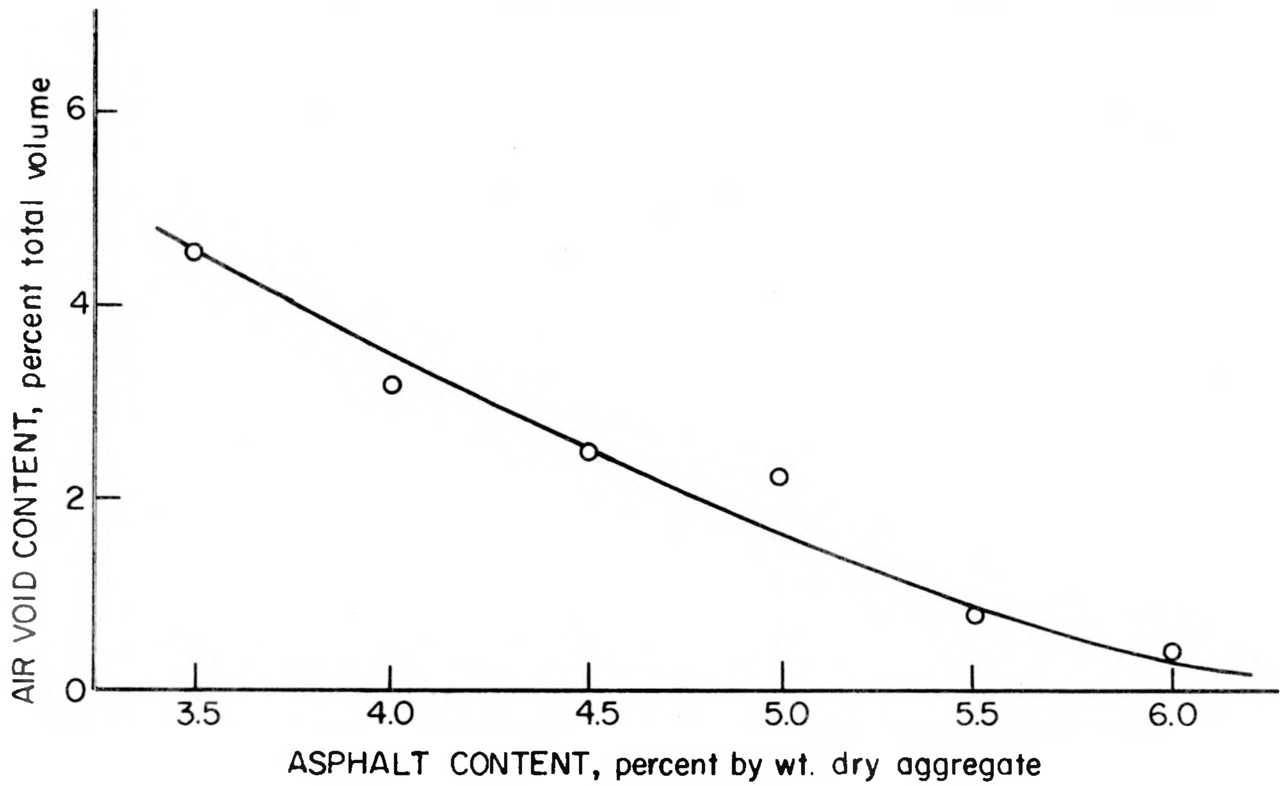

Figure B9. Air void content of Hveem specimens using crushed limestone.

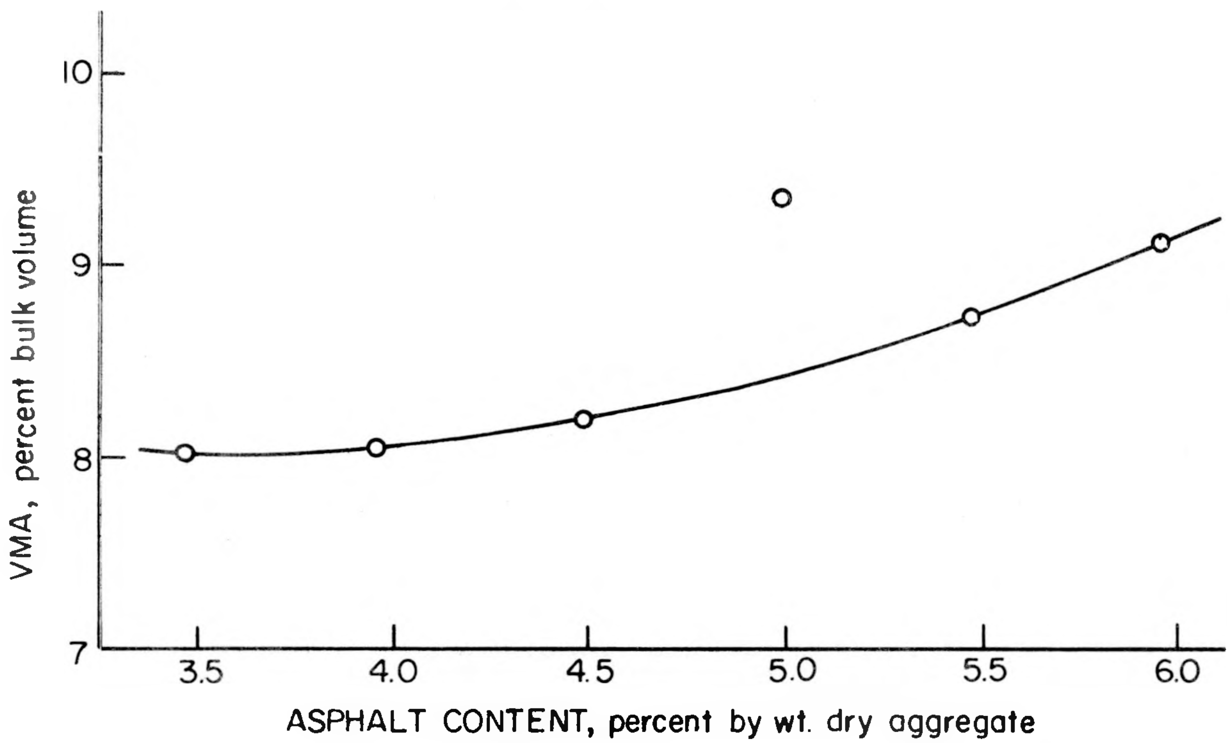

Figure B10. Voids in mineral aggregate for Hveem specimens using crushed limestone.

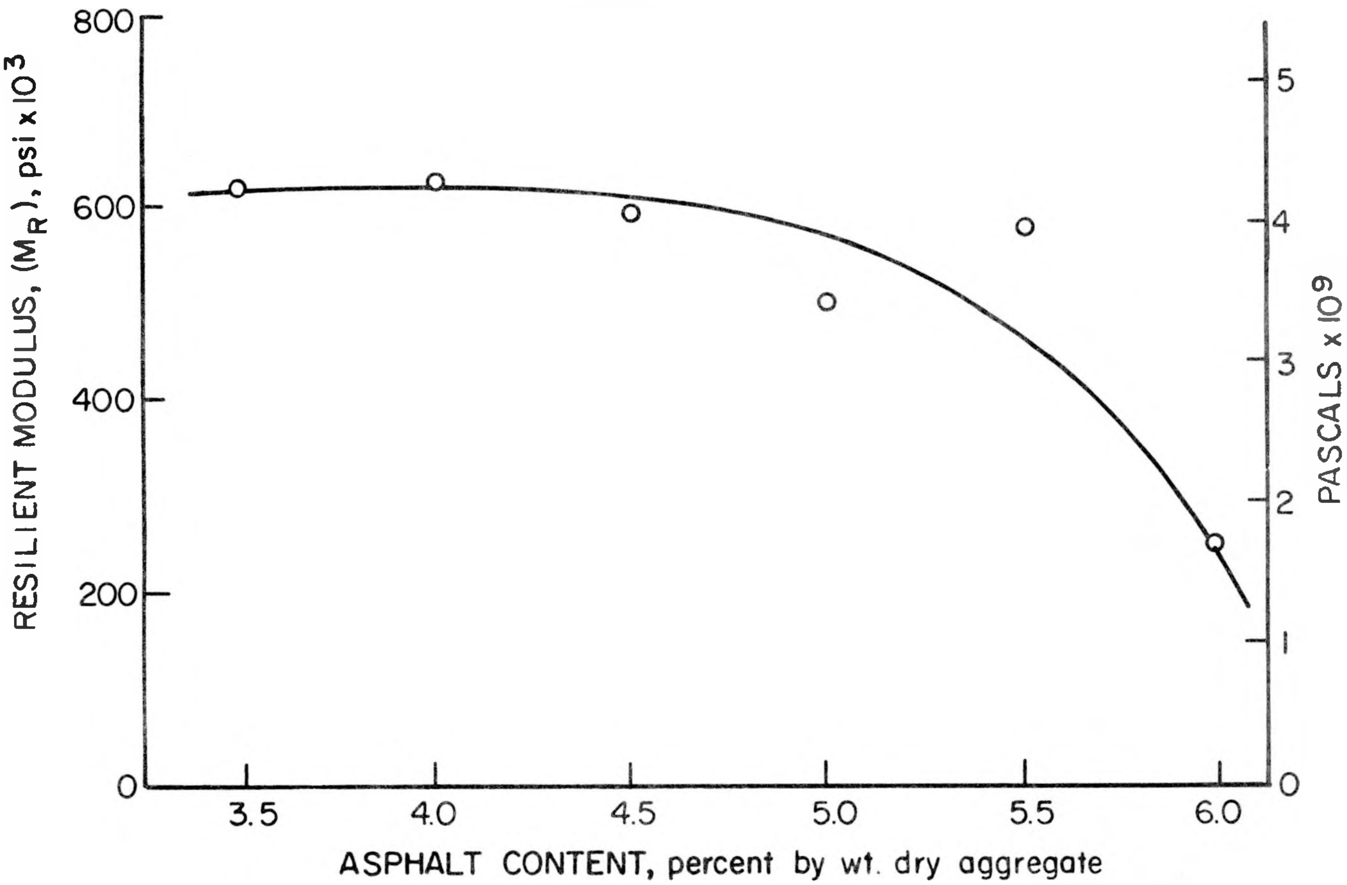

Figure B11. Resilient modulus of Hveem specimens at 68°F using crushed limestone.

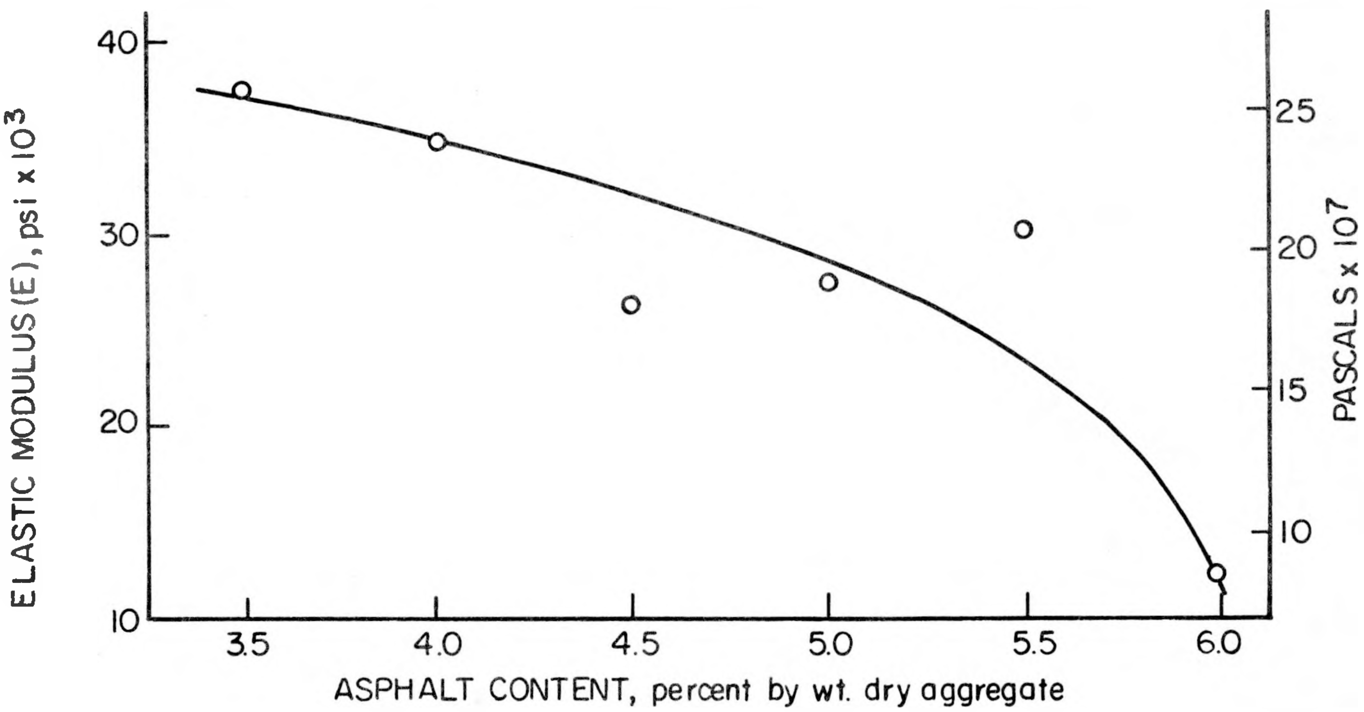

Figure B12. Splitting tensile modulus at failure for Hveem specimens at 68°F using crushed limestone.

APPENDIX C

Resilient Modulus Data for Individual Test Specimens

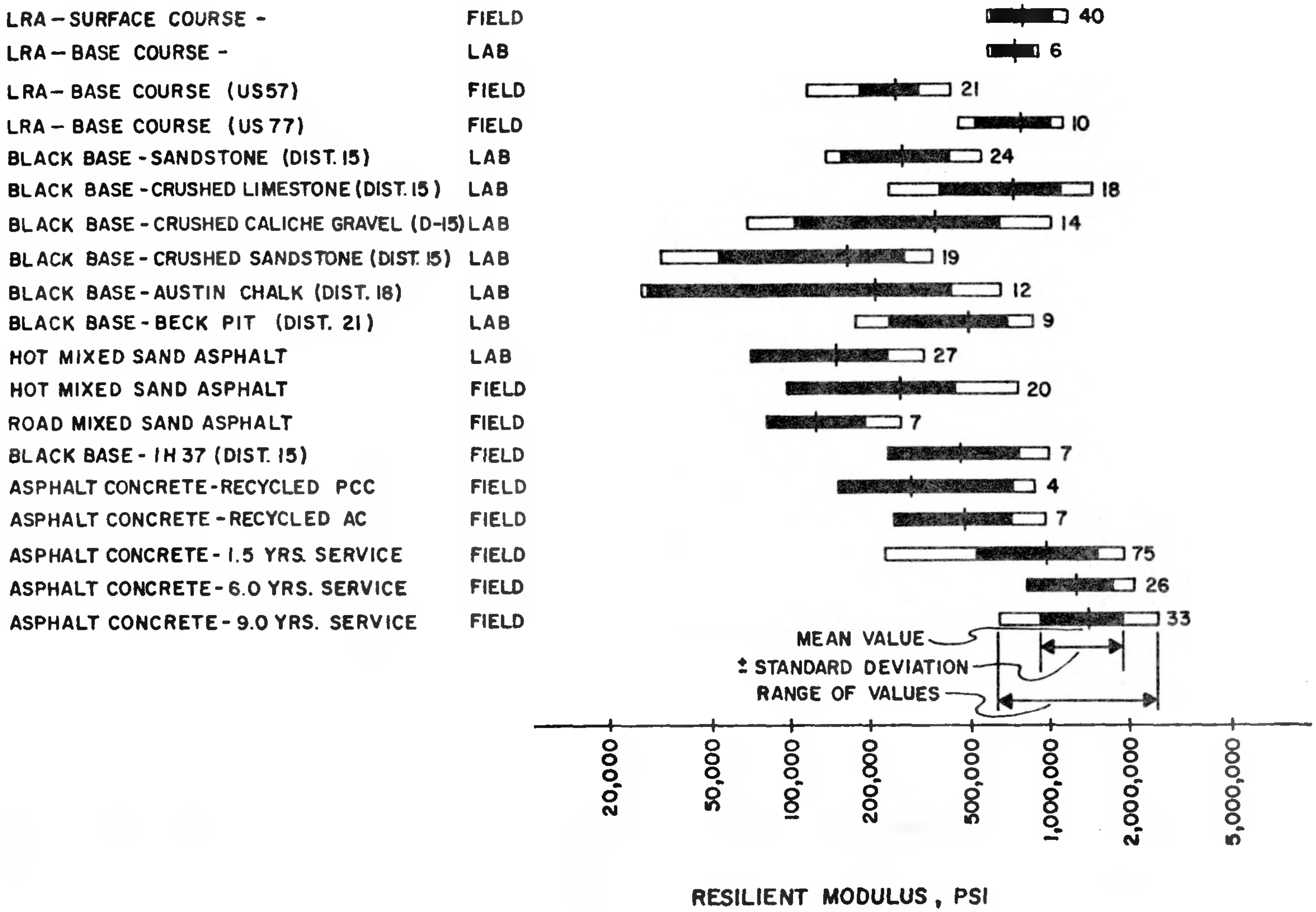

Figure C1. Ranges of Resilient Moduli at 73°F (23°C) for Various Types Asphalt-Aggregate Mixture.

TABLE C1. Resilient Modulus of Gyratory Compacted Specimens with Gravel

Lab Std		SO AC-5		SO AC-10		SO AC-20	
Sample Number	Resilient Modulus, psi x 10^{-6}	Sample Number	Resilient Modulus, psi x 10^{-6}	Sample Number	Resilient Modulus, psi x 10^{-6}	Sample Number	Resilient Modulus, psi x 10^{-6}
GA-1	0.48	S05-1	0.70	GDW-1	1.76	S020-1	1.21
GA-2	0.51	S05-2	0.66	GDW-2	1.98	S020-2	1.00
GA-3	0.51	S05-3	0.79	GDW-3	1.98	S020-3	1.07
GA-4	0.48	S05-4	0.97	GDW-4	2.06	S020-5	1.22
GA-5	0.52	S05-5	0.96	GDW-5	1.94	S020-5	1.14
GA-6	0.41	S05-6	0.78	GDW-6	1.93	S020-6	1.28
GA-7	0.53	S05-7	0.81	GDW-7	1.92	S020-7	1.09
GA-8	0.54	S05-8	0.91	GDW-8	2.12	S020-8	1.23
GA-9	0.51	S05-9	1.00	GDW-9	2.07	S020-9	1.20
GA-10	0.66	S05-10	1.01	GDW-10	2.12	S020-10	1.38
GA-11	0.47	S05-11	0.78	GDW-11	1.75	S020-11	1.04
GA-12	0.56	S05-12	0.73	GDW-12	1.82	S020-12	0.91
GA-13	----	S05-13	0.95	GDW-13	1.87	S020-13	1.38
GA-14	----	S05-14	0.75	GDW-14	1.78	S020-14	1.10
GA-15	----	S05-15	1.22	GDW-15	1.86	S020-15	1.29
GA-16	----	S05-16	1.03	GDW-16	1.96	S020-16	1.37
GA-17	----	S05-17	1.10	GDW-17	1.62	S020-17	1.38
GA-18	----	S05-18	1.14	GDW-18	1.79	S020-18	1.33
GA-19	----	S05-19	0.87	GDW-19	1.69	S020-19	1.61
GA-20	----	S05-20	0.91	GDW-20	1.66	S020-20	1.63
GA-21	----	S05-21	0.87	GDW-21	2.26	S020-21	1.07
GA-22	----	S05-22	0.99	GDW-22	1.91	S020-22	1.28
GA-23	----	S05-23	0.91	GDW-23	1.69	S020-23	1.16
GA-24	----	S05-24	0.95	GDW-24	1.94	S020-24	1.21
GA-25	----	S05-25	1.10	GDW-25	1.76	S020-25	1.55
GA-26	----	S05-26	1.04	GDW-26	1.86	S020-26	0.87
GA-27	----	S05-27	0.89	GDW-27	1.72	S020-27	1.15
GA-28	----	S05-28	1.09	GDW-27	1.72	S020-28	1.04
GA-29	----	S05-29	1.29	GDW-29	2.05	S020-29	1.18
GA-30	----	S05-30	1.29	GDW-30	1.74	S020-30	1.50

English to Metric Conversion: 1 psi = 6.895 x 10^3 pascals

TABLE C2. Resilient Modulus of Gyratory Compacted Specimens with Limestone

Lab Std		SO AC-5		SO AC-10		SO AC-20	
Sample Number	Resilient Modulus, psi x 10^{-6}	Sample Number	Resilient Modulus, psi x 10^{-6}	Sample Number	Resilient Modulus, psi x 10^{-6}	Sample Number	Resilient Modulus, psi x 10^{-6}
LA-1	0.63	S05-1	0.98	LDW-1	1.68	S020-1	1.43
LA-2	0.78	S05-2	0.86	LDW-2	1.74	S020-2	1.18
LA-3	0.71	S05-3	1.10	LDW-3	2.03	S020-1	1.62
LA-4	0.67	S05-4	1.07	LDW-4	1.96	S020-4	1.33
LA-5	0.77	S05-5	1.15	LDW-5	1.88	S020-5	1.73
LA-6	0.75	S05-6	1.12	LDW-6	2.00	S020-6	1.44
LA-7	0.67	S05-7	1.16	LDW-7	2.11	S020-7	1.36
LA-8	0.80	S05-8	1.05	LDW-8	2.20	S020-8	1.39
LA-9	0.56	S05-9	1.12	LDW-9	1.76	S020-9	1.48
LA-10	0.77	S05-10	0.88	LDW-10	2.10	S020-10	1.61
LA-11	0.83	S05-11	1.00	LDW-11	1.80	S020-11	1.23
LA-12	0.66	S05-12	1.17	LDW-12	2.13	S020-12	1.49
LA-13	0.73	S05-13	0.94	LDW-13	2.00	S020-13	1.27
LA-14	0.72	S05-14	0.93	LDW-14	2.12	S020-14	1.25
LA-15	0.82	S05-15	0.94	LDW-15	2.01	S020-15	1.73
LA-16	0.73	S05-16	1.06	LDW-16	2.07	S020-16	1.35
LA-17	0.66	S05-17	1.17	LDW-17	2.05	S020-17	1.12
LA-18	0.72	S05-18	1.04	LDW-18	1.99	S020-18	1.51
LA-19	0.79	S05-19	0.98	LDW-19	2.12	S020-19	1.44
LA-20	0.58	S05-20	0.92	LDW-20	1.94	S020-20	1.52
LA-21	0.80	S05-21	1.05	LDW-21	1.53	S020-21	1.41
LA-22	0.62	S05-22	1.05	LDW-22	1.69	S020-22	1.44
LA-23	0.42	S05-23	1.13	LDW-23	1.24	S020-23	1.44
LA-24	0.74	S05-24	1.15	LDW-24	2.03	S020-24	1.54
LA-25	0.74	S05-25	1.25	LDW-25	1.94	S020-25	1.49
LA-26	0.72	S05-26	1.25	LDW-26	2.04	S020-26	1.24
LA-27	0.74	S05-27	1.23	LDW-27	1.85	S020-27	1.28
LA-28	0.88	S05-28	1.14	LDW-28	2.00	S020-28	1.31
LA-29	0.72	S05-29	1.07	LDW-29	2.14	S020-29	1.58
LA-30	0.94	S05-30	1.03	LDW-30	2.25	S020-30	1.39

English to Metric Conversion: 1 psi = 6.895 x 10^3 pascals

APPENDIX D

Indirect Tension Test Data for Individual Test Specimens

TABLE D1. Splitting Tensile Test Data for Lab Std. Asphalt With Gravel

Displacement Rate, in/min. (cm/min)	Temperature °F (°C)	Sample Number	Stress* psi	Strain* in/in	Modulus* psi
2.0 (5.1)	68° (20°)	AG-8	110	0.0027	41,000
		AG-20	110	0.0031	35,000
		AG-24	110	0.0030	37,000
	33° (1°)	AG-4	320	0.0038	108,000
		AG-18	400	0.0025	160,000
		AG-28	460	0.0019	241,000
	-13° (-25°)	GA-1	.410	0.0010	430,000
		GA-9	520	0.0013	405,000
		GA-7	530	0.0015	358,000
0.20 (0.051)	68° (20°)	AG-9	50	0.0036	13,000
		AG-17	50	0.0061	8,000
		AG-25	50	0.0033	15,000
	33° (1°)	AG-22	270	0.0023	120,000
		AG-2	230	0.0019	123,000
		AG-12	260	0.0018	148,000
	-13° (-25°)	AG-6	370	0.0005	680,000
		AG-14	400	0.0007	586,000
		AG-27	380	0.0016	229,000
0.02 (0.051)	68° (20°)	AG-3	20	0.0047	5,000
		AG-13	20	0.0036	6,000
		AG-23	20	0.0039	5,000
	33° (1°)	AG-7	100	0.0014	73,000
		AG-19	110	0.0020	55,000
		AG-29	110	0.0022	50,000
	-13 (-25°)	GA-12	410	0.0010	417,000
		AG-26	330	0.0013	245,000
		AG-16	290	------	-------

* All values measured at the point of failure.

English to Metric Conversion: 1 psi = 6.895×10^3 pascals

TABLE D2. Splitting Tensile Data for SO AC-5 With Gravel

Displacement Rate in/min (cm/min)	Temperature °F (°C)	Sample Number	Stress*, psi	Strain*, in/in	Modulus*, psi
		S05-6	130	0.0033	39,000
	68° (20°)	S05-16	140	0.0025	60,000
		S05-26	160	0.0021	76,000
		S05-8	420	0.0013	331,000
2.0 (5.1)	38° (1°)	S05-18	430	0.0019	225,000
		S05-28	380	0.0008	505,000
		S05-1	300	0.0005	641,000
	-13 (-25°)	S05-11	410	0.0007	627,000
		S05-21	360	0.0006	606,000
		S05-9	70	0.0035	21,000
	68°(20°)	S05-19	80	0.0033	24,000
		S05-29	90	0.0029	30,000
		S05-2	390	0.0019	206,000
0.020 (0.051)	33° (1°)	S05-12	370	0.0019	191,000
		S05-22	390	0.0016	239,000
		S05-4	440	0.0007	628,000
	-13 (-25°)	S05-14	450	0.0009	504,000
		S05-24	490	0.0008	601,000
		S05-3	30	0.0030	11,000
	68° (20°)	S05-13	30	0.0033	10,000
		S05-23	30	0.0050	6,000
		S05-5	180	0.0019	94,000
0.002 0.051)	33° (1°)	S05-15	70	0.0028	25,000
		S05-25	90	0.0014	64,000
		S05-7	300	0.0012	251,000
	-13 (-25°)	S05-17	270	0.0010	272,000
		S05-27	240	0.0011	215,000

*All values measured at the point of failure.

English to Metric Conversion: 1 psi = 6.895×10^3 pascals

TABLE D3. Splitting Tensile Test Data for SO AC-10 with Gravel

Displacement Rate in/min (cm/min)	Temperature °F (°C)	Sample Number	Stress* psi	Strain* in/in	Modulus* psi
2.0 (5.1)	68 (20)	GDW-24	300	0.0045**	67,000
		GDW-9	310	0.0032**	97,000
		GDW-7	310	0.0038**	82,000
	33 (1)	GDW-3	390	0.0004	1,112,000
		GDW-11	520	0.0003	1,520,000
		GDW-25	440	0.0014**	311,000
	-13 (-25)	GDW-17	340	0.0003	1,287,000
		GDW-6	350	0.0003	1,399,000
		GDW-20	320	0.0007**	439,000
0.20 (0.51)	68 (20)	GDW-19	340	0.0020	164,000
		GDW-18	180	0.0041	44,000
		GDW-4	180	0.0034	53,000
	33 (1)	GDW-21	330	0.0016	208,000
		GDW-5	360	0.0011	327,000
		GDW-28	505	0.0021**	236,000
	-13 (-25)	GDW-8	360	0.0007	542,000
		GDW-2	350	0.0007	499,000
		GDW-14	390	0.0012	329,000
0.02 (0.051)	68 (20)	GDW-13	60	0.0050	13,000
		GDW-29	90	0.0045**	20,000
		GDW-14	100	0.0049**	20,000
	33 (1)	GDW-10	170	0.0022	77,000
		GDW-15	320	0.0025	126,000
		GDW-23	---	------	-------
	-13 (-25)	GDW-16	390	0.0014	271,000
		GDW-22	---	------	-------
		GDW-27	---	------	-------

*All values measured at the point of failure
English to Metric Conversion: 1 psi = 6.895×10^3 pascals
**Strain was computed based on vertical deformation of specimen.

TABLE D4. Splitting Tensile Test Data for SO AC-20 With Gravel

Displacement Rate, in/min. (cm/min)	Temperature °F (°C)	Sample Number	Stress*, psi	Strain*, in/in	Modulus*, psi
2.0 (5.1)	68° (20°)	S020-1	160	0.0016	104,000
		S020-11	170	0.0039	45,000
		S020-21	160	0.0020	77,000
	33° (1°)	S020-6	400	0.0010	408,000
		S020-16	390	0.0010	396,000
		S020-26	410	0.0008	544,000
	-13°(-25°)	S020-8	360	0.0004	904,000
		S020-18	380	0.0007	525,000
		S020-28	360	0.0006	575,000
0.020 (0.51)	68° (20°)	S020-4	100	0.0015	62,000
		S020-14	100	0.0028	36,000
		S020-24	110	0.0027	39,000
	33° (1°)	S020-9	300	0.0017	175,000
		S020-19	270	0.0015	181,000
		S020-29	330	0.0010	340,000
	-13°(-25°)	S020-2	390	0.0008	490,000
		S020-12	520	0.0007	710,000
		S020-22	440	0.0012	356,000
0.02 (0.051)	68° (20°)	S020-7	70	0.0028	23,000
		S020-17	70	0.0026	30,000
		S020-27	60	0.0007	36,000
	33° (1°)	S020-3	360	0.0008	476,000
		S020-13	300	0.0010	317,000
		S020-23	370	0.0015	252,000
	-13° (-25°)	S020-5	390	0.0009	446,000
		S020-15	400	0.0010	418,000
		S020-25	430	0.0015	291,000

* All values measured at the point of failure.

English to Metric Conversion: 1 psi = 6.895×10^3 pascals.

TABLE D5. Splitting Tensile Test Data for Lab Std. Asphalt With Limestone

Displacement Rate, in/min (cm/min)	Temperature °F (°C)	Sample Number	Stress*, psi	Strain*, in/in	Modulus*, psi
2.0 (5.1)	68° (20°)	LA-6	140	0.0023	60,000
		LA-14	150	0.0026	58,000
		LA-30	150	0.0025	62,000
	33° (1°)	LA-19	530	0.0018	293,000
		LA-13	490	0.0018	273,000
		LA-17	530	0.0017	308,000
	-13° (-25°)	LA-2	650	0.0015	437,000
		LA-38	600	0.0009	669,000
		LA-15	---	------	-------
0.20 (0.51)	68° (20°)	LA-16	120	0.0047	26,000
		LA-9	80	0.0045	17,000
		LA-8	80	0.0032	26,000
	33° (1°)	LA-24	330	0.0019	179,000
		LA-27	310	0.0023	139,000
		LA-8	290	0.0022	131,000
	-13° (-25°)	LA-7	600	0.0040	158,000
		LA-10	610	0.0021	293,000
		LA-23	670	------	-------
0.02 (0.051)	68° (20°)	LA-20	40	0.0041	11,000
		LA-26	40	0.0039	11,000
		LA-4	40	0.0040	10,000
	33° (1°)	LA-3	140	0.0021	65,000
		LA-22	150	0.0020	78,000
		LA-29	140	0.0022	65,000
	-13° (-25°)	LA-5	380	0.0026	147,000
		LA-12	380	0.0032	117,000
		LA-18	460	0.0031	205,000

* All values measured at the point of failure.

English to Metric Conversion: 1 psi = 6.895×10^3 pascals.

TABLE D6. Splitting Tensile Test Data for SO AC-5 With Limestone

Displacement Rate, in/min (cm/min)	Temperature °F (°C)	Sample Number	Stress*, psi	Strain*, in/in	Modulus*, psi
2.0 (5.1)	68° (20°)	S05-3	140	0.0018	79,000
		S05-13	130	0.0035	37,000
		S05-23	130	0.0015	90,000
	33° (1°)	S05-8	---	------	------
		S05-18	470	0.0011	419,000
		S05-28	490	0.0010	505,000
	-13° (-25°)	S05-1	480	0.0006	870,000
		S05-11	450	0.0012	382,000
		S05-21	580	0.0014	408,000
0.02	68° (20°)	S05-9	70	0.0033	20,000
		S05-19	60	0.0037	17,000
		S05-29	70	0.0033	21,000
	33° (1°)	S05-2	360	0.0010	356,000
		S05-12	460	0.0016	280,000
		S05-22	440	0.0012	376,000
	-13° (-25°)	S05-4	580	0.0012	468,000
		S05-14	490	0.0013	375,000
		S05-24	540	0.0009	595,000
0.02 (0.051)	68° (20°)	S05-6	40	0.0029	13,000
		S05-16	40	0.0026	14,000
		S05-26	30	0.0030	10,000
	33° (1°)	S05-5	450	0.0013	342,000
		S05-15	480	0.0015	327,000
		S05-25	470	0.0014	352,000
	-13° (-25°)	S05-7	550	0.0008	708,000
		S05-17	500	0.0013	398,000
		S05-27	450	0.0013	388,000

* All values measured at the point of failure.

English to Metric Conversion: 1 psi = 6.895×10^3 pascals.

TABLE D7. Splitting Tensile Test Data for SO AC-10 with Limestone

Displacement Rate in/min (cm/min)	Temperature °F(°C)	Sample Number	Stress* psi	Strain* in/in	Modulus* psi
		LDW-7	250	0.0024**	104,000
	68 (20)	LDW-19	240	0.0033**	73,000
		LDW-24	260	0.0029**	90,000
		LDW-15	590	0.0004	1,382,000
2.0	33 (1)	LDW-3	540	0.0008	700,000
(5.1)		LDW-11	640	0.0005	1,185,000
		LDW-17	520	0.0004	1,300,000
	-13 (-25)	LDW-6	430	0.0005	814,000
		LDW-26	450	0.0006**	750,000
		LDW-12	280	0.0025	111,000
	68 (20)	LDW-9	350	0.0026	137,000
		LDW-4	180	0.0040	45,000
		LDW-18	540	0.0011	475,000
0.20	33 (1)	LDW-5	470	0.0020	137,000
(0.51)		LDW-28	450	0.0012**	375,000
		LDW-2	400	0.0013**	308,000
	-13 (-25)	LDW-8	440	0.0009	497,000
		LDW-30	562	0.0010**	562,000
		LDW-20	90	0.0046	19,000
	68 (20)	LDW-13	80	0.0041	20,000
		LDW-29	90	0.0039**	23,000
		LDW-14	370	0.0023	163,000
0.02	33 (1)	LDW-10	390	0.0016	237,000
(0.051)		LDW-23	---	------	-------
		LDW-22	450	0.0033	138,000
	-13 (-25)	LDW-16	500	0.0014	271,000
		LDW-21	---	------	-------

*All values measured at the point of failure
English to Metric Conversion: 1 psi = 6.895×10^3 pascals

**Strain was computed based on vertical deformation of specimen.

TABLE D8. Splitting Tensile Test Data for SO AC-20 With Limestone

Displacement Rate in/min (cm/min)	Temperature °F (°C)	Sample Number	Stress*, psi	Strain*, in/in	Modulus*, psi
2.0 (5.1)	68° (20°)	S020-1	180	0.0016	116,000
		S020-4	100	0.0020	49,000
		S020-7	180	0.0015	117,000
	33° (1°)	S020-6	510	0.0010	518,000
		S020-16	500	0.0010	513,000
		S020-26	500	0.0012	406,000
	-13° (-25°)	S020-8	530	0.0011	497,000
		S020-18	620	0.0010	619,000
		S020-28	620	0.0009	676,000
0.20 (0.51)	68° (20°)	S020-11	110	0.0014	78,000
		S020-17	130	0.0020	63,000
		S020-27	110	------	-------
	33° (1°)	S020-9	370	0.0015	255,000
		S020-19	410	0.0013	306,000
		S020-29	420	0.0015	285,000
	-13° (-25°)	S020-2	640	0.0011	562,000
		S020-12	610	0.0012	527,000
		S020-22	560	0.0013	415,000
0.02 (0.051)	68° (20°)	S020-21	70	0.0025	28,000
		S020-14	70	0.0023	33,000
		S020-24	70	0.0021	35,000
	33° (1°)	S020-3	200	0.0016	121,000
		S020-13	210	0.0015	147,000
		S020-23	180	0.0019	93,000
	-13° (-25°)	S020-5	580	0.0013	450,000
		S020-15	530	0.0015	343,000
		S020-25	600	0.0010	590,000

* All values measured at the point of failure.

English to Metric Conversion: 1 psi = 6.895×10^3 pascals.

TABLE D9. Splitting Tensile Test Data for Water Saturated Samples*

Aggregate	Asphalt	Sample Number	Stress,* psi	Strain,* in/in	Modulus,* psi
Gravel	Lab Std	GA-2	100	0.0043	27,000
		GA-6	100	0.0057	17,000
		GA-11	100	0.0063	15,000
	SO AC-5	S05-19	180	0.0026	68,000
		S05-20	210	0.0028	74,000
		S05-30	210	0.0024	86,000
	SO AC-10	GDW-22	180	0.0027	66,000
		GDW-20	220	0.0032	66,000
		GDW-10	190	0.0054	34,000
	SO AC-20	S020-10	210	0.0018	117,000
		S020-20	240	0.0020	121,000
		S020-30	230	0.0021	102,000
Limestone	Lab Std.	LA-1	90	0.0041	21,000
		LA-11	100	0.0086	11,000
		LA-21	80	0.0051	16,000
	SO AC-5	S05-10	110	0.0038	30,000
		S05-20	120	0.0044	28,000
		S05-30	130	0.0033	39,000
	SO AC-10	LDW-22	170	0.0024	72,000
		LDW-10	190	0.0038	49,000
		LDW-8	200	0.0030	67,000
	SO AC-20	S020-10	220	0.0023	96,000
		S020-20	250	0.0020	126,000
		S020-30	250	0.0024	105,000

* All tested at 68°F (20°C) at a rate of 2.0 in/min (5.08 cm/min.)

English to Metric Conversion: 1 psi = 6.895×10^3 pascals.

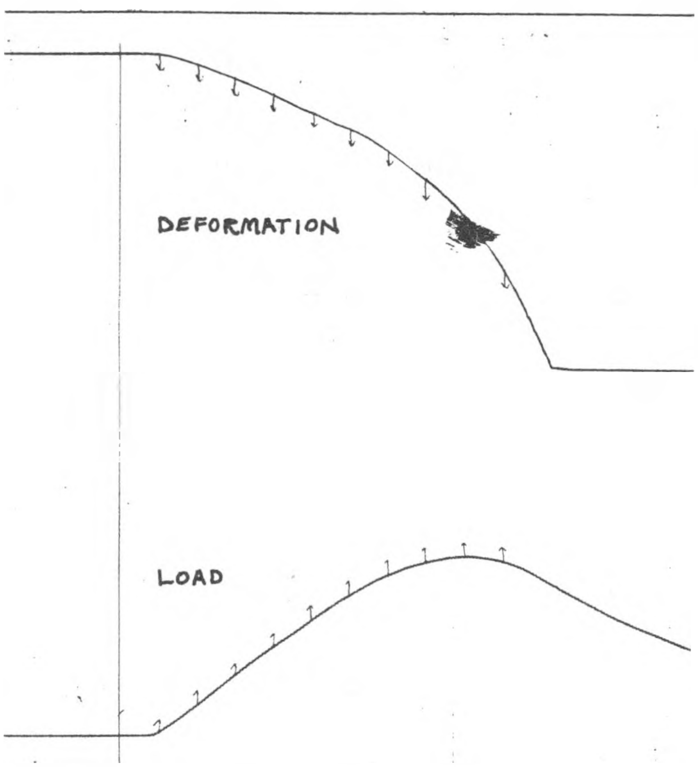

FIGURE D1. Splitting Tensile Test at 2 in/min (5.1 cm/min) and 68°F (20°C)

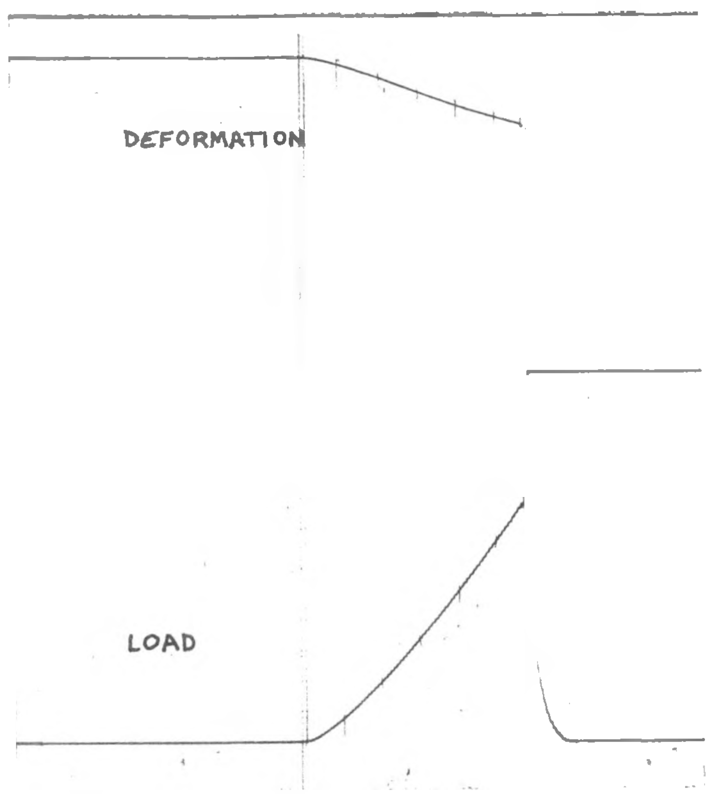

FIGURE D2. Splitting Tensile Test at 2 in/min (5.1 cm/min) and -10°F (25°C)

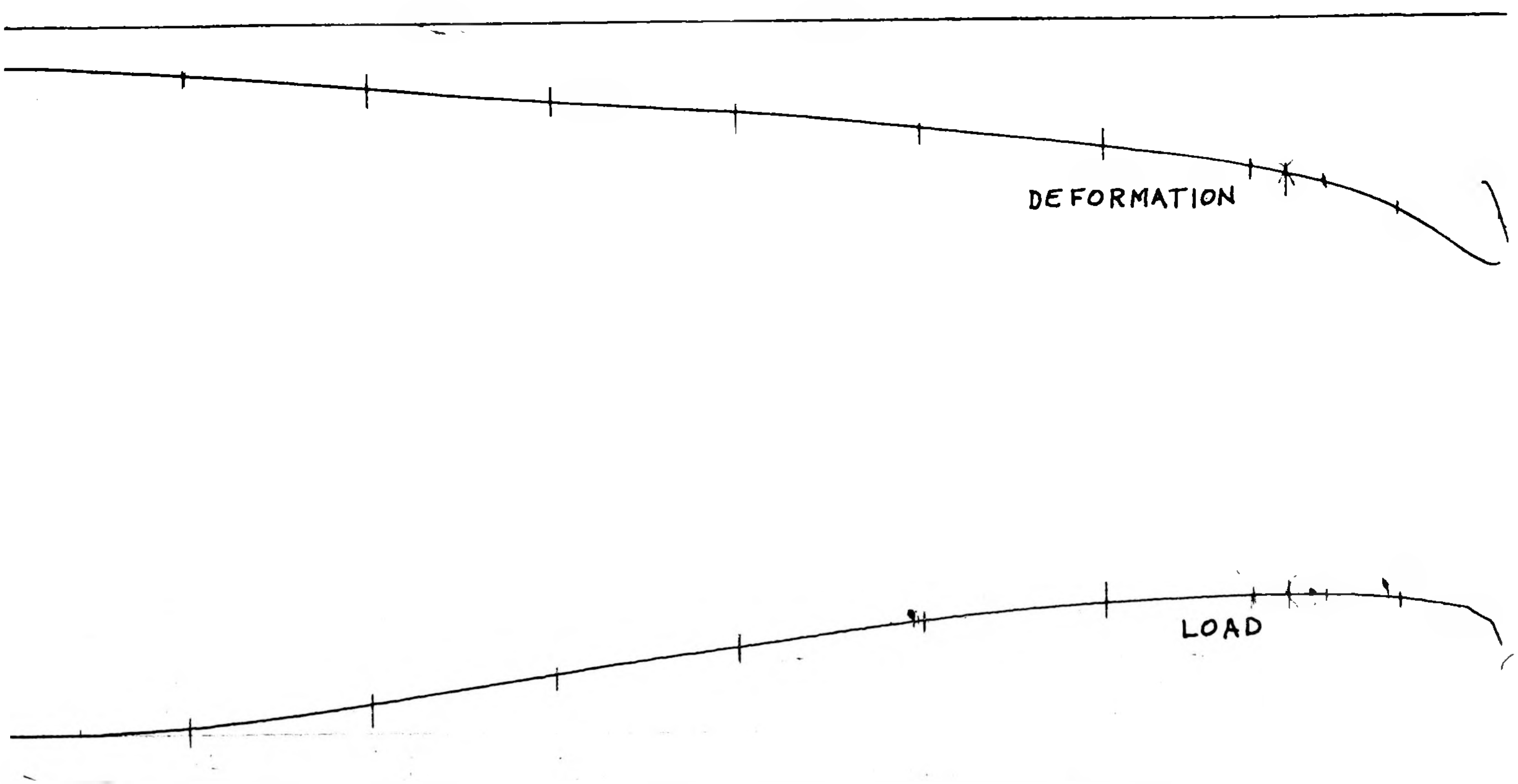

FIGURE D3. Splitting Tensile Test at 0.02 in/min (0.051 cm/min) and 33°F (1°C)

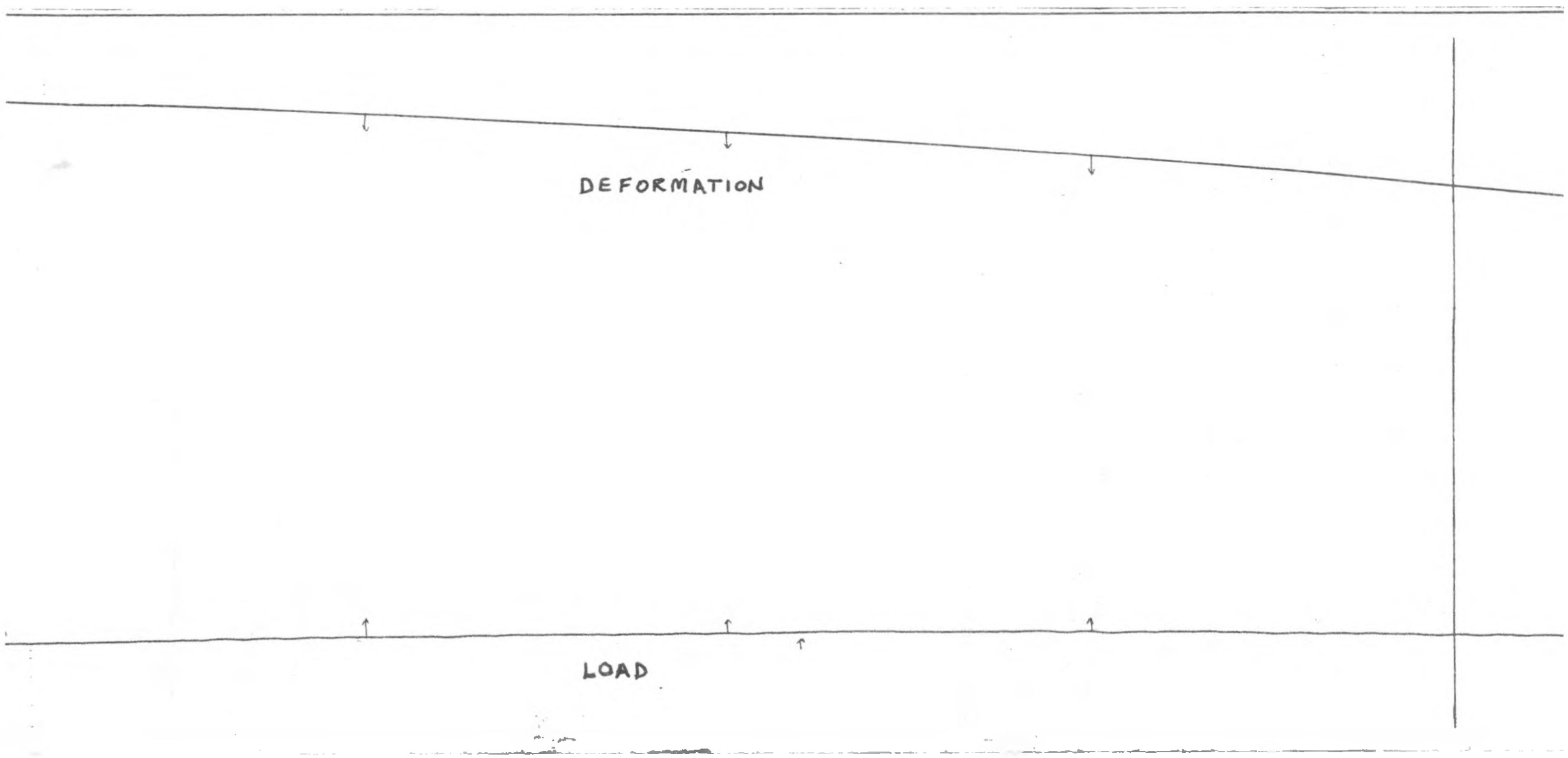

FIGURE D4. Splitting Tensile Test at 0.02 in/min (0.051 cm/min) and 68°F (20°C)

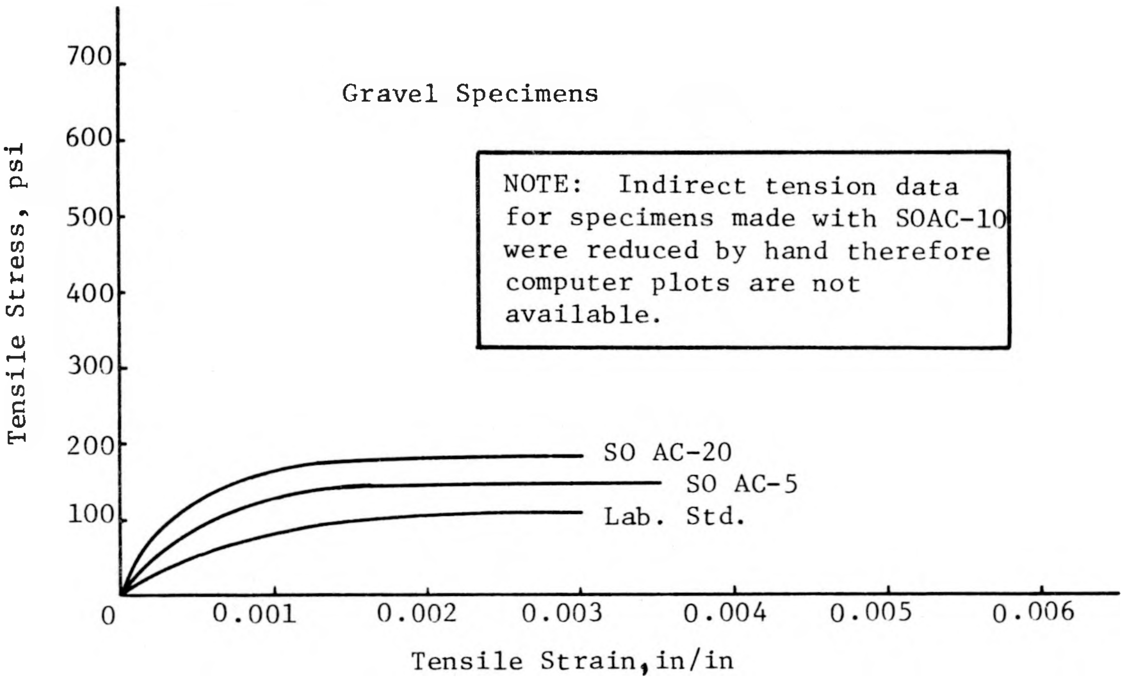

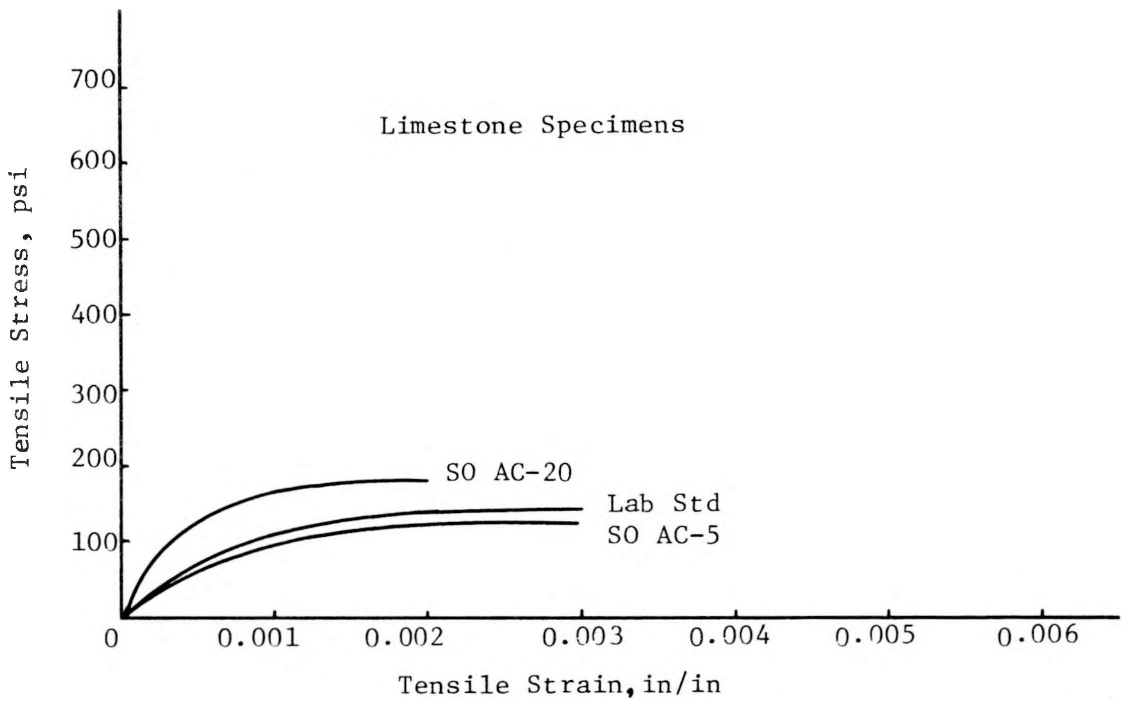

Figure D5. Sketches of Computer Plots from Splitting Tensile Tests at 68°F (20°C) and 2 in/min (5.1 cm/min)

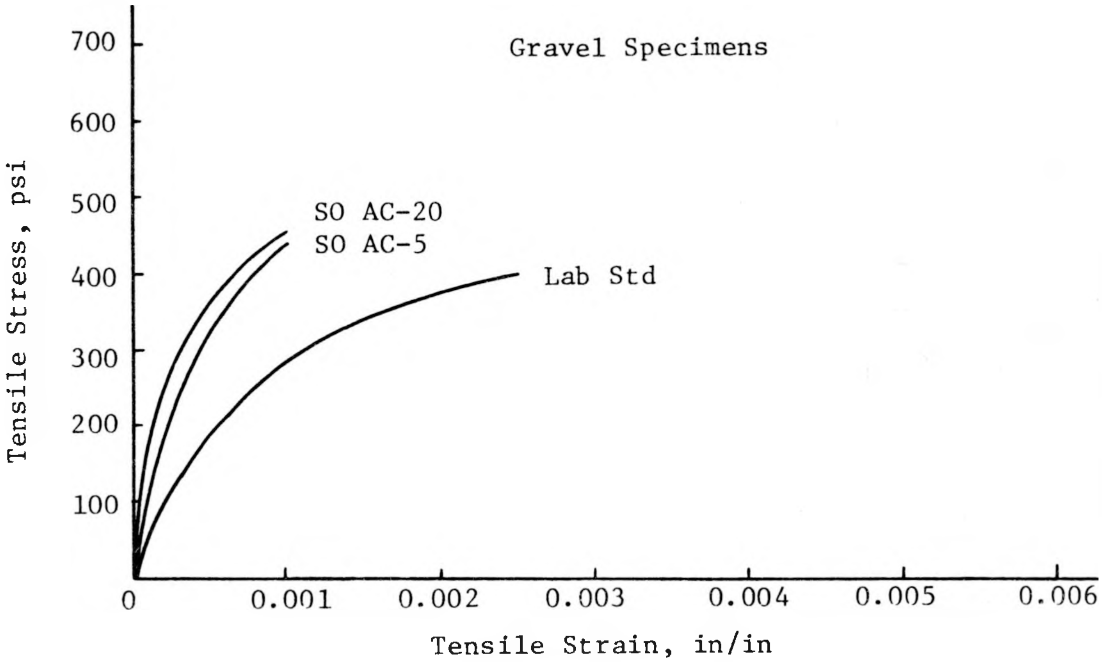

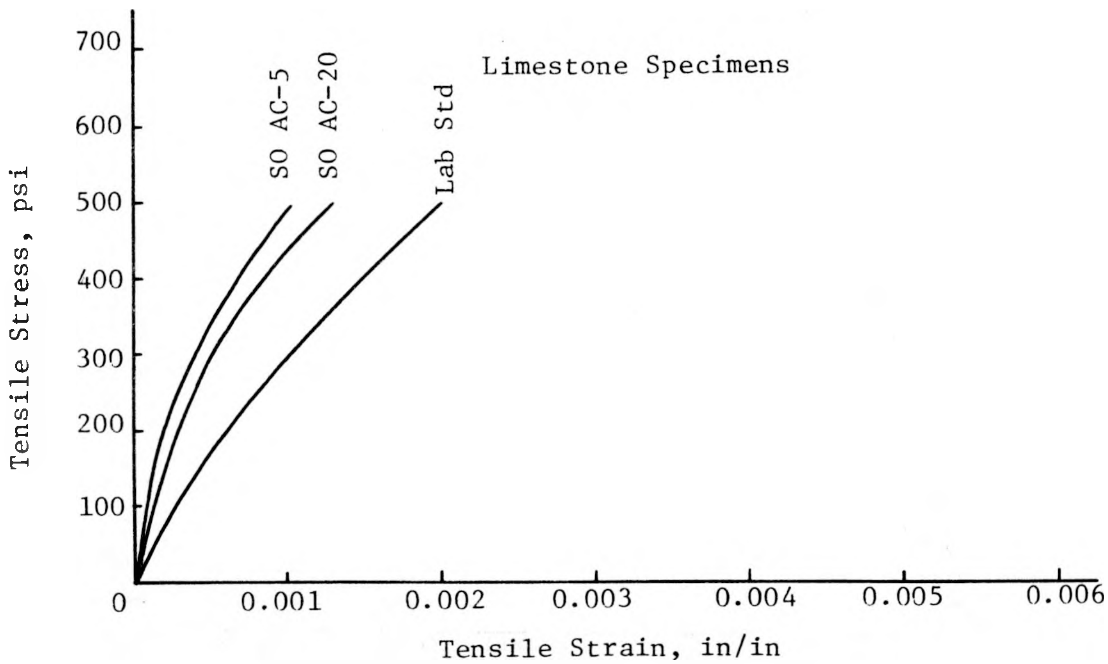

Figure D6. Sketches of Computer Plots from Splitting Tensile Tests at 33°F (1°C) and 2 in/min (5.1 cm/min)

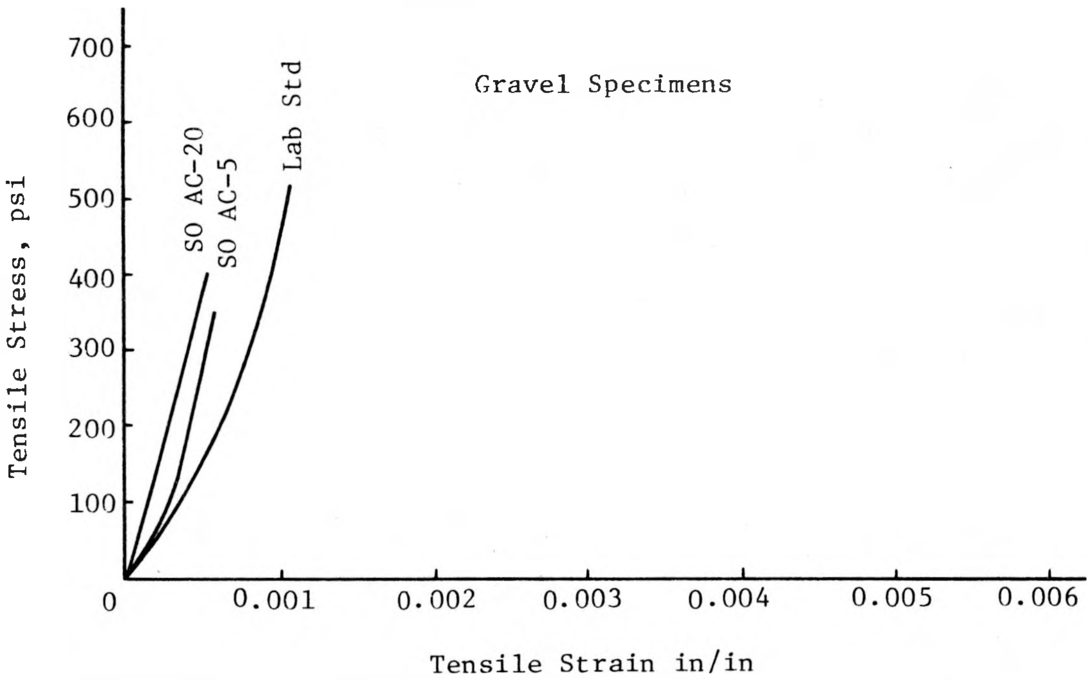

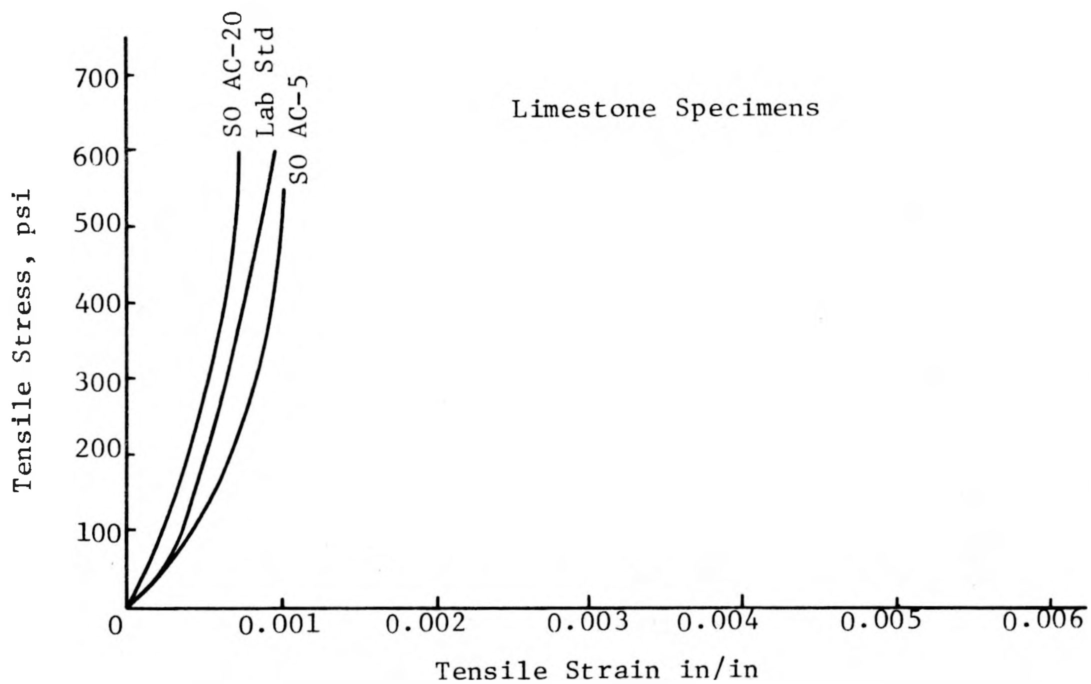

Figure D7. Sketches of Computer Plots from Splitting Tensile Tests at -13°F (-25°C) and 2 in/min (5.1 cm/min)

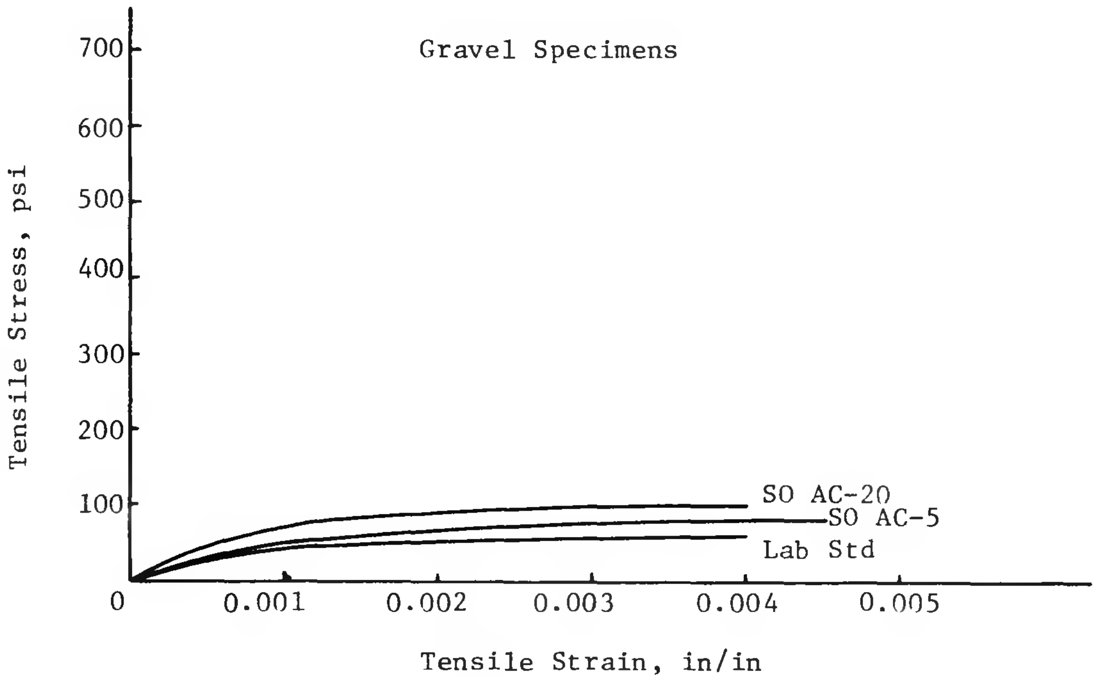

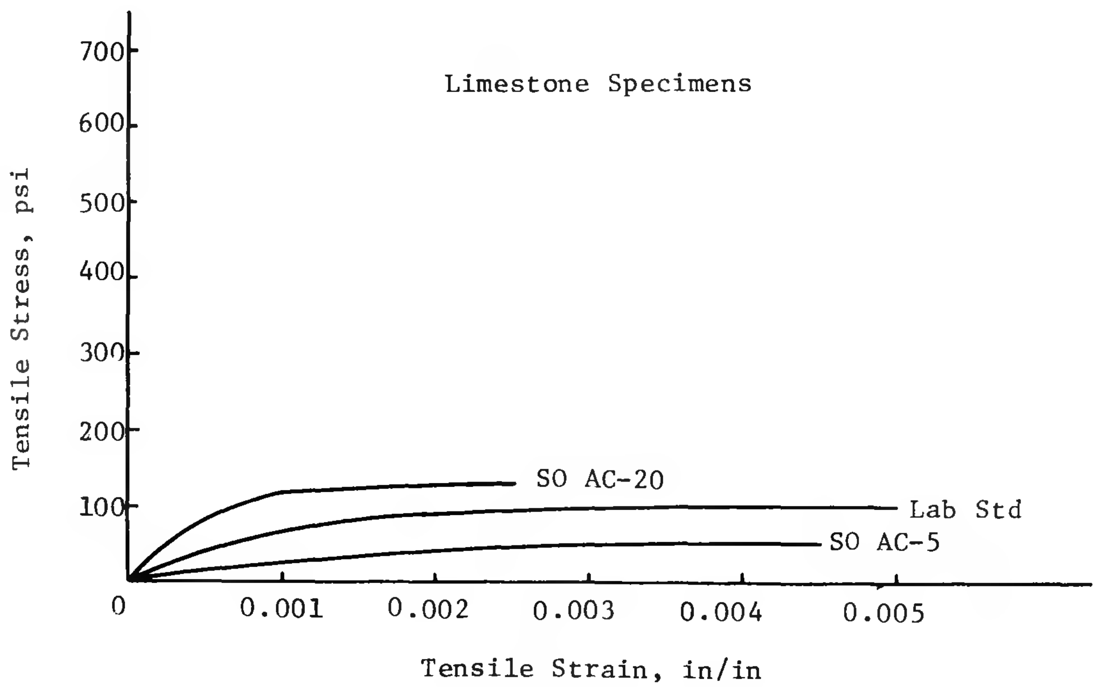

Figure D8. Sketches of Computer Plots from Splitting Tensile Tests at 68°F (20°C) and 0.2 in/min (0.51 cm/min)

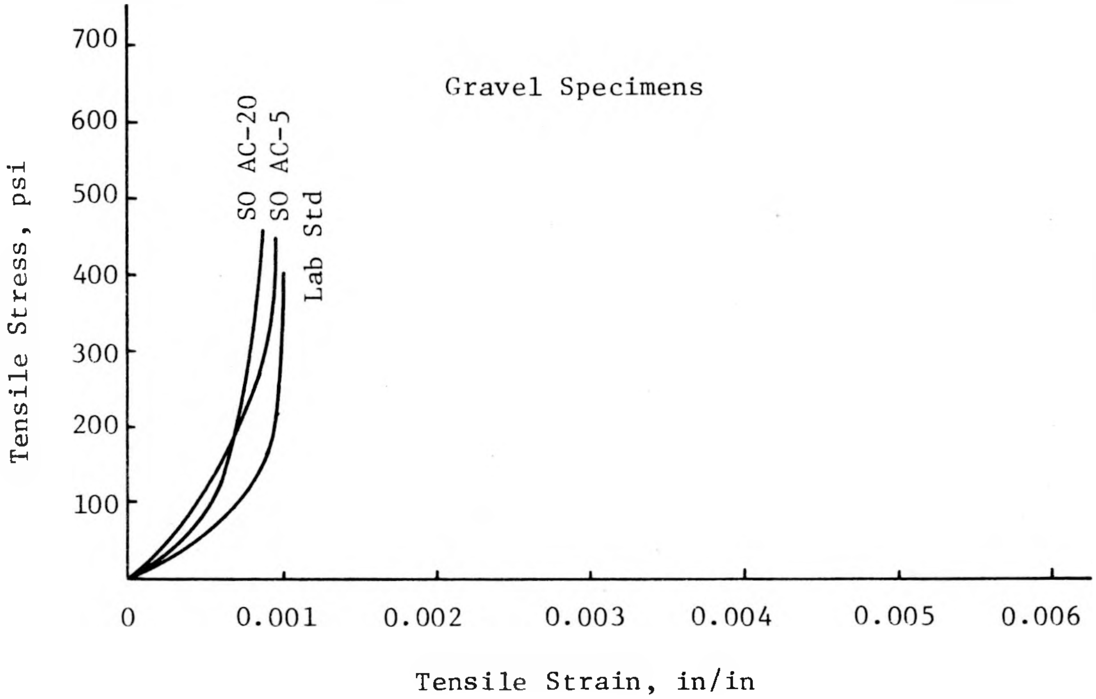

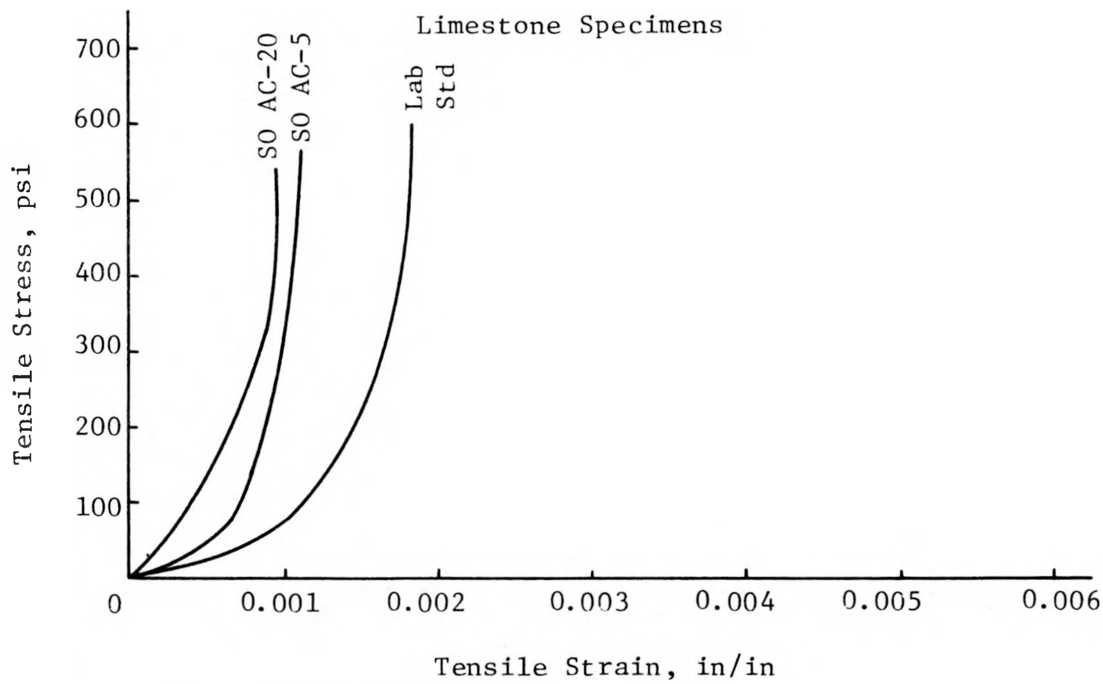

Figure D10. Sketches of Computer Plots from Splitting Tensile Tests at -13°F (-25°C) and 0.2 in/min (0.51 cm/min)

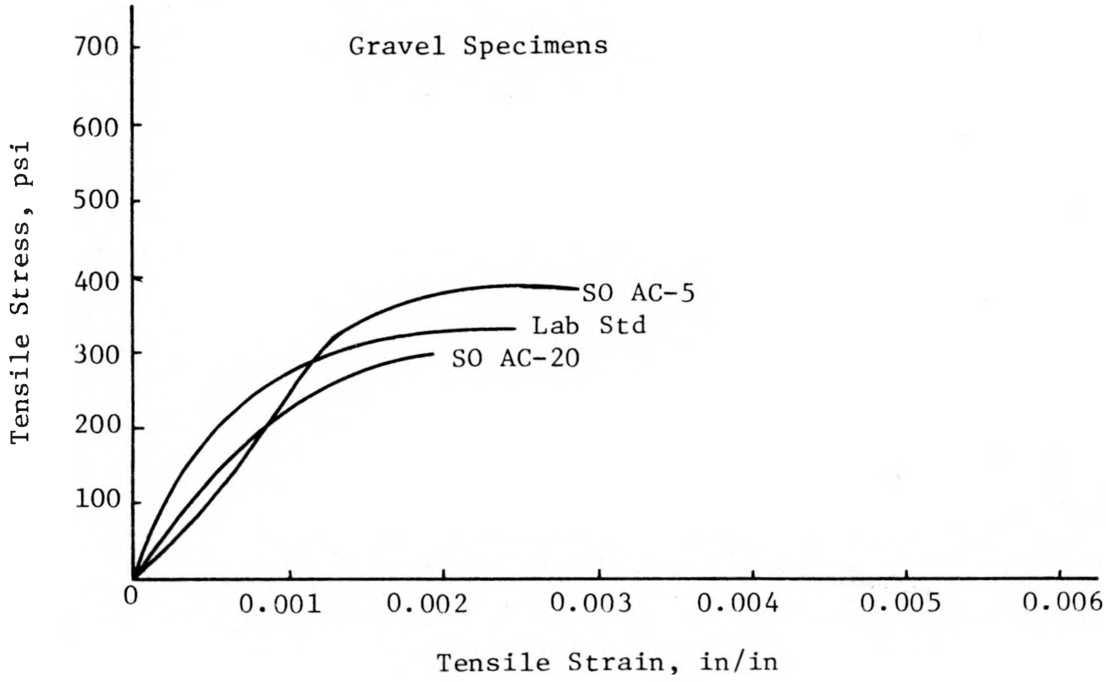

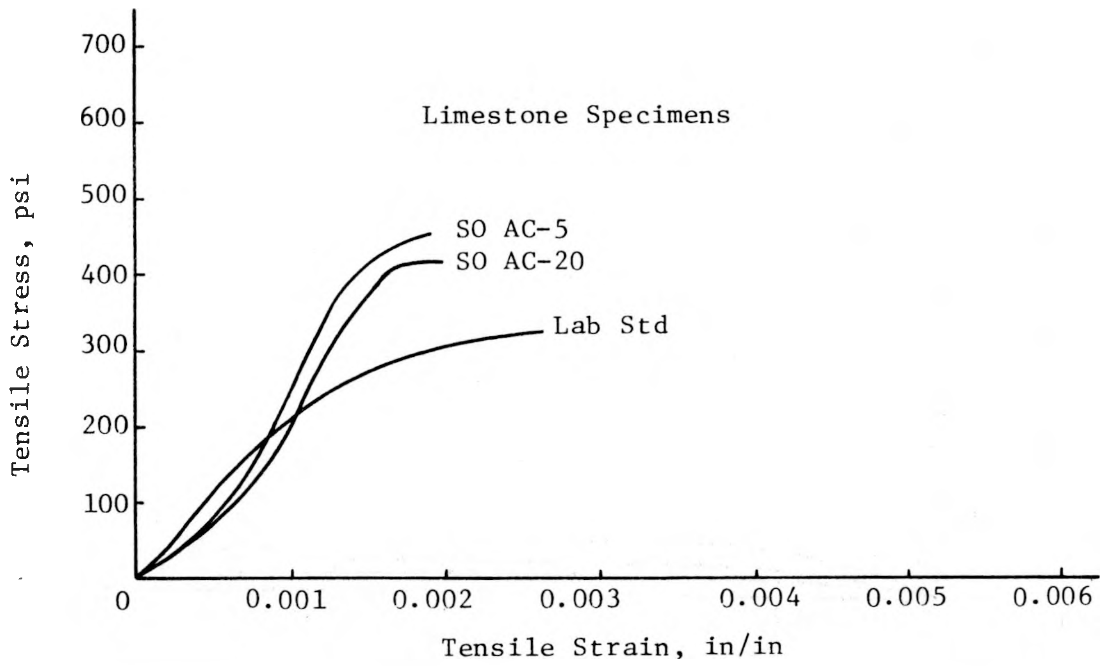

Figure D9. Sketches of Computer Plots from Splitting Tensile Tests at 33°F (1°C) and 0.2 in/min (0.51 cm/min)

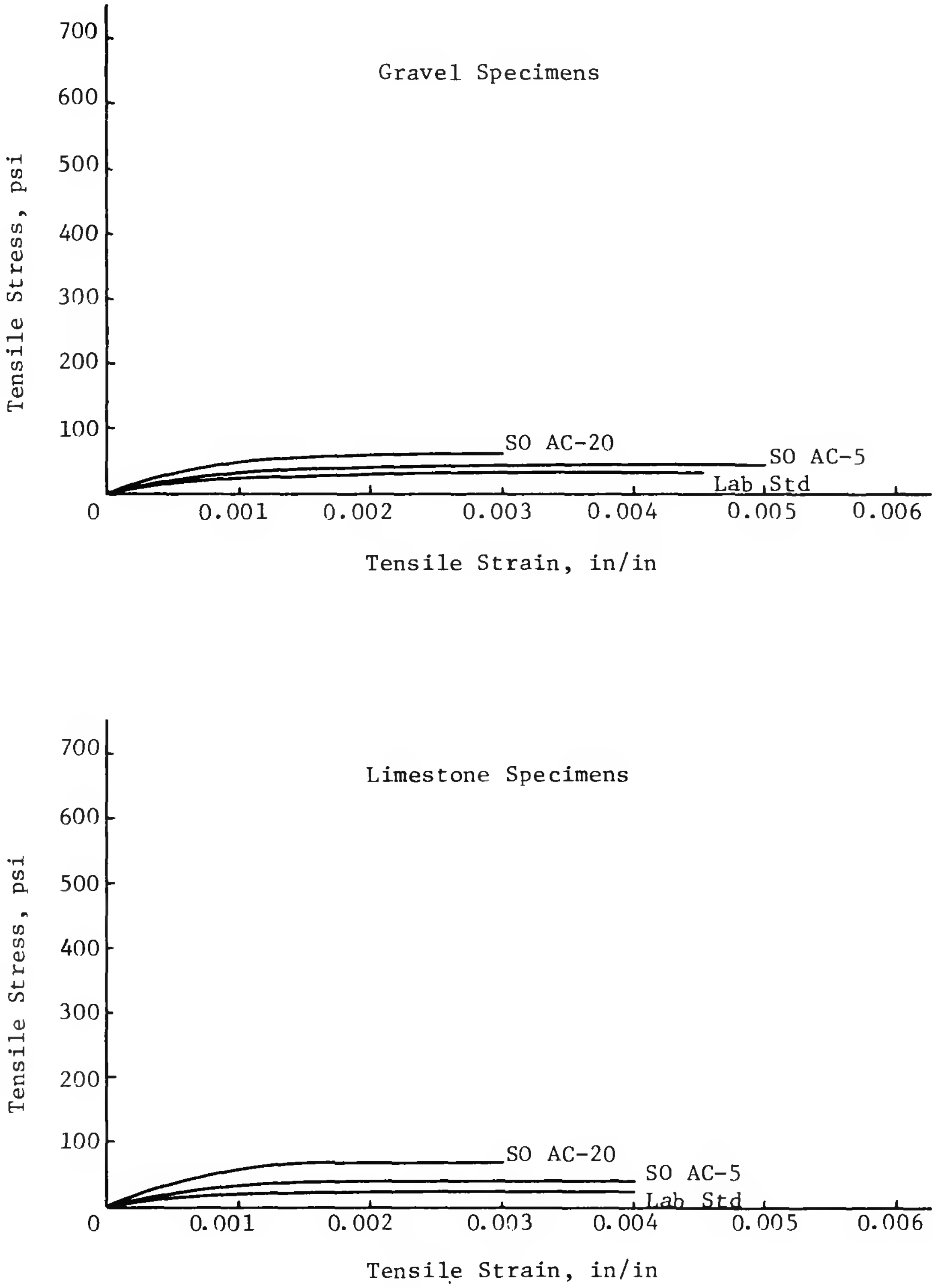

Figure D11. Sketches of Computer Plots from Splitting Tensile Tests at 68°F (20°C) and 0.02 in/min (0.051 cm/min)

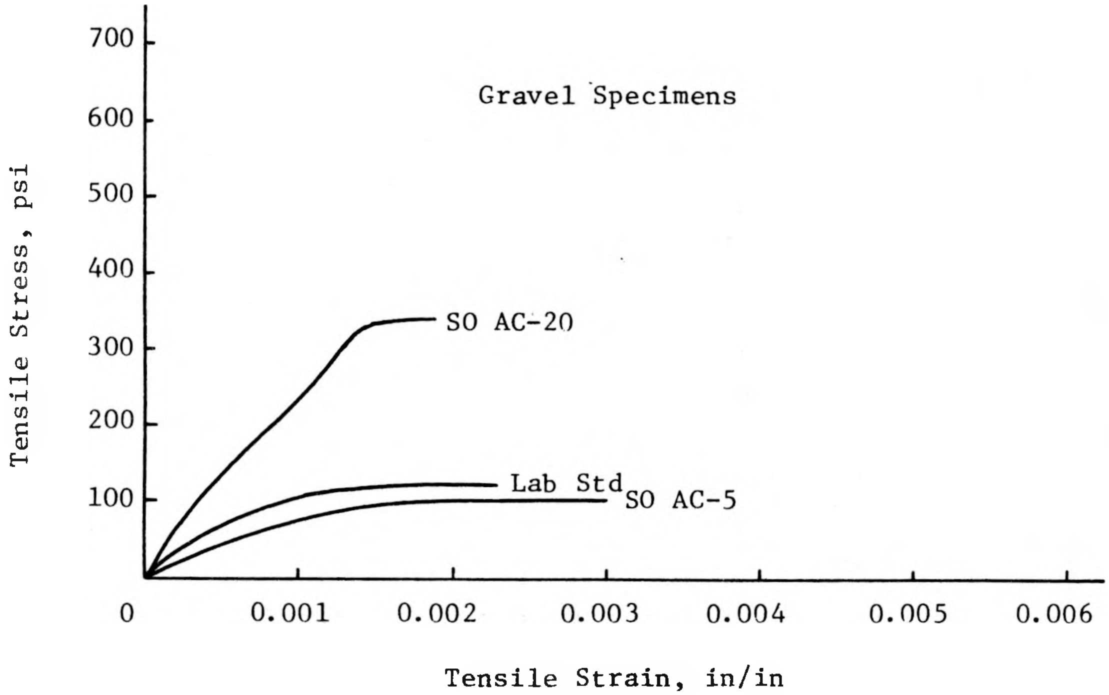

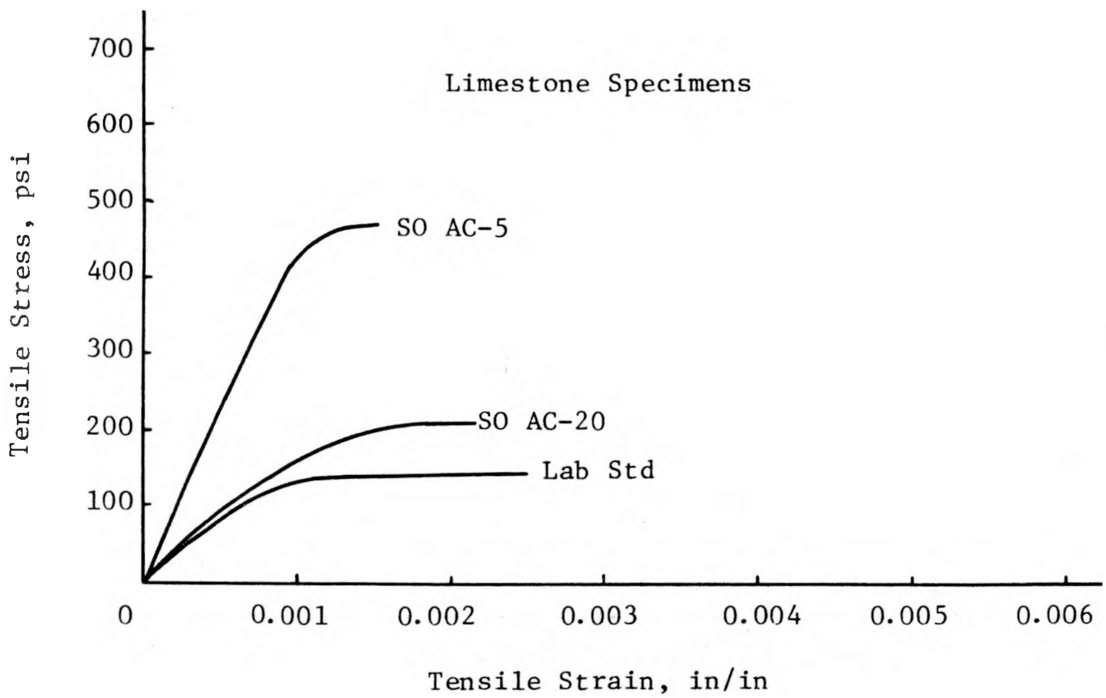

Figure D12. Sketches of Computer Plots from Splitting Tensile Tests at 33°F (1°C) and 0.02 in/min (0.051 cm/min)

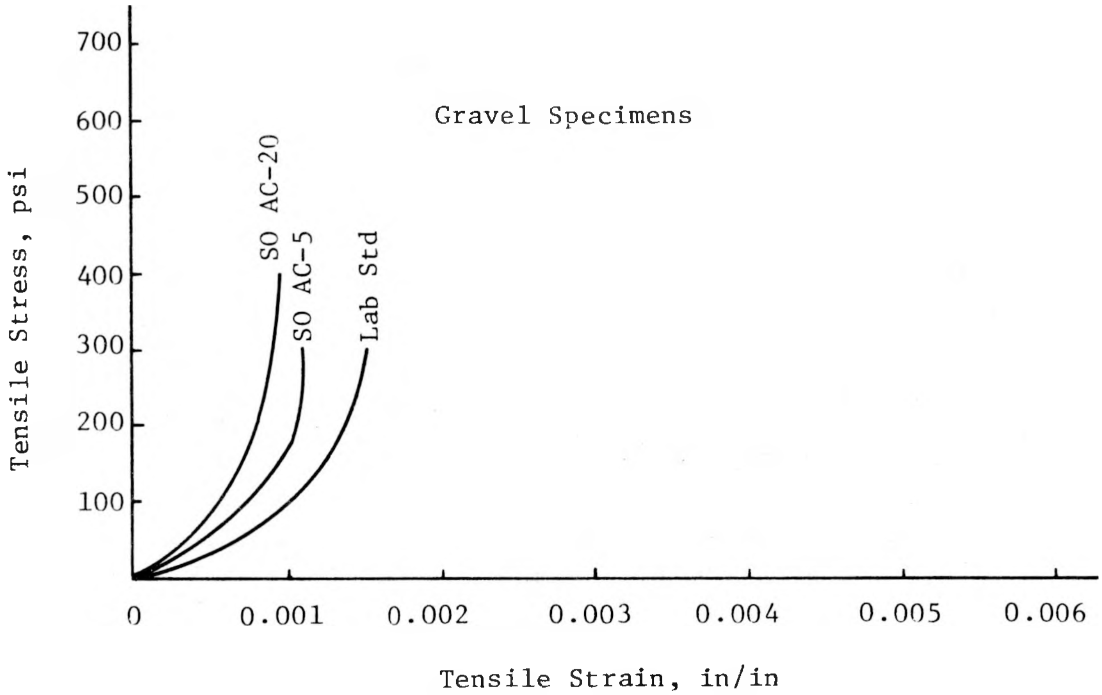

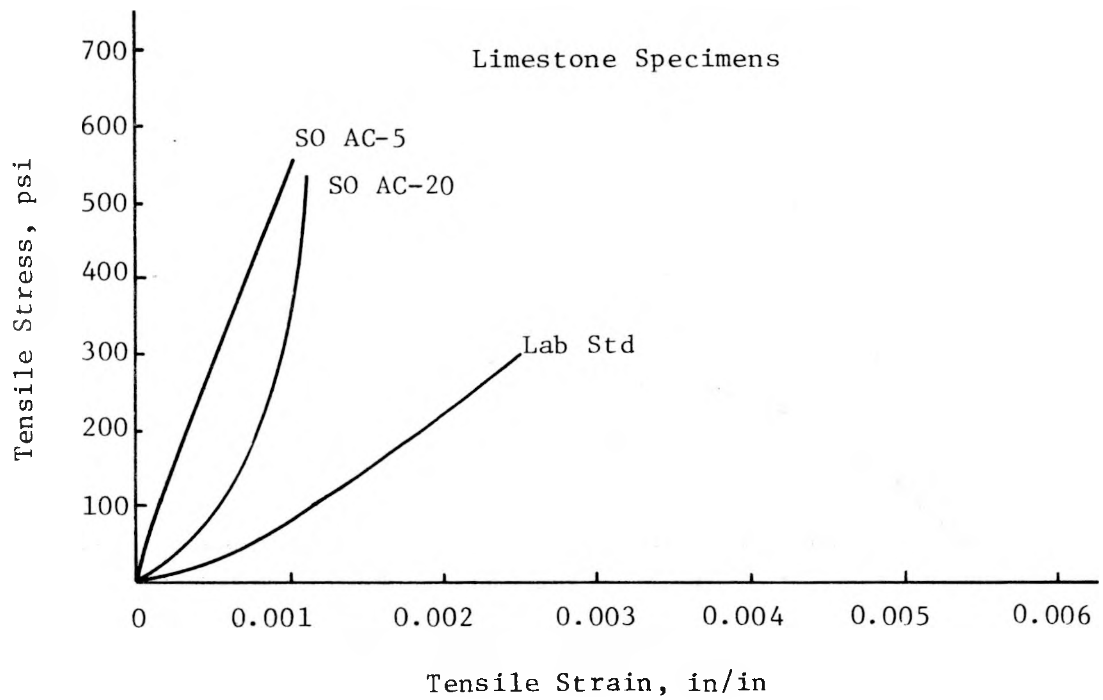

Figure D13. Sketches of Computer Plots from Splitting Tensile Tests at -13°F (-25°C) and 0.02 in/min (0.02 cm/min)

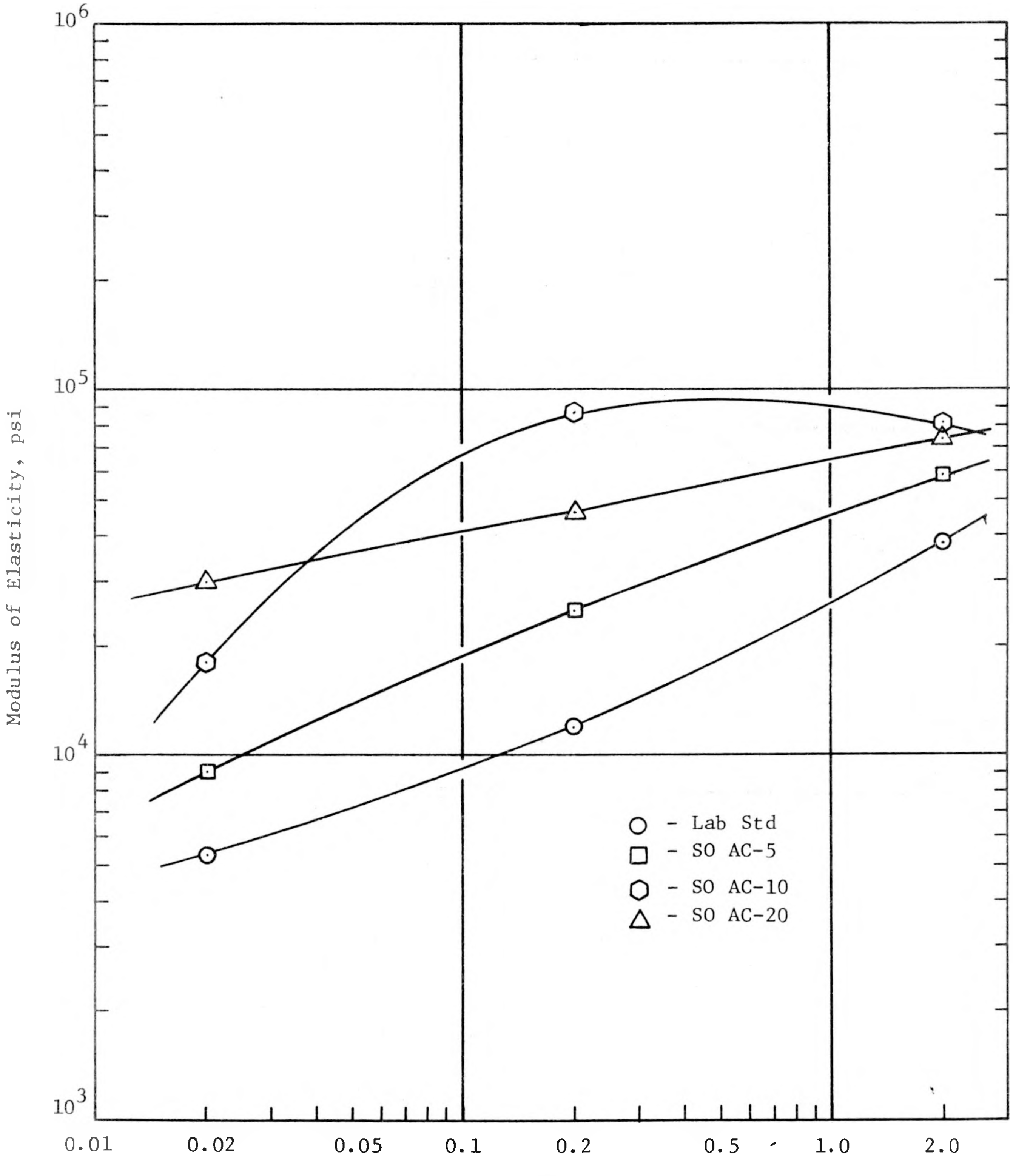

Figure D14. Modulus of Elasticity as a Function of Loading Rate for Gravel Specimens at 68°F (20°C)

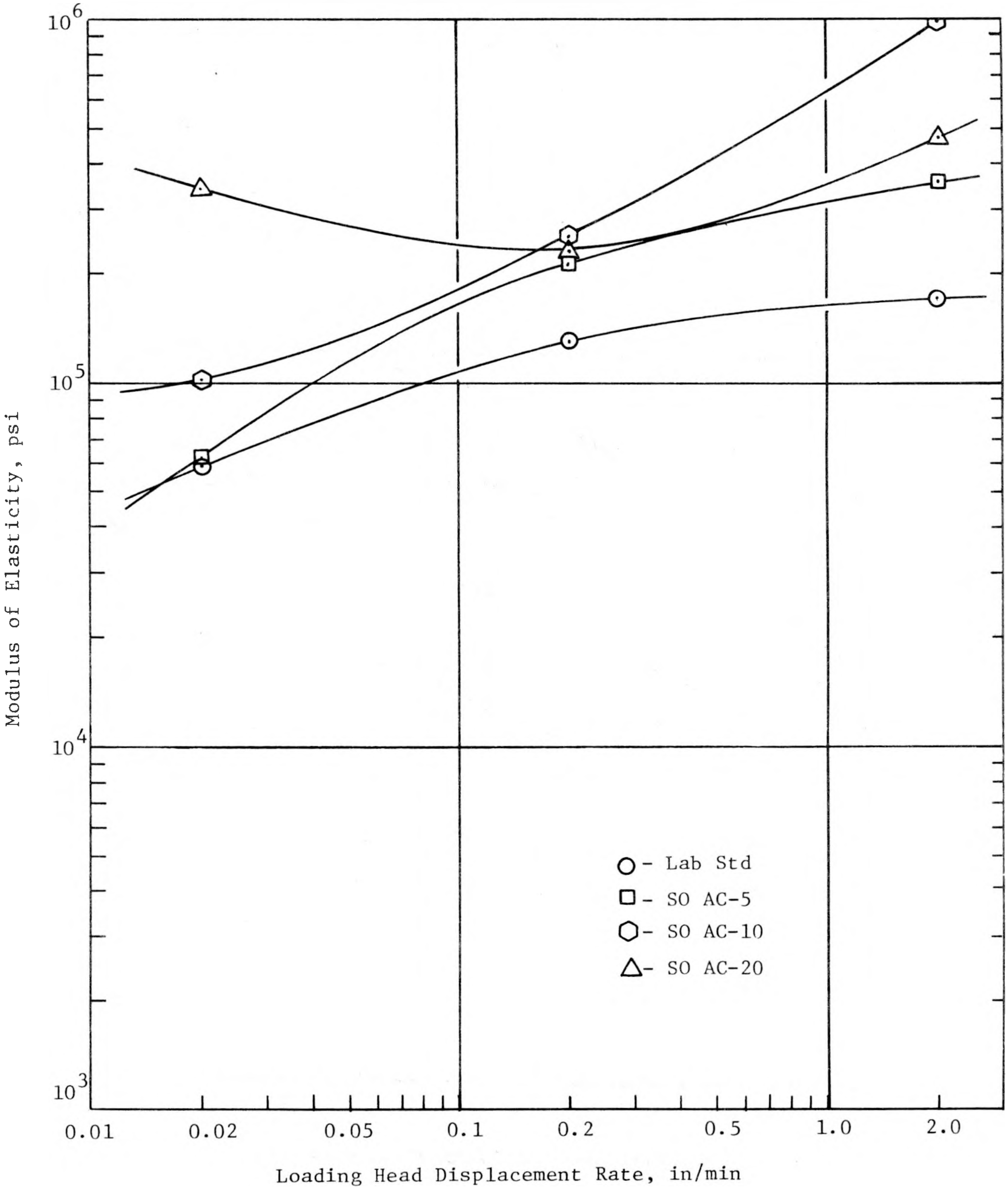

Figure D15. Modulus of Elasticity as a Function of Loading Rate for Gravel Specimens at 33°F (1°C)

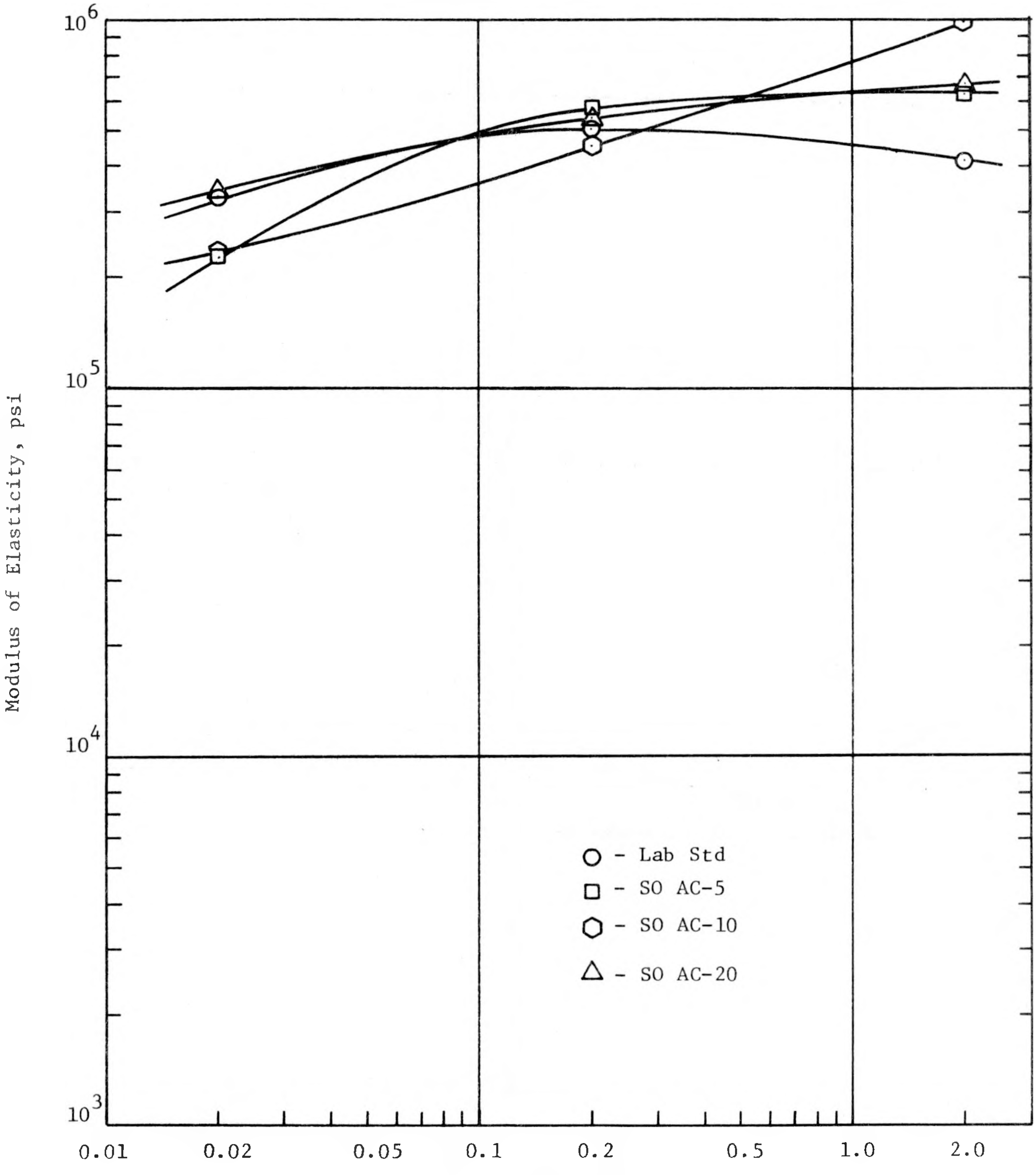

Figure D16. Modulus of Elasticity as a Function of Loading Rate for Gravel Specimens at -10°F (-25°C)

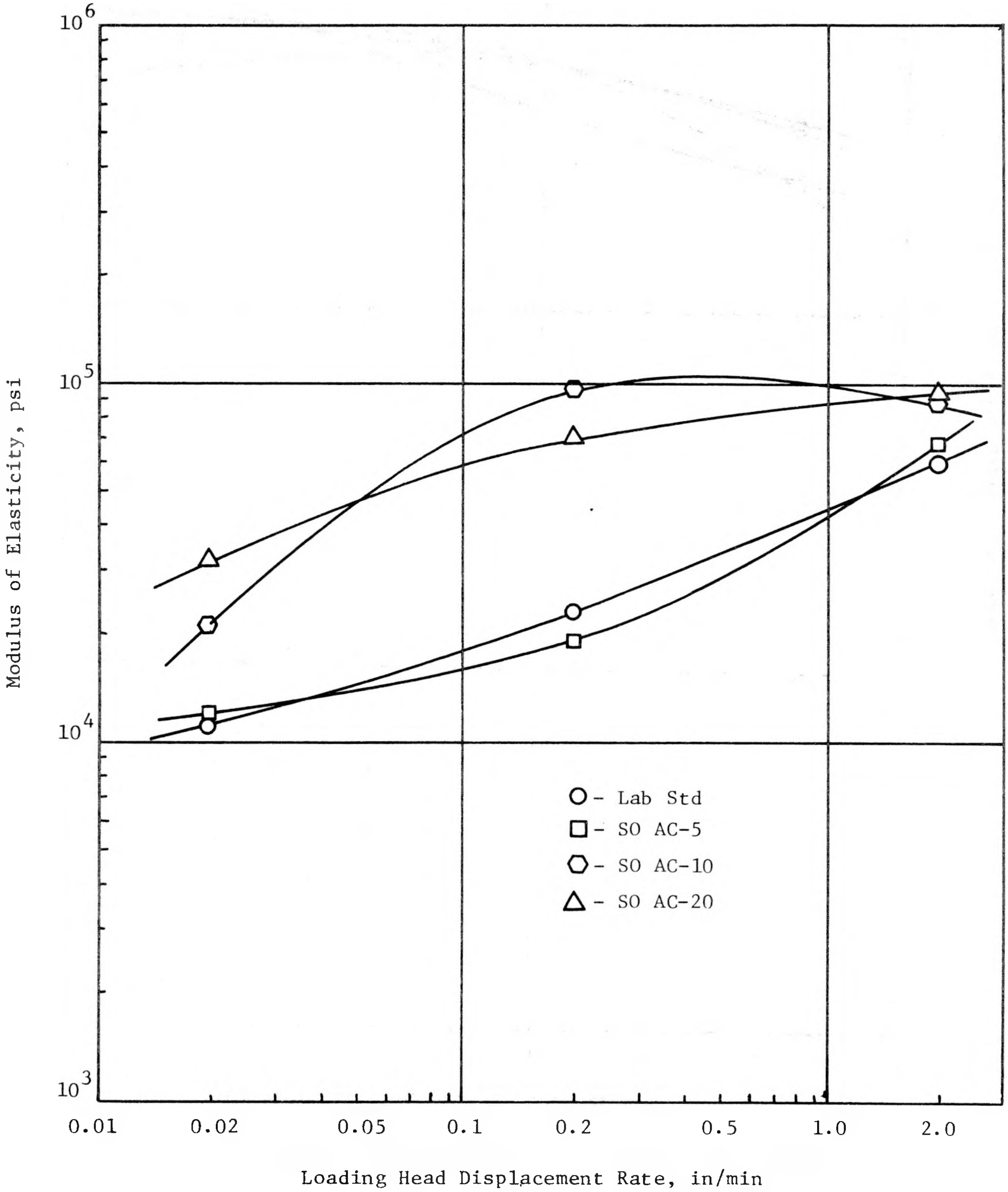

Figure D17. Modulus of Elasticity as a Function of Displacement Rate for Limestone Specimens at 68°F (20°C)

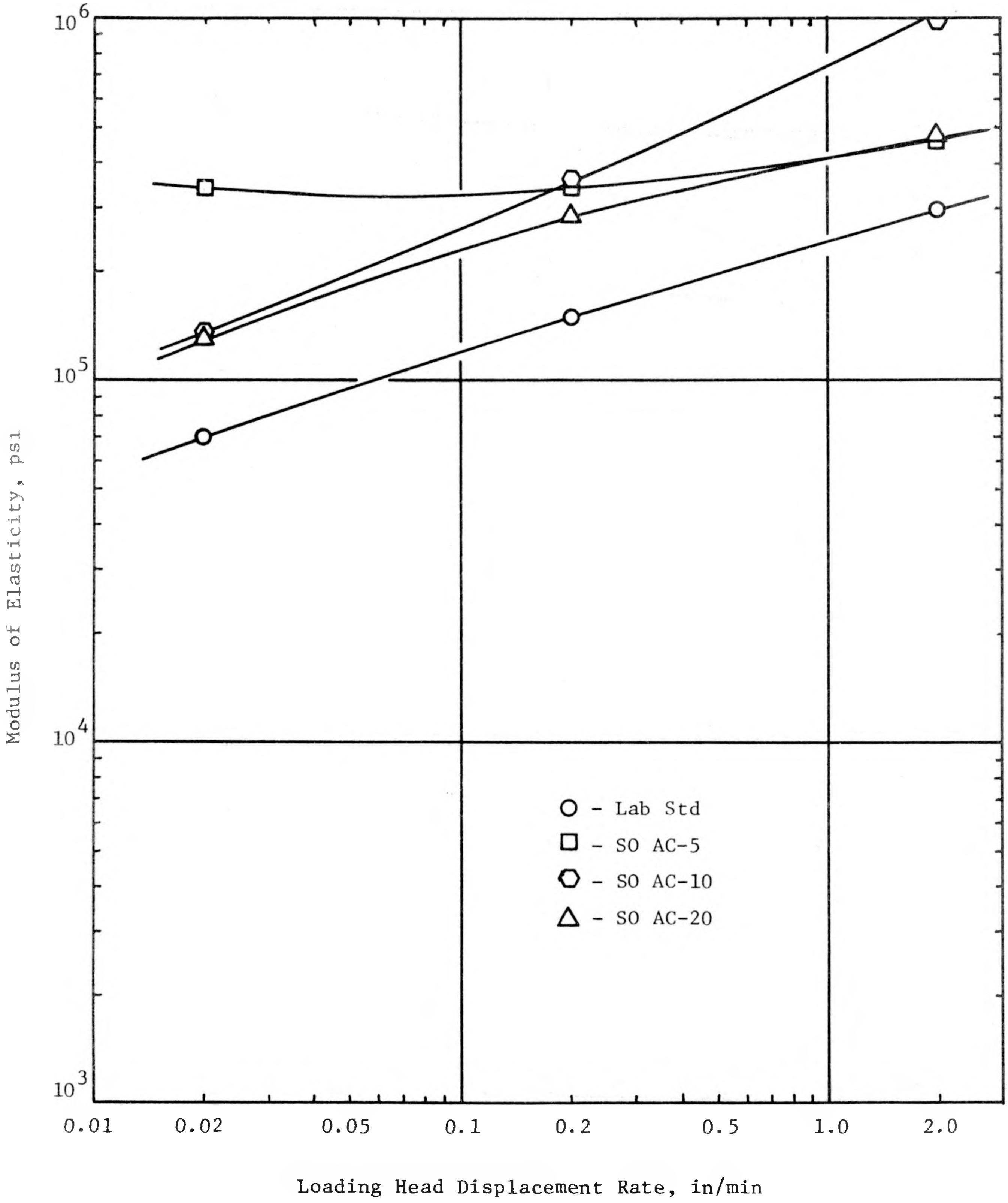

Figure D18. Modulus of Elasticity as a Function of Loading Rate for Limestone Specimens at 33°F (1°C)

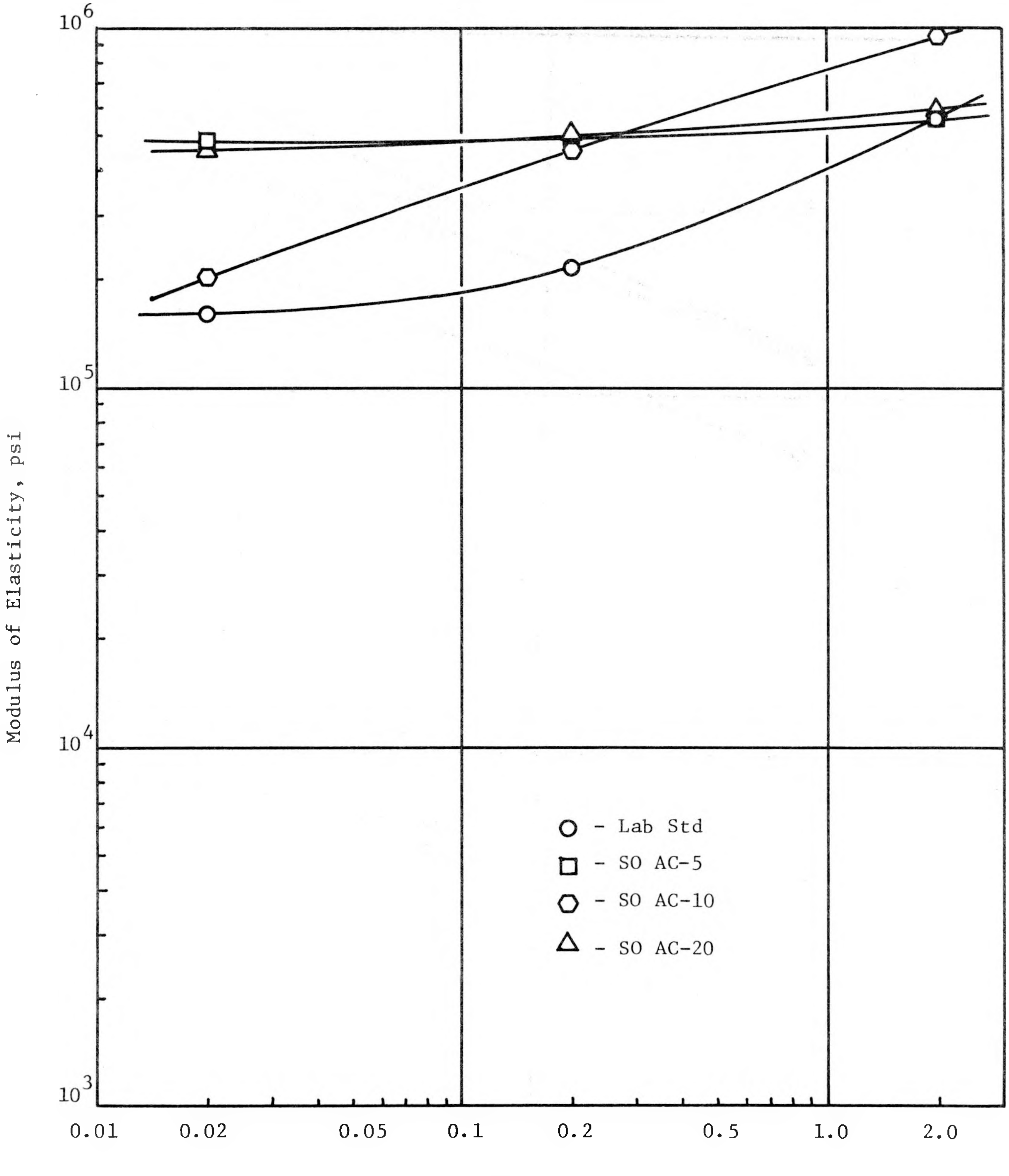

Figure D19. Modulus of Elasticity as a Function of Loading Rate for Limestone Specimens at -10°F (-25°C)

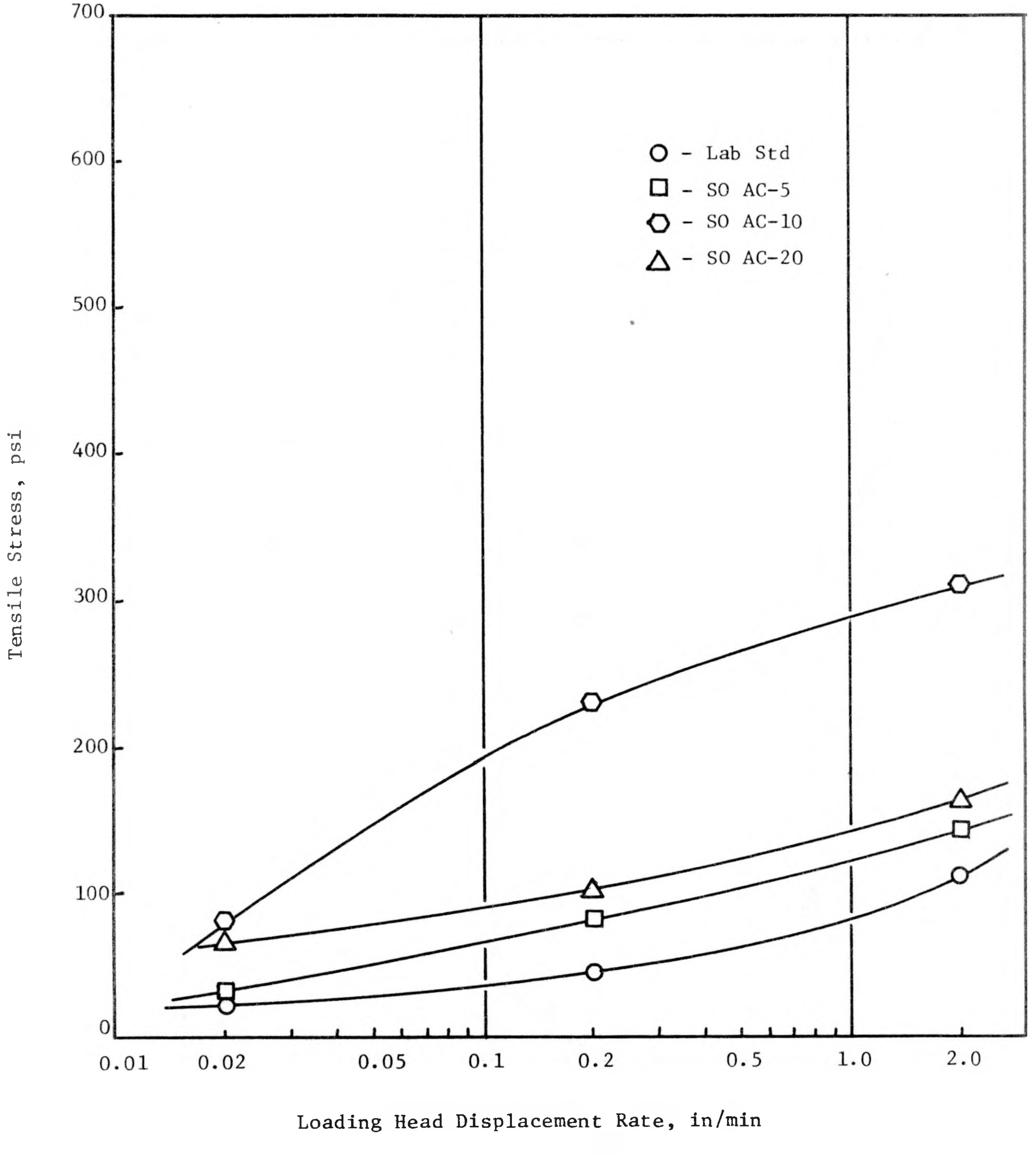

Figure D20. Indirect Tensile Stress as a Function of Loading Rate for Gravel Specimens at 68°F (20°C)

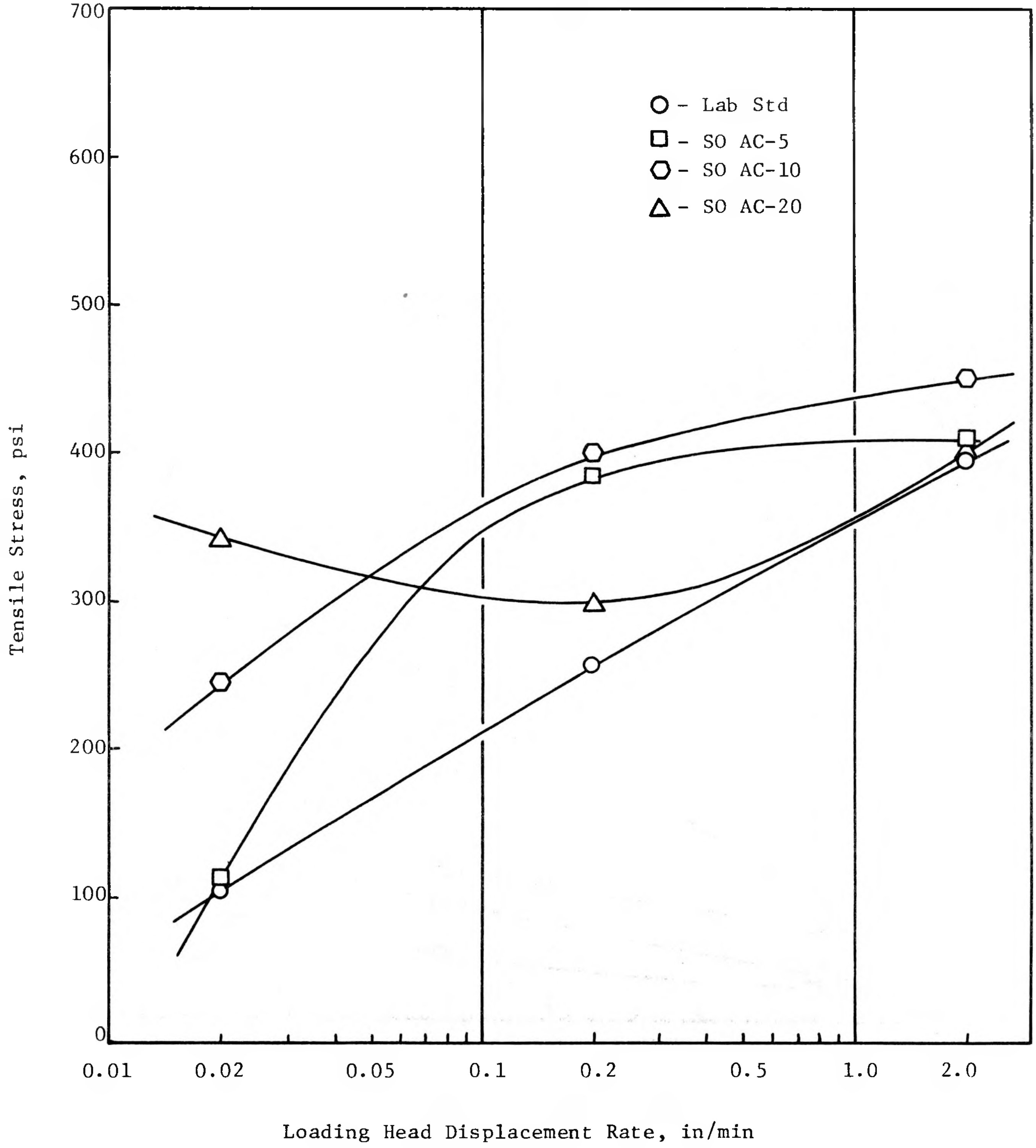

Figure D21. Indirect Tensile Stress as a Function of Loading Rate for Gravel Specimens at 33°F (1°C)

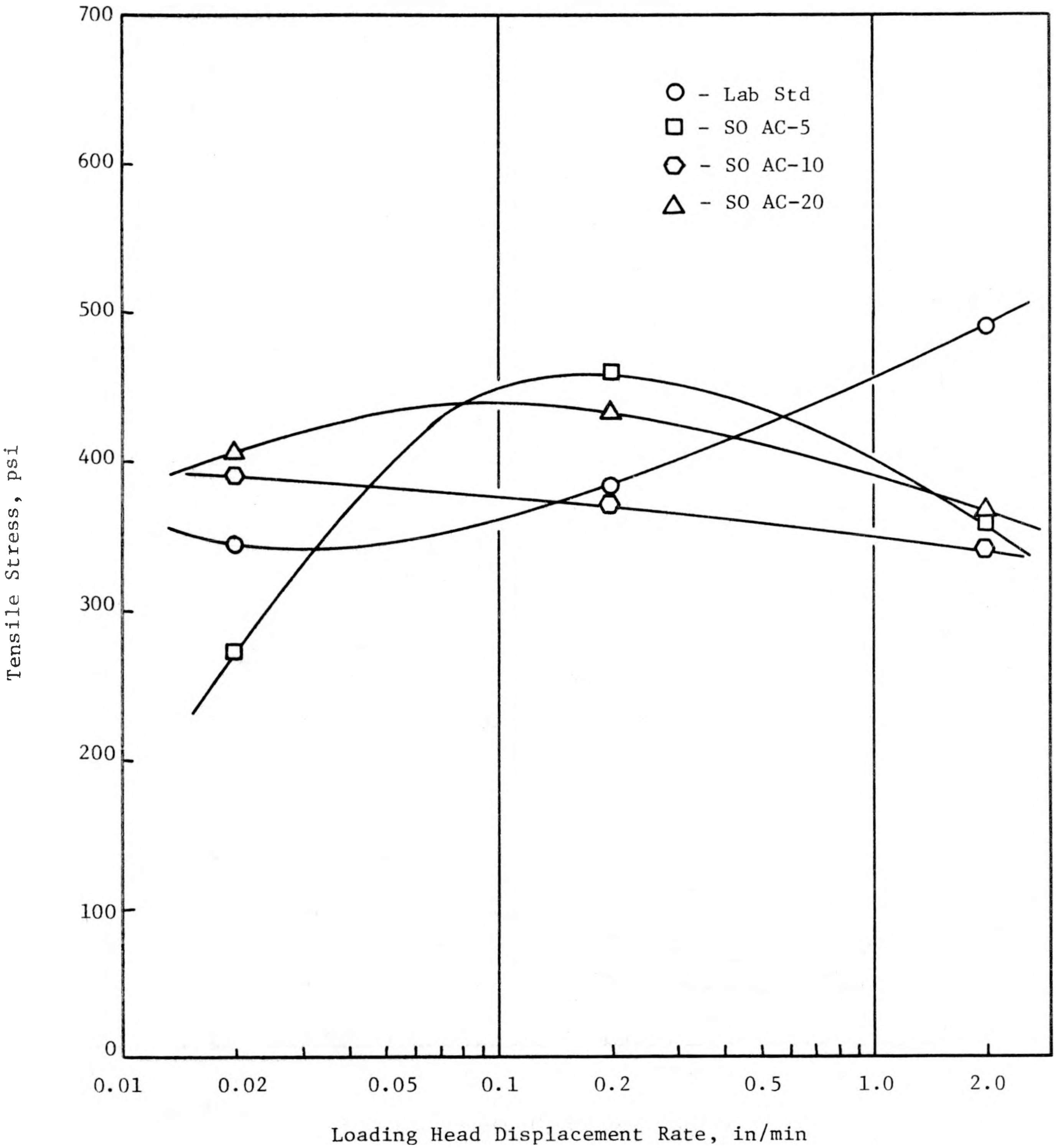

Figure D22. Indirect Tensile Stress as a Function of Loading Rate for Gravel Specimens at -10°F (-25°C)

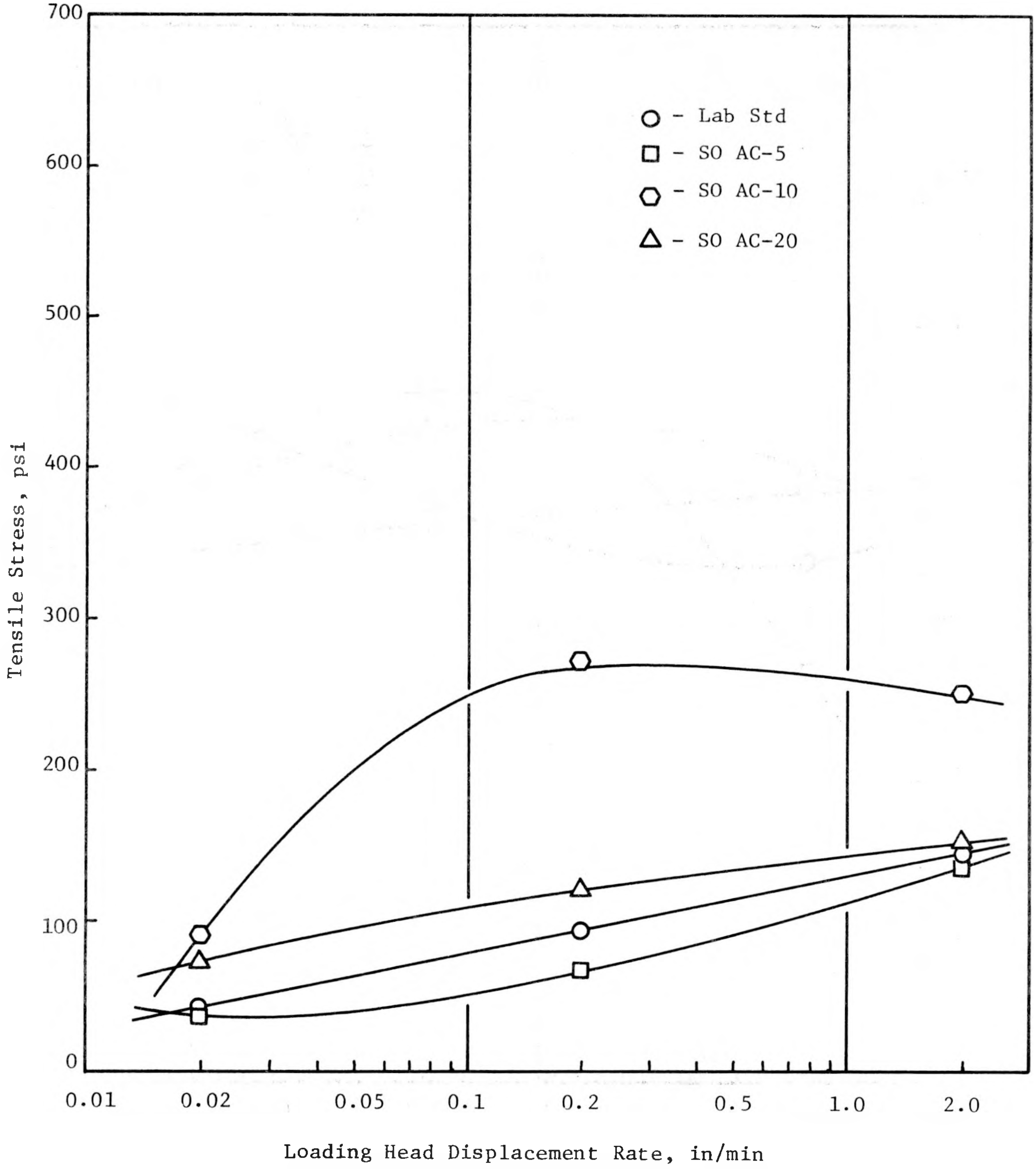

Figure D23. Indirect Tensile Stress as a Function of Loading Rate for Limestone Specimens at 68°F (20°C)

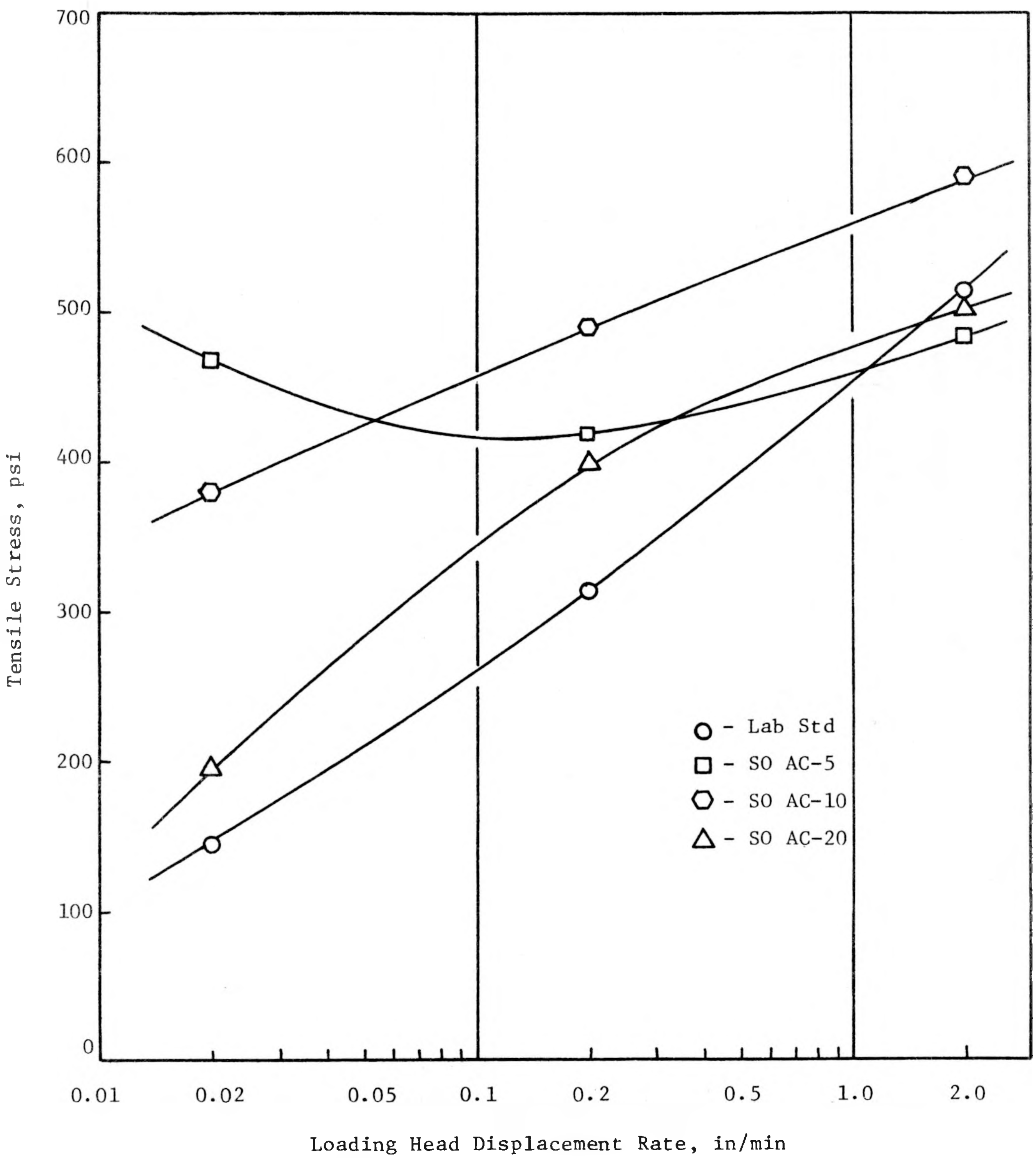

Figure D24. Indirect Tensile Stress as a Function of Loading Rate for Limestone Specimens at 33°F (1°C)

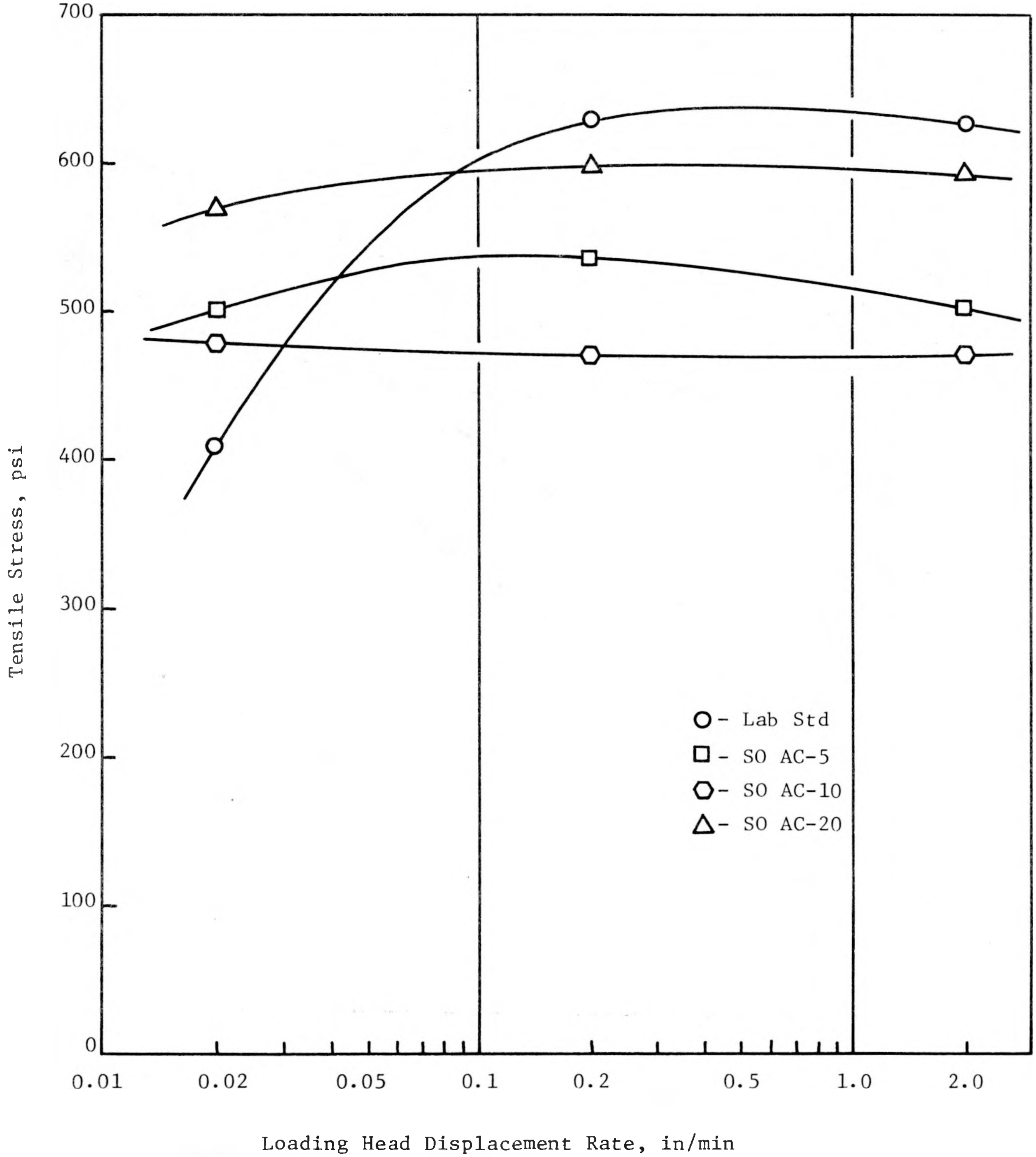

Figure D25. Indirect Tensile Stress as a Function of Loading Rate for Limestone Specimens at -10°F (-25°C)

APPENDIX E

METHOD OF EXTRACTION AND RECOVERY OF BITUMENS

Extraction and Recovery of Bitumen

From Bituminous Paving Mixtures

I. Extraction

Bitumen was extracted from the paving mixtures in accordance with ASTM Designation D 2172, Method B procedure. However, in place of trichloroethylene, a mixture of 6 parts benzene to 1 part ethyl alcohol by volume was substituted for the extracting solvent.

II. Recovery

The recovery process was a modification of the procedure devised by Traxler (12) to recover asphalt from an asphalt-solvent solution in a manner that would least influence its properties. However, since the published procedure has been modified, the revised procedure is described below.

The sample consists of the benzene-alcohol solvent and the bitumen which was extracted from the asphalt pavement mixture. This solution was centrifuged for a minimum of 30 minutes at 770 times gravity in 8-ounce wide-mouth bottles. The solution was then transferred to a boiling flask for bitumen recovery.

The boiling flask containing the extracted asphalt was attached to a rotary film evaporator and placed into a mineral oil bath (any nonvolatile oil is suitable) at an angle of approximately 30°. While continuously rotating, the partially evacuated flask was maintained between 220° and 240°F.

The vacuum was monitored by means of a manometer. A drop in manometer pressure indicated the recovery was nearing completion. In the final stages of seperation, bubbles in the asphalt could be observed. When flask rotation was stopped and no bubbles appeared, the asphalt was considered to be free of solvent. As a precaution, the process was allowed to continue for 15 to 20 minutes. At this point, the flask was removed from the system and the recovered asphalt was transferred to a covered container for storage until further evaluation.

A list of the apparatus required along with available manufacturer's information is as follows:

1. Rotary Film Evaporator
   Labline "Flash-Vac" Rotary Film Evaporator
   Catalogue Number 5100

2. Flask, Boiling, Round Bottom, Short Neck, Tapered Sleeve Joint
   Corning, C. G. W. Code Number 400223
   1000 ml., Tapered Joint 24/40

3. Oil Bath*
   Thermostatic Control 0° - 400°F

4. Mineral Oil

5. Thermometer
   Temperature Range 50° - 500°F
   ASTM

*A sunbeam "Cooker and Fryer" deep fryer has been found to fulfill the necessary requirements for the oil bath.

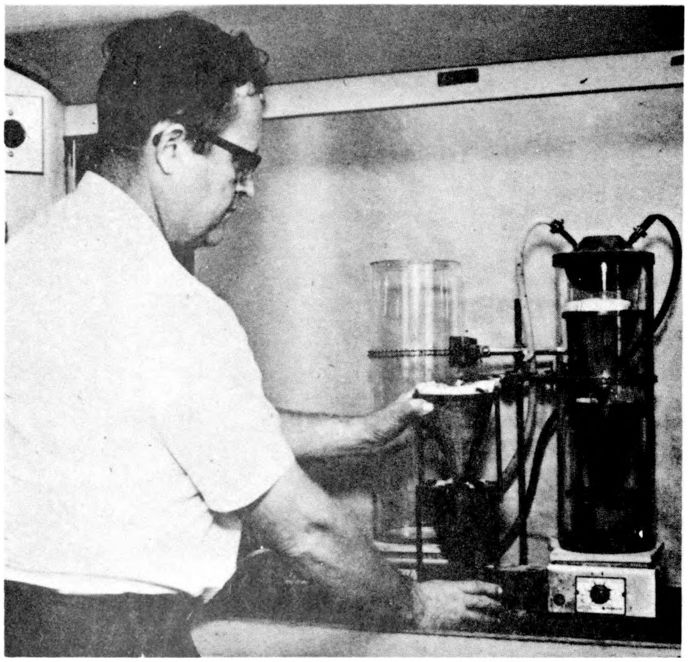

Figure E1. Asphalt Extraction Tower

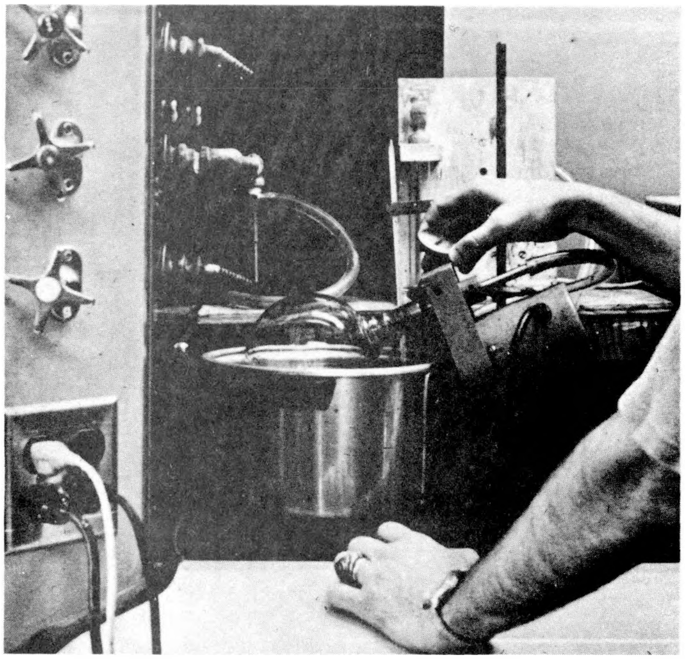

Figure E2. Asphalt Recovery Apparatus

APPENDIX F

Resilient Modulus Data for Water Susceptibility Specimens

Table F1. Resilient Modulus of Water Susceptibility Specimens made with Gravel

Asphalt	Condition	Temperature °F (°C)	Sample Number	Resilient Modulus psi x 10^{-6} (KPa x 10^{-6})	Average Res. Mod. psi x 10^{-6} (KPa x 10^{-6})
Lab Std.	Before Soaking	-13 (-25)	GA-2 GA-6 GA-11	7.35(50.6) 7.85(54.1) 8.30(57.2)	7.83 (53.9)
		33 (1)	GA-2 GA-6 GA-11	2.95(20.3) 3.29(22.7) 3.32(22.9)	3.19 (21.9)
		68 (20)	GA-2 GA-6 GA-11	0.48(3.3) 0.41(2.8) 0.47(3.2)	0.45(3.1)
		77 (25)	GA-2 GA-6 GA-11	0.23(1.6) 0.20(1.4) 0.21(1.4)	0.21(1.4)
		104 (40)	GA-2 GA-6 GA-11	0.043(.29) 0.040(.27) 0.043(.29)	0.042 (.29)
	After Soaking	68 (20)	GA-2 GA-6 GA-11	0.36(2.4) 0.27(1.8) 0.27(1.8)	0.030(2.1)
SO AC-5	Before Soaking	-13 (-25)	S05-G1 S05-G2 S05-G3	8.78(60.5) 7.09(48.9) 6.55(45.2)	7.47(51.5)
		33 (1)	S05-G1 S05-G2 S05-G3	3.25(22.4) 2.86(19.7) 4.31(29.7)	3.47(23.9)
		68 (20)	S05-G1 S05-G2 S05-G3	0.78(5.38) 0.78(5.38) 0.95(6.55)	0.84(5.79)
		68 (20)	S05-10 S05-20 S05-30	1.01(6.9) 0.91(6.3) 1.29(8.9)	1.07(7.4)

Table F1. Continued

Asphalt	Condition	Temperature °F(°C)	Sample Number	Resilient Modulus psi x 10^{-6} (KPa x 10^{-6})	Average Res. Mod. psi x 10^{-6} (KPa x 10^{-6})
SO AC-5	Before Soaking	77 (25)	S05-G1 S05-G2 S05-G3	0.39 (2.7) 0.39 (2.7) 0.42 (2.9)	0.40 (2.8)
		104 (40)	S05-G1 S05-G2 S05-G3	0.023 (.16) 0.021 (.15) 0.036 (.25)	0.023 (.16)
	After Soaking	68 (20)	S05-10 S05-20 S05-30	0.86 (5.9) 0.99 (6.8) 1.45 (9.9)	1.10 (7.6)
SO AC-10	Before Soaking	-13 (-25)	GDW-1 GDW-11 GDW-21	7.23 (49.8) 7.18 (49.5) 5.94 (40.9)	6.80 (46.8)
		33 (1)	GDW-1 GDW-11 GDW-21	4.05 (27.9) 4.81 (33.2) 4.64 (31.4)	4.50 (31.6)
		68 (20)	GDW-1 GDW-11 GDW-21	1.76 (12.1) 1.75 (12.1) 2.26 (15.6)	1.92 (13.2)
		77 (25)	GDW-1 GDW-11 GDW-21	2.03 (13.9) 1.18 (8.1) 1.01 (6.9)	1.41 (9.7)
		104 (40)	GDW-1 GDW-11 GDW-21	0.042 (.29) 0.038 (.26) 0.036 (.25)	.039 (.27)
	After Soaking	68 (20)	GDW-1 GDW-11 GDW-21	0.959 (6.6) 1.258 (8.7) 1.299 (8.9)	1.17 (8.1)

Table F1. Continued

Asphalt	Condition	Temperature °F (°C)	Sample Number	Resilient Modulus psi x 10^{-6} (KPa x 10^{-6})	Average Res. Mod. psi x 10^{-6} (KPa x 10^{-6})
SO AC-20	Before Soaking	-13 (-25)	S020-G1 S020-G2 S020-G3	6.12 (4.22) 5.45 (37.6) 5.91 (40.7)	5.83 (40.2)
		33 (1)	S020-G1 S020-G2 S020-G3	3.09 (21.3) 3.20 (22.1) 3.59 (24.8)	3.19 (21.9)
		68 (20)	S020-G1 S020-G2 S020-G3	1.03 (7.10) 0.89 (6.14) 0.92 (6.34)	0.95 (6.55)
		68 (20)	S020-10 S020-20 S020-30	1.38 (9.5) 1.37 (9.4) 1.50 (10.3)	1.42 (9.8)
		77 (25)	S020-G1 S020-G2 S020-G3	0.60 (4.1) 0.49 (3.4) 0.54 (3.7)	0.55 (3.8)
		104 (40)	S020-G1 S020-G2 S020-G3	0.091 (.63) 0.10 (.69) 0.10 (.69)	0.10 (.69)
	After Soaking	68 (20)	S020-10 S020-20 S020-30	1.47 (10.1) 1.69 (11.6) 1.76 (12.1)	1.64 (11.3)

Table F2. Resilient Modulus of Water Susceptibility Specimens made with Limestone

Asphalt	Condition	Temperature °F (°C)	Sample Number	Resilient Modulus psi x 10^{-6} (KPa x 10^{-6})	Average Res. Mod. psi x 10^{-6} (KPa x 10^{-6})
Lab Std	Before Soaking	-13 (-25)	LA-1 LA-11 LA-21	4.95 (34.1) 5.68 (39.2) 6.74 (46.5)	5.79 (39.9)
		33 (1)	LA-1 LA-11 LA-21	3.30 (22.8) 3.37 (23.2) 2.85 (19.7)	3.17 (21.9)
		68 (20)	LA-1 LA-11 LA-21	0.63 (4.3) 0.83 (5.7) 0.80 (5.5)	0.75 (5.2)
		77 (25)	LA-1 LA-11 LA-21	0.39 (2.7) 0.40 (2.8) 0.41 (2.8)	0.40 (2.8)
		104 (40)	LA-1 LA-11 LA-21	0.086 (.59) 0.090 (.62) 0.104 (.72)	0.093 (.64)
	After Soaking	68 (20)	LA-1 LA-11 LA-21	0.40 (2.8) 0.45 (3.1) 0.50 (3.5)	0.45 (3.1)
SO AC-5	Before Soaking	-13 (-25)	SO5-L1 SO5-L2 SO5-L3	7.60 (52.4) 4.92 (33.9) 4.78 (32.9)	5.77 (39.8)
		33 (1)	SO5-L1 SO5-L2 SO5-L3	3.34 (23.0) 3.47 (23.9) 3.37 (23.2)	3.39 (23.4)
		68 (20)	SO5-L1 SO5-L2 SO5-L3	1.09 (7.52) 1.04 (7.17) 1.04 (7.17)	1.06 (7.31)
		68 (20)	SO5-10 SO5-20 SO5-30	0.88 (6.1) 0.92 (6.3) 1.03 (7.1)	0.94 (6.5)

Table F2. Continued

Asphalt	Condition	Temperature °F (°C)	Sample Number	Resilient Modulus psi x 10^{-6} (KPa x 10^{-6})	Average Res. Mod. psi x 10^{-6} (KPa x 10^{-6})
SO AC-5	Before Soaking	77 (25)	S05-L1 S05-L2 S05-L3	0.68 (4.7) 0.65 (4.5) 0.63 (4.3)	0.66 (4.5)
		104 (40)	S05-L1 S05-L2 S05-L3	0.077 (.53) 0.068 (.47) 0.076 (.52)	0.074 (.51)
	After Soaking	68 (20)	S05-10 S05-20 S05-30	0.93 (6.4) 1.08 (7.5) 1.04 (7.2)	1.02 (7.0)
SO AC-10	Before Soaking	-13 (-25)	LDW-1 LDW-11 LDW-21	4.86 (33.5) 7.28 (50.2) 6.70 (46.2)	6.28 (43.3)
		33 (1)	LDW-1 LDW-11 LDW-21	3.78 (26.1) 4.98 (34.3) 4.12 (28.4)	4.29 (29.6)
		68 (20)	LDW-1 LDW-11 LDW-21	1.67 (11.5) 1.80 (12.4) 1.53 (10.5)	1.67 (11.5)
		77 (25)	LDW-1 LDW-11 LDW-21	1.51 (10.4) 1.66 (11.4) 1.67 (11.5)	1.61 (11.1)
		104 (40)	LDW-1 LDW-11 LDW-21	0.14 (.97) 0.14 (.97) 0.11 (.76)	0.13 (.89)
	After Soaking	68 (20)	LDW-1 LDW-11 LDW-21	1.30 (8.9) 1.23 (8.5) 1.15 (7.9)	1.22 (8.4)

Table F2. Continued

Asphalt	Condition	Temperature °F (°C)	Sample Number	Resilient Modulus psi x 10^{-6} (KPa x 10^{-6})	Average Res. Mod. psi x 10^{-6} (KPa x 10^{-6})
SO AC-20	Before Soaking	-13 (-25)	S020-L1 S020-L2 S020-L3	4.46 (30.8) 4.25 (29.3) 4.62 (31.9)	4.44 (30.6)
		33 (1)	S020-L1 S020-L2 S020-L3	3.23 (22.3) 3.42 (23.6) 3.28 (22.6)	3.31 (22.8)
		68 (20)	S020-L1 S020-L2 S020-L3	1.13 (7.79) 1.09 (7.52) 1.13 (7.79)	1.12 (7.72)
		68 (20)	S020-10 S020-20 S020-30	1.61 (11.1) 1.52 (10.5) 1.39 (9.6)	1.51 (10.4)
		77 (25)	S020-L1 S020-L2 S020-L3	0.83 (5.7) 0.97 (6.7) 0.96 (6.6)	0.92 (6.3)
		104 (40)	S020-L1 S020-L2 S020-L3	0.22 (1.5) 0.21 (1.4) 0.23 (1.6)	0.22 (1.5)
	After Soaking	68 (20)	S020-10 S020-20 S020-30	1.26 (8.7) 1.41 (9.7) 1.58 (10.9)	1.42 (9.8)

DISCLAIMER

Available from the National Technical Information Service, U. S. Department of Commerce, Springfield, Virginia 22161.

Price: Printed Copy $7.25
Microfiche $3.00

Printed in the United States of America
USDOE Technical Information Center, Oak Ridge, Tennessee